NASA TECHNICAL NOTE

NASA TN D-7454

NASA TN D-7454

SIMULATOR EVALUATION OF THE LOW-SPEED FLYING QUALITIES OF AN EXPERIMENTAL STOL CONFIGURATION WITH AN EXTERNALLY BLOWN FLAP WING OR AN AUGMENTOR WING

by Bruce G. Powers and David A. Kier

Flight Research Center
Edwards, Calif. 93523

NATIONAL AERONAUTICS AND SPACE ADMINISTRATION • WASHINGTON, D. C. • OCTOBER 1973

1. Report No.	2. Government Accession No.	3. Recipient's Catalog No.
NASA TN D-7454		

4. Title and Subtitle	5. Report Date
SIMULATOR EVALUATION OF THE LOW-SPEED FLYING QUALITIES OF AN EXPERIMENTAL STOL CONFIGURATION WITH AN EXTERNALLY BLOWN FLAP WING OR AN AUGMENTOR WING	October 1973
	6. Performing Organization Code
7. Author(s)	8. Performing Organization Report No.
Bruce G. Powers and David A. Kier	H-780
	10. Work Unit No.
9. Performing Organization Name and Address	501-26-01-00
NASA Flight Research Center P. O. Box 273 Edwards, California 93523	11. Contract or Grant No.
	13. Type of Report and Period Covered
12. Sponsoring Agency Name and Address	Technical Note
National Aeronautics and Space Administration Washington, D. C. 20546	14. Sponsoring Agency Code

15. Supplementary Notes

16. Abstract

The low-speed flying qualities of an experimental STOL configuration were evaluated by using a fixed-base six-degree-of-freedom simulation. The configuration had either an externally blown flap (EBF) wing or an augmentor wing (AW). The AW configuration was investigated with two tails, one sized for the AW configuration and a larger one sized for the EBF configuration. The emphasis of the study was on the 70-knot approach task. The stability and control characteristics were compared with existing criteria. Several control systems were investigated for the normal four-engine condition and for the engine-out transient condition. Minimum control and stall speeds were determined for both the three- and four-engine operation.

17. Key Words (Suggested by Author(s))	18. Distribution Statement
STOL Externally blown flap Augmentor wing Flying qualities	Unclassified - Unlimited

19. Security Classif. (of this report)	20. Security Classif. (of this page)	21. No. of Pages	22. Price*
Unclassified	Unclassified	73	Domestic, $3.50 Foreign, $6.00

*For sale by the National Technical Information Service, Springfield, Virginia 22151

SIMULATOR EVALUATION OF THE LOW-SPEED FLYING QUALITIES OF AN EXPERIMENTAL STOL CONFIGURATION WITH AN EXTERNALLY BLOWN FLAP WING OR AN AUGMENTOR WING

Bruce G. Powers and David A. Kier
Flight Research Center

SUMMARY

The low-speed flying qualities of an experimental STOL configuration were evaluated by using a fixed-base six-degree-of-freedom simulation. The airplane was configured with either an externally blown flap (EBF) or an augmentor wing (AW). The AW configuration was investigated with two tails, one sized for the AW configuration and a larger one sized for the EBF configuration. The study emphasized the 70-knot approach task. The stability and control characteristics were compared with existing criteria. Several control system configurations were investigated for the normal four-engine condition and for the engine-out transient condition. Minimum control and stall speeds were determined for both three- and four-engine operation.

Without stability augmentation, all three configurations were characterized by poor flight path control, large trim changes, and lightly damped phugoid motions in the longitudinal mode and poor Dutch-roll damping and strong roll-yaw coupling in the lateral-directional mode. In addition, the transient motion due to a sudden engine failure was difficult to control with the EBF configuration.

Satisfactory longitudinal handling qualities were obtained by using a pitch attitude command system with the piloting technique of controlling speed with attitude and flight path with thrust. For the piloting technique of controlling speed with thrust and flight path with attitude, automatic speed control was required. The stability augmentation required for satisfactory lateral-directional handling qualities during four-engine operation consisted of a turn coordinator and a Dutch-roll damper based on sideslip rate. To reduce the transient motions resulting from a sudden engine failure with the EBF configuration, automatic deflection of the differential flaps and a roll attitude command system were required.

INTRODUCTION

Air traffic congestion has become a major operational problem for commercial transport operators, and it prompted the Civil Aviation Research and Development [CARD] Policy Study (ref. 1). The study emphasized the losses incurred in terms of time and money and suggested a short-takeoff-and-landing, or STOL, system as one means of alleviating the problem.

The National Aeronautics and Space Administration and its predecessor, the National Advisory Committee for Aeronautics, first conducted wind-tunnel tests on jet-powered-lift STOL aircraft in 1956 (ref. 2). More recent wind-tunnel tests have been made on externally blown flap and augmentor wing configurations (refs. 3 to 9).

Simulator studies of the flying characteristics of jet-powered-lift STOL transport aircraft have also been conducted (refs. 10 to 12). However, an experimental airplane is needed to provide flight verification of the design and operational procedures for jet-powered-lift STOL airplanes. One approach for developing an experimental STOL airplane is to design a vehicle that accommodates more than one type of lift concept. By adapting this approach, two of the most studied configurations, the externally blown flap and the augmentor wing, could be tested by replacing only the wing/engine assembly on the common fuselage.

In this study the low-speed flying qualities of a research vehicle capable of both lift concepts were evaluated by using a fixed-base six-degree-of-freedom simulation. The stability and control characteristics were compared to existing criteria to provide a guide for defining the control system. Several control systems were investigated for the normal four-engine condition and for the engine-out transient condition. Minimum control and stall speeds were determined for both three- and four-engine operation. In addition, since the empennage designed for the EBF configuration was larger than that required by the AW configuration, the study evaluated the effect of using the EBF-sized tail with the AW configuration. The takeoff and landing performance of the EBF configuration is described in reference 13.

SYMBOLS

Physical quantities in this report are given in the International System of Units (SI) and parenthetically in U.S. Customary Units. The measurements were taken in Customary Units. Factors relating the two systems are presented in reference 14.

a_n normal acceleration, g

b wingspan, m (ft)

C_D drag coefficient, $\frac{\text{Drag}}{\bar{q}S}$

C_L lift coefficient, $\frac{\text{Lift}}{\bar{q}S}$

C_l rolling moment coefficient, $\frac{\text{Rolling moment}}{\bar{q}Sb}$

C_m pitching moment coefficient, $\frac{\text{Pitching moment}}{\bar{q}S\bar{c}}$

C_n yawing moment coefficient, $\frac{\text{Yawing moment}}{\bar{q}Sb}$

C_Y side force coefficient, $\frac{\text{Side force}}{\bar{q}S}$

C_μ thrust coefficient

$\bar{c}$ mean aerodynamic chord, m (ft)

g	acceleration of gravity, m/sec^2 (ft/sec^2)
$\dot{h}$	rate of climb, m/sec (ft/min)
I_X, I_Y, I_Z	moments of inertia about the roll, pitch, and yaw axis, $kg\text{-}m^2$ ($slug\text{-}ft^2$)
I_{XZ}	cross product of inertia, $kg\text{-}m^2$ ($slug\text{-}ft^2$)
$j\omega$	imaginary part of the complex number, rad/sec
K, k	control system gains
L_{δ_c}	dimensional variation of lift coefficient with column deflection, $\frac{rad/sec}{cm}$ ($\frac{rad/sec}{in.}$)
M_{δ_c}	dimensional pitch sensitivity derivative, $\frac{rad/sec^2}{cm}$ ($\frac{rad/sec^2}{in.}$)
N_{Z_α}	normal acceleration per angle of attack, g/rad
p, q, r	rolling, pitching, and yawing angular velocity, deg/sec or rad/sec
$\bar{q}$	dynamic pressure, N/m^2 (lb/ft^2)
S	wing area, m^2 (ft^2)
s	Laplace operator, per sec
$T_{1/2}, T_2$	time to half amplitude and time to double amplitude, sec
T/W	ratio of static thrust to weight
t	time, sec
$t_{\varphi=30}$	time to bank to 30°, sec
V	velocity, knots or m/sec (ft/sec)
V_{min}	minimum speed, knots
W	airplane gross weight, N (lb)
α, β	angle of attack and angle of sideslip, deg
$\dot{\beta}$	rate of change in β, deg/sec

γ	flight path angle, deg
Δ	incremental change
$\frac{\Delta\beta}{K}$	maximum sideslip excursion for applicable roll performance, deg
δ_a	aileron deflection, deg
δ_{ddc}	third flap element deflection, deg
δ_f	flaperon deflection, deg
δ_h	horizontal stabilizer deflection, deg
δ_r	rudder deflection, deg
δ_{sp}	spoiler deflection, deg
δ_w	wheel deflection, deg
ζ	damping ratio of the longitudinal short-period mode
ζ_d	damping ratio of the Dutch-roll mode
Θ	angle of pitch, deg
$\ddot{\Theta}_{max}$	maximum pitch angular acceleration, rad/sec^2
σ	real part of complex number, rad/sec
φ	angle of bank, deg
$\varphi_{t=2}$	bank angle after 2 seconds, deg
ψ_β	sideslip phase angle, deg
ω_d	damped frequency, rad/sec
ω_n	longitudinal undamped natural frequency, rad/sec
ω_{n_d}	lateral-directional undamped natural frequency, rad/sec
$\omega_\varphi, \zeta_\varphi$	natural frequency and damping ratio of the roll per aileron transfer function numerator, rad/sec

TEST CONFIGURATIONS

The externally blown flap configuration and the two augmentor wing configurations that were evaluated are shown in figures 1(a) to 1(f), and their physical characteristics are listed in table 1. All three configurations used the same fuselage. The AW configuration was evaluated with the AW tail described in reference 8 or the EBF tail. The weight used in this study was 213,500 newtons (48,000 pounds), which resulted in a wing loading of 3830 N/m^2 (80 lb/ft^2). The airplane inertial characteristics are given in table 2.

Externally Blown Flap Configuration

The basic EBF configuration was a spread-engined, high-winged, triple-slotted flap transport with a large T-tail (figs. 1(a) to 1(d) and table 1). References 5 and 6 describe the configuration in detail, the only major difference being that the configuration used in this study incorporated the double-hinged slotted rudder shown in figure 1(c). No boundary-layer control was used on the control surfaces or on the wing leading edge. The aerodynamic characteristics are summarized in table 3.

Longitudinal control was provided by the horizontal stabilizer with a geared elevator and a leading-edge Krueger flap on the stabilizer (fig. 1(d)). At the full trailing-edge-up (TEU) stabilizer position (-10°), the Krueger flap was fully extended and the elevator was deflected 50° TEU relative to the stabilizer. At the full trailing-edge-down (TED) stabilizer position (10°), the Krueger flap was fully retracted and the elevator was deflected 10° TED.

Lateral control was provided by ailerons, spoilers, and differential flaps. The configuration had full-span flaps. The flaps on the outer 28 percent of the semispan served as ailerons and had a deflection range of 0° to 60° TED. Wing spoilers (fig. 1(a)), which were just forward of the flaps and covered the outer two-thirds of the semispan, were also capable of deflecting from 0° to 60°. The center span flap segments (flaperons) were deflected differentially for additional control of engine-out rolling moments. The flaperons had a deflection range of ±20° on each side. Directional control was achieved with a double-hinged slotted rudder (fig. 1(c)) which could be deflected ±45°.

The auxiliary controls were the spoilers, which were operated symmetrically for direct lift control, and the third flap elements of the inboard flap segments (fig. 1(b), direct drag control), which were used for thrust-minus-drag modulation for flight path control. The spoilers had a deflection range of 0° to 60°, and the drag flap had a deflection range of ±20°.

The thrust characteristics of the EBF configuration were based on data for a TF34-GE-2 turbofan jet engine, which had a bypass ratio of 6 and a maximum uninstalled sea level static thrust of 41,300 newtons (9280 pounds). To accommodate the low noise requirements for STOL aircraft, it was assumed that the engines were throttled to an installed thrust level of 30,000 newtons (6750 pounds) per engine, for a total airplane thrust-to-weight ratio of 0.56.

Augmentor Wing With Augmentor Tail Configuration

The AW configuration that used the tail tested in reference 8 is shown in figures 1(e)

and 1(f) and is designated the AW/AW configuration. Aerodynamic data for this configuration were derived from references 7 to 9 and are summarized in table 4.

Longitudinal control was provided by the stabilizer with an elevator geared so that at the -10° (TEU) stabilizer position the elevator was deflected -30° (TEU). (When the stabilizer was deflected 10° (TED), the elevator was deflected 10° (TED)). Roll control was provided by ailerons with boundary-layer control and deflection limits of 10° TEU and 45° TED and spoilers with a deflection range of 0° to 60°. Yaw control was provided by a double-hinged rudder with a ±45° deflection range.

Data for direct lift and drag control were not available for the AW configurations; however, thrust vectoring and augmentor choke controls can provide these features. For this simulation the EBF data were used for the direct lift and drag modulation increments.

The engine data were derived from Lycoming ALF 502A engines modified with high-power extraction turbines and operated in a derated condition. The normal total thrust level for one engine was 20,500 newtons (4600 pounds), of which 16,500 newtons (3700 pounds) was from the fan. With assumed losses, this provided 14,100 newtons (3170 pounds) of thrust per engine at the wing nozzles.

Augmentor Wing With Externally Blown Flap Tail Configuration

The AW configuration was also evaluated with the EBF tail (fig. 1(e)) and is designated the AW/EBF configuration. This configuration was identical to the AW/AW configuration except for the tail assembly, and its aerodynamic characteristics are summarized in table 5. The assumptions made to correct the AW aerodynamic data for the change in tail configuration are as follows:

(1) The basic pitching moment, lift, and drag coefficients are the same for the two AW configurations at zero horizontal tail deflection.

(2) The downwash fields of the two wings are similar, so the angle of attack of the tail and therefore the values of tail effectiveness are also similar.

(3) To account for the difference in tail dihedral (the dihedral of the EBF tail was -3.5° whereas that of the AW tail was 0°), the effective dihedral of the AW/EBF configuration was decreased 18 percent for the zero thrust condition by using the Datcom methods described in reference 15. In addition, the side force and directional stability were increased approximately 10 percent and 5 percent, respectively.

The longitudinal and directional control characteristics were the same as those used for the EBF configuration. The roll control characteristics were the same as for the AW/AW configuration.

SIMULATION DESCRIPTION

A hybrid six-degree-of-freedom fixed-base simulation was used in this study. The equations of motion were solved on a digital computer, and the control systems were simulated on an analog computer. The fixed-base cockpit is shown in figure 2. The cockpit instruments included indicators of angle of attack, angle of sideslip, airspeed,

normal acceleration, percent of power, control positions, and rate of climb, as well as a flight director, standard ILS cross pointers, a conventional altimeter, and a radar altimeter.

The linear cockpit control characteristics used in the simulator, which are shown in table 6, were selected by the pilots as representative of this class of aircraft. The control wheel had a four-position trim button for longitudinal and lateral trim. Rudder trim was controlled by a center console switch. Engine failure could be initiated from either the cockpit or the computer console.

The visual display was generated by a Dalto point source system. A model of Edwards Air Force Base and the surrounding area, including Rogers Dry Lake and its runway complex, was used in the visual display. At 610 meters (2000 feet) above the ground, runways and hangars could be distinguished at a distance of approximately 5600 meters (3 miles). Height judgment for flare or other low-altitude maneuvers was difficult below 30 meters (100 feet) and virtually impossible below 15 meters (50 feet).

CONTROL SYSTEM DESCRIPTION

Pitch Control System

A block diagram of the pitch control system is shown in figure 3(a). Several control system configurations were simulated by changing various gains. The configurations investigated were a proportional system with and without rate damping, rate and attitude command systems, and a system with a combination of pitch rate and normal acceleration feedbacks.

Roll Control System

A block diagram of the roll control system is shown in figure 3(b). Roll rate damping and roll rate or attitude command systems were investigated with a proportional plus integral network, $K\left(1 + \frac{k}{s}\right)$, as well as a simple proportional network, K. The flaperons were used as an emergency roll control and were activated by an engine failure.

Directional Control System

A block diagram of the directional control system is shown in figure 3(c). Dutch-roll damping was augmented with a washed-out yaw rate feedback or a combination of yaw rate and bank angle feedback to give an approximation of $\dot{\beta}$ feedback (ref. 16). Turn coordination was provided by a roll rate feedback and a wheel-to-rudder interconnect.

Flight Path Control System

Flight path control systems included an autothrottle system, in which airspeed error caused a power change; an autospeed system, in which airspeed error caused a change in the drag through the last element of the innermost flap segment; and a direct lift control system, in which symmetrical spoiler deflection caused a change in lift.

TEST PROCEDURES

During the study the pilot evaluated the handling characteristics of all three configurations during low-speed flight. Four-engine approaches, which included go-arounds at various altitudes, were made with various stability augmentation systems. Three-engine characteristics were evaluated with an outboard engine failure occurring during the approach. The 1g stall and minimum control speeds were determined for each configuration at various thrust settings.

The pilot rating scale from reference 17, presented here as table 7, was used during the evaluations. Although several pilots made evaluations, one research pilot made most of the evaluations presented.

RESULTS AND DISCUSSION

Comparison of the Basic Configuration Characteristics With Criteria

The stability and control characteristics of the three basic configurations were compared with several criteria (refs. 18 to 24). The configuration characteristics were calculated for the approach flap setting with approach thrust and maximum thrust. The criteria were used to provide an indication of stability augmentation requirements in terms of both the type of augmentation and the degree of reliability required.

References 22 and 23 use levels 1, 2, and 3 to describe criteria boundaries that correspond approximately to pilot ratings of 3.5, 6.5, and 9.5, respectively. If a basic airplane met the level 1 requirements, its handling qualities were considered to be satisfactory without stability augmentation. If an airplane's handling qualities met the level 2 or 3 requirements, the airplane was considered to be flyable, but stability augmentation would be necessary to improve its handling qualities. Under these circumstances the basic airplane could be used as a backup system in case of stability augmentation system failure. An airplane with handling qualities worse than level 3 would require a highly reliable full-time stability augmentation system, since the basic airplane would not be suitable as a failure mode for a stability augmentation system failure. The satisfactory boundary in references 18 to 20 corresponds to level 1 in references 22 and 23. Reference 18 also specifies a single failure limit and reference 20 a level for safe operation, and these levels correspond approximately to level 2 in references 22 and 23.

The configurations were evaluated as conventional transport aircraft, and conventional and STOL criteria were used when available rather than VTOL criteria. When the configurations were compared with data from references 22 and 23, they were considered to be in Class II (mediumweight, low-to-medium maneuverability), Category C (approach and landing).

Longitudinal characteristics. - The pitch control power available with the three configurations is shown in figure 4 with the criteria from references 19 and 20. The values of pitch acceleration shown were calculated for the maximum available control deflection from trim in the pitchup direction, which was the more critical direction. The

EBF and AW/EBF configurations exceed the satisfactory requirements set by reference 19 and are near the minimum satisfactory level specified by reference 20. The AW/AW configuration, which had a smaller, less effective horizontal tail, does not meet the reference 20 criteria but does fall within the satisfactory range defined by reference 19.

A time history of the EBF configuration's response is shown in figure 5 for a longitudinal control step input of sufficient magnitude to reach approximately stall angle of attack. The 25 deg/sec control surface rate limit provides maximum angular acceleration in less than 0.2 second for the control deflection shown. This satisfies the reference 23 criterion, which calls for reaching the maximum angular acceleration in less than 0.3 second. Reference 18 specifies a time delay of less than 2 seconds to the point of inflection in both angular rate and normal acceleration response. The inflection point for the pitch angular rate occurs at approximately 0.2 second, and the normal acceleration inflection point occurs at approximately 1.0 second.

Another criterion for the evaluation of the normal acceleration response (ref. 21) is shown in figure 6. In this criterion the lift loss due to a longitudinal control input is compared with the pitch angular acceleration generated by that input. This criterion is a measure of the severity of the lag in the initial normal acceleration response (shown in fig. 5 during the first second) which is caused by the lift loss due to the horizontal tail deflection. These criteria indicate that the EBF and both AW configurations would have satisfactory response characteristics.

The frequency and damping characteristics of the configurations are shown in figure 7 along with criteria from references 19 and 22. Both criteria indicate that all the configurations would have satisfactory dynamic characteristics. Another criterion from reference 22, for frequency and normal acceleration sensitivity, is shown in figure 8. This criterion indicates that all the configurations exhibit a value of N_{Z_α} that is too low for satisfactory control of normal acceleration, and that some other method of producing normal acceleration would be required. However, most of the N_{Z_α} values were within the level 2 limits.

Figures 9(a) to 9(c) show the longitudinal control required for steady-state trim for two flap settings and airspeeds as a function of thrust level. The longitudinal control/speed relationship is stable, that is, increasing pull force on the column is required for decreasing speed for all the configurations. Significant trim changes accompany flap changes as well as thrust changes.

Reference 22 defines flight path stability in terms of the flight path angle change due to a speed change when speed is changed with the longitudinal control. Curves of trim flight path angle as a function of speed are shown for each configuration at approach thrust and maximum thrust in figures 10(a) and 10(b). At the lower speeds the slope of the curves is positive, which indicates flight path instability, commonly referred to as operation on the back side of the power curve. In this region a speed reduction requires an increase in thrust to remain trimmed at a constant flight path angle, and an increase in speed requires a decrease in thrust. Since this is opposite to the normal control technique, the reference 22 criterion defines the allowable values of instability in terms of the slope $\frac{\Delta\gamma}{\Delta V}$. A comparison of the slopes at the 70-knot approach speed with the

reference 22 criterion is shown in figure 10(c). All the configurations are at or beyond the level 3 boundary, indicating that a full-time speed control system would be required since the basic airplane would not be acceptable as a failure mode.

Lateral-directional characteristics.- The lateral-directional frequency and damping characteristics are shown in figure 11 along with criteria from references 19, 20, and 22. Both references 20 and 22 have a minimum frequency or stability requirement that all the configurations easily meet. Dutch-roll damping for the AW/AW configuration is less than the level 3 boundary in reference 22 and less than the single failure limit of reference 19. This indicates that the basic airplane would not be suitable as a failure mode and that a full-time augmentation system would be required. The EBF and the AW/EBF configurations were slightly better damped, but would be only marginally acceptable as a failure mode.

The roll control characteristics for four-engine operation are presented in figures 12 and 13. The time to bank to 30° (fig. 12) was calculated for a step input of the maximum wheel deflection and the aileron and spoiler rate limits shown in figure 3(b). The data shown include the effect of the ailerons and spoilers but do not include differential flap deflections for the EBF configuration or differential flap choking action for the AW configurations. The aileron/spoiler system meets the bank angle response criterion of reference 20, although it has slightly less response than that required by reference 22 for level 1 (fig. 12). The static control power of all the configurations (fig. 13) meets the maneuvering requirements of reference 20 for normal four-engine operation without crosswind. For the EBF configuration with a 30-knot crosswind, approximately one-quarter of the available roll power was required to trim to a wings-level attitude. An adequate margin of roll control power remained for maneuvering. The AW/AW configuration had a greater dihedral effect than the EBF configuration, which resulted in insufficient roll power for maneuvering while trimmed in a 30-knot crosswind. Additional roll control power would have to be provided, by, for example, the differential choking of the augmentor flap. The AW/EBF configuration, with a slightly lower dihedral effect, could be trimmed in a 30-knot crosswind with sufficient roll control remaining for maneuvering.

The engine-out moments for the AW configurations consisted only of a yawing moment produced by the net thrust which could be balanced by less than 5° of rudder. No rolling moments were produced, since a symmetrical lift distribution would be provided by proper ducting from the remaining engines. For the EBF configuration, large rolling moments were produced by the loss of an outboard engine. The control surface deflections required to trim to a constant heading are shown in figure 14. At an approach speed of 70 knots, the aileron/spoiler roll control could be used to compensate for the engine-out moment, although it would require approximately 75 percent of the total roll control power. Since the remaining roll control power would not be adequate for maneuvering, a flaperon deflection of 40° was used for engine-out trim in the approach configuration. This reduced the aileron/spoiler deflection to approximately 10 percent of that available and also resulted in a performance benefit because the drag of the flaperons was lower than that of the aileron/spoiler system.

The roll damping characteristics (fig. 15) are nominally satisfactory when compared with the criteria of references 18 and 22. Slightly greater roll damping would be desirable for normal approach conditions. The spiral characteristics are compared with criteria from references 20 and 22 in figure 16. The EBF configuration has unacceptable spiral

characteristics, with a time to double amplitude of approximately 5 seconds; however, the basic airplane characteristics would be marginally acceptable as a failure mode. The AW spiral characteristics are acceptable, although unsatisfactory for the approach power setting and satisfactory for the full power setting. The spiral instability in all the configurations is due to the relatively high directional stability compared with the dihedral effect.

The yaw control power available and that required for trim is shown in figure 17. The crosswind trim values were calculated for a 30-knot crosswind with wings level. Without crosswind, all the configurations have sufficient yaw control power to trim a critical engine-out condition and meet the maneuvering requirements of references 19 and 20. To provide sufficient yaw control power for simultaneous crosswind trim, engine-out trim, and maneuvering, all the configurations would require approximately double the yaw control power present.

Roll-yaw coupling characteristics are shown in terms of the reference 22 parameters $\frac{\Delta\beta}{\kappa}$ and ψ_β in figure 18(a) and in terms of the reference 24 parameter $\omega_\varphi/\omega_{n_d}$ in figure 18(b). The reference 22 parameters were calculated for a step input of the aileron/spoiler that would satisfy the roll requirement of 30° of bank angle change in 1.8 seconds. All the configurations fall in the unacceptable region in figure 18(a). Compared with the $\omega_\varphi/\omega_{n_d}$ summary data from reference 24 (fig. 18(b)), the EBF and AW/EBF configurations are satisfactory, and the AW/AW configuration is acceptable. The AW/AW configuration has a much lower $\omega_\varphi/\omega_{n_d}$ than the other configurations because of its higher dihedral effect. The $\omega_\varphi/\omega_{n_d}$ comparison may not be entirely valid, since the reference 24 data shown can be generally applied only when $\zeta_\varphi \approx \zeta_d$, and this was not true of the configurations in this study.

A time history of the response to a roll control input is shown in figure 19. A small (6°) aileron and spoiler input generates a large sideslip angle of approximately 10°. The divergent Dutch-roll damping of the AW/AW configuration is readily apparent, as is the divergent spiral mode of the EBF configuration.

Simulator Evaluations and Control System Development

Simulator evaluation of the basic longitudinal characteristics. - The overall longitudinal characteristics of all three basic airplane configurations were given pilot ratings of 6 to 7 for the approach task. The flight path stability criterion (fig. 10(c)) indicated that control of flight path with attitude would be unacceptable, and this was confirmed during the simulator evaluations. As a result, the back side of the power curve control technique, that is, using attitude to control speed and thrust to control flight path, had to be used. This produced a somewhat unnatural condition in that trim angle of attack had to be reduced to increase the rate of climb. To go from the 6° approach glide slope to level flight, thrust had to be advanced to maximum power and angle of attack reduced approximately 4°. After becoming familiar with this control technique, however, the pilots were able to perform acceptable approaches without stability augmentation.

Pitch response was generally considered acceptable and was rated 3.5 to 4. The short-period dynamic response characteristics were acceptable, but the phugoid characteristics

dominated the dynamic responses. The phugoid for all the configurations had a nominal period of 20 seconds and was very lightly damped or unstable. A time history for the EBF configuration that is typical of other configurations is shown in figure 20. Pitch control inputs easily excited the phugoid, and the dynamic response characteristics were rated near 6 for the 70-knot approach condition. Both phugoid period and damping became more unacceptable as velocity decreased; the pilot ratings at 90 knots were 4 to 5, but at 60 knots they deteriorated to 7 to 8.

Trim changes were large and objectionable, with pilot ratings of 4 to 5 for a 50 percent to 100 percent power change for all configurations. For the EBF configuration, the trim change from takeoff flaps (30°) to landing flaps (60°) was rated 4 to 5. For the AW configurations the ratings were 5 to 6. The large trim changes were most difficult to control during the go-around, especially with an engine out. The pilot had to retrim the airplane for a climb condition during a flap and power change while retaining reasonably precise control.

Longitudinal control system. - The longitudinal control system was developed to alleviate deficiencies in the basic airplane, which included dynamic oscillations, trim changes, and flight path instability. These deficiencies were common to the EBF and AW configurations. A simple pitch rate damper proved to be ineffective because the short-period damping of the basic airplane was already high and because the pitch rate damper had little effect on the phugoid. Both pitch rate command system and a pitch rate with normal acceleration control system reduced the dynamic oscillations due to the phugoid and the trim changes due to configuration and power changes. However, a pitch attitude command system proved to be the most desirable. This system alleviated the phugoid and trim changes. In addition it acted as a speed command system when the technique of controlling speed with attitude was used. This reduced pilot workload considerably, and a pilot rating of 2 was given for the approach task with this system.

Although the pitch attitude command system made satisfactory approaches possible, it did not overcome the flight path instability problem. As a result, an autospeed control system was developed to allow the use of the normal control technique of controlling flight path with pitch attitude. In a conventional airplane an autothrottle could be used for this purpose; however, because of the lift that accompanied changes in thrust, an autothrottle did not produce the desired results. Since the third element of the inboard flap produced primarily drag changes, it was used to control speed. Before satisfactory operation could be achieved with this device, however, proportionate deflection of the spoilers was required to remove the small lift increments of the flap deflection. Operating as a direct drag device, this flap/spoiler combination provided speed control similar to that provided by a conventional autothrottle. With this system, satisfactory approaches could be made with the normal technique of controlling flight path with attitude. Manual control of the direct drag device was also evaluated, but did not prove to be as effective as using the throttles with the pitch attitude command system.

Simulator evaluation of the basic lateral-directional characteristics. - The unaugmented lateral-directional characteristics were unacceptable in the approach and were given a pilot rating of 8 to 10. Low or negative Dutch-roll damping, strong roll-yaw coupling, and a divergent spiral mode were characteristic of all the configurations. Lateral control activity (which was constantly required because of the divergent spiral) produced large directional motions which excited the Dutch-roll mode. The pilots hesitated to make large or quick roll inputs because of the large sideslips generated. The

AW configurations were slightly more objectionable to the pilots because of the divergent Dutch-roll damping, which required constant attention. In addition to these characteristics during the normal approach, the EBF configuration presented serious control problems after the loss of an engine. Although sufficient control power was available to balance the engine-out moments, large, rapid inputs were necessary which generally led to loss of control.

Lateral-directional control system.- Various feedback loops were evaluated to improve the airplane's lateral-directional characteristics, and the results were generally the same for all the configurations. The EBF configuration is used to illustrate the effects of several control system feedback loops on the airplane's lateral-directional characteristics, and a summary of the pilot ratings for these variations is shown in table 8. The lateral-directional characteristics of the basic airplane without stability augmentation were given a pilot rating of 8. A roll and yaw damper (roll rate feedback to the ailerons and yaw rate feedback to the rudder) improved the airplane's Dutch-roll damping and spiral characteristics, but it did little for the roll-yaw coupling problem. This configuration received a pilot rating of 6. The basic airplane with only a turn coordinator (roll rate feedback to the rudder) improved the roll-yaw coupling and increased the Dutch-roll damping slightly but did not improve the airplane's spiral characteristics. This configuration also received a pilot rating of 6. Either of these systems could be used as the minimum level of stability augmentation for acceptable handling qualities. With both the rate dampers and the turn coordinator, the pilot rating improved to a value of 4. To further improve the roll-yaw coupling characteristics, an improved Dutch-roll damper was used. In this damper, which was like the one described in reference 16, a bank-angle-to-rudder feedback was added to the yaw damper to approximate a sideslip rate ($\dot{\beta}$) damper. With this system the handling qualities improved to the satisfactory level (pilot ratings of 3). With the addition of an aileron-to-rudder interconnect, a further improvement was obtained (pilot ratings of 2 to 3).

Additional refinements to the stability augmentation system were necessary for the EBF engine-out condition. To provide adequate roll control power for an engine failure, the flaperons were activated as an emergency roll control device. With this system an engine failure was followed by the automatic deflection of the flaperons. The pilot provided the additional inputs through the aileron/spoiler system to correct for the transient motions. Prompt pilot action was necessary to minimize the transient motions, and a pilot rating of 10 was given for engine failure control with this system without stability augmentation. A pilot rating of 6 was given with stability augmentation. The addition of a rate command system provided some reduction of the transient response motions, but a bank angle command system proved to be better, with pilot ratings of 3 to 4 for engine failure control. A time history of an engine failure with this configuration is shown in figure 21.

Minimum speed determination.- Minimum speeds were determined on the simulator by using a deceleration rate of approximately 1 knot/sec for three- and four-engine operation. Minimum speed was defined as the 1g stall speed or the speed at which loss of control occurred in any axis. For the three-engine case, sideslip was kept at zero and bank angle was used to give constant heading.

The three- and four-engine minimum speeds for the EBF configuration are shown in figure 22(a). As expected, the minimum speed decreased with increasing thrust-to-weight ratio. At the nominal approach power ($T/W \approx 0.3$) the four-engine minimum speed was 53 knots, whereas the three-engine minimum speed was 61 knots. Since the wing with

the failed engine stalls at a lower angle of attack than the other wing, the three-engine cases stall at a lower angle of attack than the four-engine cases and are characterized by a large rolloff at stall. For thrust-to-weight ratios greater than approximately 0.25, the three-engine minimum speed was defined by loss of control in roll.

The results for the AW configurations are shown in figures 22(b) and 22(c). Since it was assumed that the flow was cross-ducted between the wings for the engine-out condition, there was negligible difference between the three- and four-engine cases at the same thrust-to-weight ratio. The minimum speeds were the result of a pitchup in the 22° to 28° angle-of-attack range, which was generally more severe with the AW/AW configuration. Because of the pitchup characteristics of the AW configurations and the rolloff characteristics of the three-engine EBF configuration, a stall warning device would be required for all the configurations.

The effect of wing loading on the minimum speed is shown in figures 23(a) and 23(b) for the four- and three-engine EBF approach configurations, respectively. At the lower thrust-to-weight ratios for the four-engine cases, the minimum speed follows the general trend of wing loading, as in conventional airplanes. At the higher thrust-to-weight ratios, wing loading had almost no effect. The three-engine minimum speeds do not show the latter trend and exhibit the conventional relationship with wing loading for all thrust-to-weight ratios.

Effect of approach speed on control system complexity. - As shown in the preceding sections, the capability for approaching at 70 knots was achieved by using a stability augmentation system that is complex compared with that used in current transport airplanes, which usually consists of only a yaw damper. As a result, the influence of approach speed (which is converted to field length in reference 13) on control system complexity was determined using the EBF 60° flap setting configuration. Some of the more important handling qualities characteristics for the basic airplane are summarized in figures 24(a) to 24(e) as a function of approach speed. The engine-out characteristics (fig. 24(b)) are shown as the bank angle change in 2 seconds due to a sudden engine failure with no pilot control input. The control system requirements are summarized in figure 25 as a function of speed and field length.

The airplane's handling qualities at an airspeed of 110 knots are typical of conventional transport airplanes. The Dutch-roll damping ratio is approximately 0.12, which is acceptable although unsatisfactory. A yaw rate damper with a washout would be necessary for satisfactory damping and turn coordination. An outboard engine failure would cause a bank angle change of approximately 15° in 2 seconds and would require approximately 25 percent of the maximum aileron/spoiler control to trim, which could be handled relatively easily with normal piloting techniques. The longitudinal control would be satisfactory with both $\frac{\Delta\gamma}{\Delta V}$ and N_{Z_α} exceeding the reference 22 level 1 requirements. The landing field length for the 110-knot approach would be approximately 1220 meters (4000 feet).

At 90 knots the handling qualities are slightly worse than at 110 knots. The Dutch-roll damping is reduced and would require further augmentation. The engine-out roll response increases from 15° in 2 seconds at 110 knots to 23° in 2 seconds, requiring approximately 45 percent of the roll control for trim. The addition of a roll rate damper would increase the Dutch-roll damping to the satisfactory level and would also

reduce the engine-out bank angle in 2 seconds to approximately 18°. In the longitudinal mode, N_{Z_α} is still satisfactory; however, flight path stability deteriorates to the unsatisfactory but acceptable level, and an autothrottle would be required for satisfactory handling qualities. The field length for the 90-knot approach would be approximately 900 meters (3000 feet).

At 80 knots the basic airplane Dutch-roll damping is unacceptable. Since turn coordination is also worse, a more complex damper with roll rate and attitude feedbacks would be necessary to improve the turn coordination as well as the Dutch-roll damping. The engine-out problem is more severe, with a bank angle in 2 seconds of 34° without roll augmentation and 27° with a roll damper. Approximately 60 percent of the roll control would be required to trim the engine-out condition. This would be unacceptable for pilot control, so a rate or attitude command control system would be required. Flight path stability has deteriorated to an unacceptable level and an autospeed stability system would be required. The value of N_{Z_α} is marginally satisfactory. The field length for the 80-knot approach would be approximately 760 meters (2500 feet).

The handling qualities at 70 knots are similar to those at 80 knots in the lateral-directional modes, with slightly higher augmentation gains required for satisfactory handling qualities. Longitudinal flight path stability has degraded beyond the level 3 requirements, and the value of N_{Z_α} is in the unsatisfactory region. An autospeed control would be required for conventional control, and the low N_{Z_α} may have to be augmented with thrust or direct lift control. The field length for the 70-knot approach would be approximately 610 meters (2000 feet).

CONCLUDING REMARKS

A simulator study was performed to evaluate the low-speed flying characteristics of a proposed 213,500-newton (48,000-pound) STOL research airplane. The airplane was configured with either an externally blown flap (EBF) wing or an augmentor wing (AW). The AW configuration was investigated with two tails, one sized for the AW configuration and a larger one sized for the EBF configuration. The emphasis of the study was on the 70-knot approach task.

Without stability augmentation, the longitudinal handling qualities of all three configurations were characterized by poor flight path control, large trim changes, and lightly damped phugoid motions and were given pilot ratings of 6 to 7. The lateral-directional handling qualities of the three configurations during the normal four-engine approach were characterized by poor Dutch-roll damping and strong roll-yaw coupling and were given pilot ratings of 8 to 10. In addition, control of the transient motion due to a sudden engine failure was difficult with the EBF configuration.

Satisfactory longitudinal handling qualities were obtained by using a pitch attitude command system and the piloting technique of controlling speed with attitude and flight path with thrust. For the conventional piloting technique of controlling speed with

thrust and flight path with attitude, automatic speed control was required. The auto-speed control used a drag device consisting of the third flap element in combination with the spoilers.

The stability augmentation required for satisfactory lateral-directional handling qualities during four-engine operation consisted of a turn coordinator and Dutch-roll damper based on sideslip rate. To reduce the transient motions resulting from a sudden engine failure with the EBF configuration, automatic deflection of the differential flaps and a roll attitude command system were required.

The stall behavior was characterized by pitchup for the AW configurations and a rapid rolloff for the three-engine EBF configuration. A stall warning system would be required for each configuration.

The handling characteristics of the EBF and AW configurations were similar. It appeared that a configuration that incorporated the EBF lift concept could be converted to one that incorporated the AW lift concept by changing only the wing/engine assembly, using the same fuselage and the EBF tail. The handling characteristics of the AW configuration with the EBF tail were better than those of the configuration with the smaller AW tail because of the lower effective dihedral and the additional longitudinal control power.

Flight Research Center,
National Aeronautics and Space Administration,
Edwards, Calif., Aug. 24, 1973

REFERENCES

1. Anon.: Civil Aviation Research and Development Policy Study. NASA SP-265, 1971.

2. Campbell, John P.; and Johnson, Joseph L., Jr.: Wind-Tunnel Investigation of an External-Flow Jet-Augmented Slotted Flap Suitable for Application to Airplanes With Pod-Mounted Jet Engines. NACA TN 3898, 1956.

3. Parlett, Lysle P.; Fink, Marvin P.; and Freeman, Delma C., Jr.: Wind-Tunnel Investigation of a Large Jet Transport Model Equipped With an External-Flow Jet Flap. NASA TN D-4928, 1968.

4. Freeman, Delma C., Jr.; Grafton, Sue B.; and D' Amato, Richard: Static and Dynamic Stability Derivatives of a Model of a Jet Transport Equipped With External-Flow Jet-Augmented Flaps. NASA TN D-5408, 1969.

5. Parlett, Lysle P.; Greer, H. Douglas; Henderson, Robert L.; and Carter, C. Robert: Wind-Tunnel Investigation of an External-Flow Jet-Flap Transport Configuration Having Full-Span Triple-Slotted Flaps. NASA TN D-6391, 1971.

6. Grafton, Sue B.; Parlett, Lysle P.; and Smith, Charles C., Jr.: Dynamic Stability Derivatives of a Jet Transport Configuration With High Thrust-Weight Ratio and an Externally Blown Jet Flap. NASA TN D-6440, 1971.

7. Koenig, David G.; Corsiglia, Victor R.; and Morelli, Joseph P.: Aerodynamic Characteristics of a Large-Scale Model With an Unswept Wing and Augmented Jet Flap. NASA TN D-4610, 1968.

8. Cook, Anthony M.; and Aiken, Thomas N.: Low Speed Aerodynamic Characteristics of a Large Scale STOL Transport Model With an Augmented Jet Flap. NASA TM X-62017, 1971.

9. Falarski, Michael D.; and Koenig, David G.: Aerodynamic Characteristics of a Large-Scale Model With a Swept Wing and Augmented Jet Flap. NASA TM X-62,029, 1971.

10. Grantham, William D.; Deal, Perry L.; and Sommer, Robert W.: Simulator Study of the Instrument Landing Approach of a Heavy Subsonic Jet Transport With an External-Flow Jet-Flap System Used for Additional Lift. NASA TN D-5862, 1970.

11. Grantham, William D.; Sommer, Robert W.; and Deal, Perry L.: Simulator Study of Flight Characteristics of a Jet-Flap STOL Transport Airplane During Approach and Landing. NASA TN D-6225, 1971.

12. Grantham, William D.; Nguyen, Luat T.; Patton, James M., Jr.; Deal, Perry L.; Champine, Robert A.; and Carter, C. Robert: Fixed Base Simulator Study of an Externally Blown Flap STOL Transport Airplane During Approach and Landing. NASA TN D-6898, 1972.

13. Washington, Harold P.; and Gibbons, John T.: Analytical Study of Takeoff and Landing Performance for a Jet STOL Transport Configuration With Full-Span, Externally Blown, Triple-Slotted Flaps. NASA TN D-7441, 1973.

14. Mechtly, E. A.: The International System of Units - Physical Constants and Conversion Factors (Revised). NASA SP-7012, 1969.

15. Anon.: USAF Stability and Control Datcom. Air Force Flight Dynamics Lab., Wright-Patterson Air Force Base, Oct. 1960 (rev. Aug. 1968).

16. Quigley, Hervey C.; Innis, Robert C.; Vomaske, Richard F.; and Ratcliff, Jack W: A Flight and Simulator Study of Directional Augmentation Criteria for a Four-Propellered STOL Airplane. NASA TN D-3909, 1967.

17. Cooper, George E.; and Harper, Robert P., Jr.: The Use of Pilot Rating in the Evaluation of Aircraft Handling Qualities. NASA TN D-5153, 1969.

18. Anon.: Recommendations for V/STOL Handling Qualities With an Addendum Containing Comments on the Recommendations. AGARD Rept. 408A, Oct. 1964.

19. Anon.: V/STOL Handling-Qualities Criteria—I - Criteria and Discussion. AGARD Rept. No. 577, Dec. 1970.

20. Innis, Robert C.; Holzhauser, Curt A.; and Quigley, Hervey C.: Airworthiness Considerations for STOL Aircraft. NASA TN D-5594, 1970.

21. Condit, Philip M.; Kimbrel, Laddie G.; and Root, Robert G.: Inflight and Ground-Based Simulation of Handling Qualities of Very Large Airplanes in Landing Approach. NASA CR-635, 1966.

22. Anon.: Flying Qualities of Piloted Airplanes. Military Specification MIL-F-8785B (ASG), Aug. 7, 1969.

23. Anon.: Flying Qualities of Piloted V/STOL Aircraft. Military Specification MIL-F-83300, Dec. 31, 1970.

24. Ashkenas, I. L.: A Consolidation of Lateral-Directional Handling Qualities. AIAA Paper No. 65-314, July 26-29, 1965.

TABLE 1.- PHYSICAL CHARACTERISTICS OF THE AIRPLANE CONFIGURATIONS

	EBF	AW
Wing -		
Area, m^2 (ft^2)	55.7 (600)	55.7 (600)
Aspect ratio	7.3	8.0
Span, m (ft)	20.2 (66.2)	21.1 (69.3)
Taper ratio	0.34	0.30
Sweep at quarter chord, deg	27.5	27.5
Dihedral, deg	-3.5	0
Incidence at mean aerodynamic chord, deg	4.5	0
Root thickness, percent chord	14	12.5
Tip thickness, percent chord	11	10.5
Mean aerodynamic chord, m (ft)	3.0 (9.8)	2.9 (9.5)
Airfoil section:		
Root	NACA 63_2-A214	RAE 104
Tip	NACA 63_2-A211	RAE 105
Flap hinge axis, percent chord	7.80	68.5
Travel, deg	0 to 60	0 to 71
Ailerons -		
Span, percent semispan	28.1	9.4
Hinge axis, percent chord	78.0	68.0
Travel, deg	0 to 60	-10 to 45
Spoilers -		
Span, percent semispan	57	9
Percent chord	10	10.5
Deflection, deg	0 to 60	0 to 60
Horizontal tail -		
Area, m^2 (ft^2)	19.0 (205)	14.8 (159)
Aspect ratio	5.3	4.5
Span, m (ft)	10.1 (33)	8.1 (26.5)
Sweep at leading edge, deg	29	25
Dihedral, deg	3.5	0
Elevator hinge axis, percent chord	73	60
Elevator travel, deg	-10 to 50	±30
Tail incidence, deg	±10	±10
Volume coefficient	1.0	0.99
Tail arm length, m (ft)	9.75 (28.7)	10.9 (35.8)
Vertical tail -		
Area, m^2 (ft^2)	11.1 (120)	8.1 (87)
Aspect ratio	1.66	1.4
Volume coefficient	0.09	0.075
Rudder hinge axis, percent chord	57	60
Rudder travel, deg	±45	±45
Engine location -		
Inboard, percent semispan	22	22
Outboard, percent semispan	42	42

TABLE 2. - WEIGHT AND INERTIAL CHARACTERISTICS OF THE AIRPLANE CONFIGURATIONS

	Configuration		
	EBF	AW/AW	AW/EBF
Weight, N (lb)	213,500 (48,000)	213,500 (48,000)	213,500 (48,000)
Center of gravity, percent $\bar{c}$	40	25	25
I_X, kg-m^2 (slug-ft^2)	289,000 (213,000)	291,000 (215,000)	290,000 (214,000)
I_Y, kg-m^2 (slug-ft^2)	315,000 (232,500)	312,000 (230,400)	314,000 (232,000)
I_Z, kg-m^2 (slug-ft^2)	546,000 (402,500)	542,000 (399,500)	544,000 (401,000)
I_{XZ}, kg-m^2 (slug-ft^2)	42,200 (31,150)	35,300 (26,000)	39,000 (28,800)

TABLE 3.- AERODYNAMIC COEFFICIENTS FOR THE EBF CONFIGURATION WITH 60° FLAPS

Coefficient	C_μ	α, deg						
		-10.0	-2.0	6.0	12.0	18.0	24.0	28.0
C_m	0	.640	.130	-.270	-.400	-.320	-.260	-.280
	.97	.380	-.040	-.400	-.530	-.540	-.460	-.380
	1.93	.080	-.240	-.530	-.680	-.780	-.680	-.500
	2.90	-.220	-.460	-.720	-.840	-.990	-.910	-.710
	3.85	-.540	-.710	-.900	-1.100	-1.210	-1.200	-1.110
C_L	0	-.100	1.000	2.100	2.300	2.200	2.000	1.810
	.97	1.900	3.150	4.100	4.500	4.490	3.600	3.150
	1.93	3.000	4.150	5.320	5.800	6.100	5.450	4.500
	2.90	3.710	4.900	6.150	6.850	7.350	7.100	6.250
	3.85	4.200	5.550	6.900	7.700	8.400	8.800	8.150
C_D	0	.250	.325	.500	.650	.875	1.080	1.140
	.97	-.120	.250	.600	.930	1.240	1.340	1.410
	1.93	-.470	.125	.640	1.125	1.520	1.640	1.720
	2.90	-.800	-.410	.525	1.120	1.680	1.970	2.080
	3.85	-1.125	-.425	.325	.975	1.750	2.350	2.600
$\frac{\partial C_m}{\partial\left(\frac{q\bar{c}}{2V}\right)}$	0	-17.0	-36.0	-37.0	-27.0	-8.0	-6.0	-14.0
	.97	-26.0	-37.0	-46.0	-38.0	-16.0	-25.0	-30.0
	1.93	-34.0	-38.0	-54.0	-47.0	-33.0	-43.0	-46.0
	2.90	-36.0	-38.0	-53.0	-47.0	-37.0	-40.0	-50.0
	3.85	-38.0	-38.0	-52.0	-47.0	-41.0	-38.0	-54.0
$\frac{\partial C_m}{\partial \delta_h}$, deg^{-1}	0	-.1088	-.1038	-.0576	-.0240	-.0100	-.0040	.0010
	.97	-.0940	-.1325	-.1045	-.0730	-.0445	-.0180	-.0190
	1.93	-.0814	-.1350	-.1424	-.1084	-.0730	-.0360	-.0380
	2.90	-.0855	-.1370	-.1535	-.1310	-.0920	-.0580	-.0580
	3.85	-.1010	-.1398	-.1482	-.1340	-.0960	-.0720	-.0720
$\frac{\partial C_L}{\partial \delta_h}$, deg^{-1}	0	.0600	.0344	.0396	.0286	.0400	-.0050	.0050
	.97	.0290	.0460	.0520	.0440	.0430	-.0120	-.0100
	1.93	.0350	.0570	.0570	.0500	.0440	.0100	-.0100
	2.90	.0490	.0650	.0570	.0540	.0355	.0260	.0050
	3.85	.0710	.0700	.0640	.0480	.0446	.0410	.0120
$\frac{\partial C_D}{\partial \delta_h}$, deg^{-1}	0	.0090	.0070	.0100	.0180	.0195	.0075	.0080
	.97	-.0060	.0075	.0120	.0160	.0240	.0150	.0130
	1.93	-.0075	.0125	.0150	.0220	.0265	.0150	.0110
	2.90	-.0080	.0150	.0160	.0220	.0265	.0215	.0155
	3.85	-.0040	.0160	.0155	.0200	.0250	.0250	.0215

TABLE 3.- AERODYNAMIC COEFFICIENTS FOR THE EBF CONFIGURATION WITH 60° FLAPS - Continued

Coefficient	C_μ	α, deg						
		-10.0	-2.0	6.0	12.0	18.0	24.0	28.0
$\frac{\partial C_l}{\partial \delta_a}$, deg^{-1}	0	.00050	.00070	.00080	.00060	.00040	.00040	.00040
	.97	.00080	.00110	.00160	.00130	.00080	.00080	.00080
	1.93	.00120	.00170	.00200	.00180	.00110	.00100	0.00000
	2.90	.00200	.00240	.00260	.00250	.00180	.00010	0.00000
	3.85	.00250	.00300	.00330	.00330	.00250	.00000	0.00000
$\frac{\partial C_n}{\partial \delta_a}$, deg^{-1}	0	.00013	.00023	.00033	.00055	.00057	.00080	.00180
	.97	.00006	.00030	.00030	.00035	.00035	.00150	.00150
	1.93	.00000	.00030	.00030	.00012	.00012	.00007	.00007
	2.90	-.00010	-.00010	.00020	.00007	.00015	.00015	.00015
	3.85	-.00019	-.00015	-.00012	.00000	.00000	.00000	.00000
$\frac{\partial C_Y}{\partial \delta_a}$, deg^{-1}	0	.00000	-.00050	-.00050	-.00050	-.00050	-.00020	.00000
	.97	-.00030	-.00050	-.00050	-.00050	-.00050	-.00070	-.00080
	1.93	-.00080	-.00050	-.00050	-.00050	-.00050	-.00070	-.00080
	2.90	-.00100	-.00050	-.00050	-.00050	-.00050	-.00070	-.00120
	3.85	-.00130	-.00050	-.00050	-.00050	-.00050	-.00070	-.00150
$\frac{\partial C_l}{\partial \delta_r}$, deg^{-1}	0	.00263	.00210	.00188	.00231	.00270	.00195	.00045
	.97	.00200	.00170	.00150	.00168	.00185	.00143	.00088
	1.93	.00138	.00130	.00113	.00105	.00100	.00090	.00130
	2.90	.00088	.00105	.00095	.00082	.00080	.00070	-.00013
	3.85	.00038	.00080	.00078	.00060	.00060	.00050	-.00155
$\frac{\partial C_n}{\partial \delta_r}$, deg^{-1}	0	-.00375	-.00338	-.00277	-.00240	-.00190	-.00087	.00026
	.97	-.00400	-.00375	-.00347	-.00325	-.00295	-.00250	-.00187
	1.93	-.00425	-.00412	-.00417	-.00410	-.00400	-.00413	-.00400
	2.90	-.00500	-.00500	-.00512	-.00535	-.00527	-.00495	-.00475
	3.85	-.00575	-.00588	-.00607	-.00660	-.00645	-.00577	-.00550
$\frac{\partial C_Y}{\partial \delta_r}$, deg^{-1}	0	.01250	.01250	.01025	.00900	.00825	.00500	.00275
	.97	.01150	.01150	.01050	.00975	.00950	.00850	.00700
	1.93	.01050	.01050	.01075	.01050	.01075	.01200	.01125
	2.90	.01000	.01100	.01350	.01425	.01450	.01500	.01525
	3.85	.00950	.01150	.01625	.01800	.01825	.01800	.01925

TABLE 3.- AERODYNAMIC COEFFICIENTS FOR THE EBF CONFIGURATION WITH 60° FLAPS - Continued

Coefficient	C_μ	α, deg						
		-10.0	-2.0	6.0	12.0	18.0	24.0	28.0
$\frac{\partial C_l}{\partial \delta_{sp}}$, deg^{-1}	0	.00070	.00090	.00120	.00110	.00080	.00020	.00000
	.97	.00150	.00150	.00150	.00150	.00150	.00040	.00000
	1.93	.00220	.00220	.00220	.00220	.00220	.00060	.00000
	2.90	.00220	.00220	.00220	.00220	.00220	.00100	.00050
	3.85	.00220	.00220	.00220	.00220	.00220	.00190	.00100
$\frac{\partial C_n}{\partial \delta_{sp}}$, deg^{-1}	0	.00037	.00037	.00037	.00025	.00013	.00000	.00000
	.97	.00037	.00037	.00041	.00032	.00021	.00000	.00000
	1.93	.00037	.00037	.00044	.00040	.00029	.00000	.00000
	2.90	.00037	.00037	.00047	.00048	.00033	.00020	.00000
	3.85	.00037	.00037	.00050	.00055	.00037	.00037	.00037
$\frac{\partial C_Y}{\partial \delta_{sp}}$, deg^{-1}	0	.00000	-.00080	-.00120	-.00120	-.00120	-.00060	.00000
	.97	.00000	-.00080	-.00120	-.00120	-.00120	-.00060	.00000
	1.93	.00000	-.00080	-.00120	-.00120	-.00120	-.00060	.00000
	2.90	.00000	-.00080	-.00120	-.00120	-.00120	-.00060	.00000
	3.85	.00000	-.00080	-.00120	-.00120	-.00120	-.00060	.00000
$\frac{\partial C_m}{\partial \delta_{sp}}$, deg^{-1}	0	.00000	-.00133	.00000	.00133	.00167	.00133	.00000
	.97	.00110	.00033	.00075	.00093	.00130	-.00017	.00000
	1.93	.00233	.00167	-.00150	.00083	.00116	-.00067	.00000
	2.90	.00167	.00067	-.00116	.00033	.00017	-.00133	.00000
	3.85	-.00150	.00050	.00100	-.00017	-.00100	-.00183	.00000
$\frac{\partial C_L}{\partial \delta_{sp}}$, deg^{-1}	0	.00333	-.00667	-.00667	-.00667	-.00333	-.00167	.00000
	.97	.00133	-.00917	-.00950	-.00883	-.00530	-.00300	-.00133
	1.93	.00033	-.01160	-.01000	-.01160	-.00750	-.00750	-.00300
	2.90	.00050	-.01000	-.01000	-.01160	-.00916	-.00583	.00083
	3.85	.00133	.00116	-.00667	-.00867	-.00925	-.01030	.00000
$\frac{\partial C_D}{\partial \delta_{sp}}$, deg^{-1}	0	.00100	.00100	.00050	.00000	-.00033	-.00033	.00000
	.97	.00133	.00116	.00017	-.00033	-.00067	-.00017	.00083
	1.93	.00150	.00133	-.00008	-.00050	-.00083	.00000	.00150
	2.90	.00167	.00200	.00200	.00100	.00017	.00000	.00000
	3.85	.00167	.00167	.00067	-.00017	-.00067	.00000	.00000

TABLE 3.- AERODYNAMIC COEFFICIENTS FOR THE EBF CONFIGURATION WITH 60° FLAPS - Continued

Coefficient	C_μ	α, deg						
		-10.0	-2.0	6.0	12.0	18.0	24.0	28.0
$\frac{\partial C_l}{\partial \beta}$	0	.0027	-.0035	-.0060	-.0052	-.0032	-.0024	-.0027
	.97	-.0001	-.0035	-.0058	-.0056	-.0051	-.0065	-.0088
	1.93	-.0030	-.0035	-.0055	-.0061	-.0070	-.0106	-.0150
	2.90	-.0025	-.0041	-.0052	-.0072	-.0077	-.0116	-.0160
	3.85	-.0020	-.0047	-.0049	-.0084	-.0084	-.0125	-.0170
$\frac{\partial C_n}{\partial \beta}$	0	.0035	.0043	.0042	.0041	.0044	.0024	.0002
	.97	.0045	.0055	.0059	.0059	.0078	.0048	.0027
	1.93	.0055	.0068	.0077	.0078	.0073	.0072	.0053
	2.90	.0055	.0071	.0080	.0078	.0079	.0079	.0066
	3.85	.0055	.0075	.0083	.0077	.0086	.0086	.0080
$\frac{\partial C_Y}{\partial \beta}$	0	-.0250	-.0250	-.0250	-.0240	-.0280	-.0260	-.0230
	.97	-.0325	-.0350	-.0375	-.0375	-.0380	-.0375	-.0305
	1.93	-.0400	-.0450	-.0500	-.0510	-.0480	-.0490	-.0380
	2.90	-.0425	-.0500	-.0520	-.0515	-.0500	-.0540	-.0500
	3.85	-.0450	-.0540	-.0540	-.0520	-.0520	-.0590	-.0620
$\frac{\partial C_l}{\partial \left(\frac{pb}{2V}\right)}$	0	-.560	-.800	-.520	-.140	-.360	-.150	-.180
	.97	-.700	-.740	-.400	-.280	-.250	.020	.010
	1.93	-.840	-.680	-.280	-.420	-.130	.180	.200
	2.90	-.810	-.640	-.280	-.440	-.280	.140	.220
	3.85	-.780	-.590	-.280	-.460	-.440	.100	.240
$\frac{\partial C_n}{\partial \left(\frac{pb}{2V}\right)}$	0	-.070	-.050	-.170	-.160	-.180	-.100	-.060
	.97	-.100	-.120	-.210	-.250	-.280	-.220	-.180
	1.93	-.120	-.180	-.240	-.320	-.380	-.300	-.260
	2.90	-.130	-.210	-.250	-.360	-.460	-.380	-.270
	3.85	-.140	-.240	-.270	-.380	-.520	-.460	-.280
$\frac{\partial C_l}{\partial \left(\frac{rb}{2V}\right)}$	0	.320	.570	.800	.880	.950	.480	.480
	.97	.410	.660	.820	.850	.780	.510	.470
	1.93	.500	.760	.840	.820	.620	.540	.470
	2.90	.430	.780	.830	.780	.720	.440	.340
	3.85	.360	.800	.820	.740	.820	.340	.220
$\frac{\partial C_n}{\partial \left(\frac{rb}{2V}\right)}$	0	-.360	-.300	-.310	-.380	-.330	-.440	-.340
	.97	-.280	-.320	-.340	-.390	-.400	-.490	-.340
	1.93	-.220	-.340	-.360	-.400	-.460	-.530	-.340
	2.90	-.210	-.410	-.420	-.410	-.460	-.550	-.470
	3.85	-.200	-.480	-.480	-.420	-.470	-.570	-.600

TABLE 3.- AERODYNAMIC COEFFICIENTS FOR THE EBF CONFIGURATION WITH 60° FLAPS - Continued

Coefficient	C_μ	α, deg						
		-10.0	-2.0	6.0	12.0	18.0	24.0	28.0
$\frac{\partial C_l}{\partial \delta_f}$, deg^{-1}	0	.00050	.00050	.00075	.00175	.00225	.00325	.00350
	.97	.00150	.00195	.00280	.00320	.00320	.00400	.00400
	1.93	.00225	.00275	.00375	.00400	.00375	.00450	.00475
	2.90	.00285	.00365	.00520	.00515	.00600	.00650	.00850
	3.85	.00350	.00450	.00650	.00625	.00825	.00875	.01125
$\frac{\partial C_n}{\partial \delta_f}$, deg^{-1}	0	.00010	.00010	.00040	.00050	.00050	.00060	.00090
	.97	.00000	.00019	.00045	.00050	.00050	.00045	.00050
	1.93	-.00005	.00025	.00050	.00050	.00050	.00030	.00025
	2.90	-.00008	.00075	.00075	.00100	.00100	.00030	-.00002
	3.85	-.00050	.00090	.00105	.00150	.00150	.00030	-.00030
$\frac{\partial C_Y}{\partial \delta_f}$, deg^{-1}	0	.00250	-.00150	-.00250	-.00250	-.00250	-.00250	-.00350
	.97	-.00450	-.00700	-.00800	-.00550	-.00600	-.00550	-.00600
	1.93	-.00800	-.01150	-.01150	-.00900	-.00850	-.00800	-.00750
	2.90	-.01350	-.01700	-.01550	-.01250	-.01250	-.01250	-.01300
	3.85	-.01850	-.02250	-.01900	-.01600	-.01700	-.01750	-.01850
$\frac{\partial C_m}{\partial \delta_{ddc}}$, deg^{-1}	0	.00500	.00200	.00300	.00250	.00300	.00250	.00400
	.97	.00500	.00150	.00250	.00300	.00300	.00200	.00300
	1.93	.00500	.00100	.00250	.00350	.00300	.00200	.00150
	2.90	.00500	.00150	.00350	.00350	.00200	.00100	.00100
	3.85	.00500	.00200	.00450	.00400	.00150	.00000	.00100
$\frac{\partial C_L}{\partial \delta_{ddc}}$, deg^{-1}	0	.00500	.00350	.00500	.00500	.01000	.01000	.01500
	.97	.01750	.01250	.01250	.01150	.01250	.01000	.01500
	1.93	.03000	.02250	.02500	.01750	.01500	.01000	.01500
	2.90	.03500	.02250	.02500	.02000	.01750	.01250	.01250
	3.85	.04250	.03250	.02750	.02250	.02000	.01500	.01000
$\frac{\partial C_D}{\partial \delta_{ddc}}$, deg^{-1}	0	.00500	.00500	.00500	.00500	.00500	.00500	.00500
	.97	.01750	.01250	.01150	.01250	.01250	.01250	.01250
	1.93	.02750	.02000	.01750	.02000	.02000	.02000	.01750
	2.90	.02750	.02500	.02500	.02500	.03000	.02750	.02750
	3.85	.02750	.03000	.03250	.03250	.03750	.03500	.03500

TABLE 3.- AERODYNAMIC COEFFICIENTS FOR THE EBF CONFIGURATION WITH 60° FLAPS - Concluded

Coefficient (engine out)	C_μ	α, deg						
		-10.0	-2.0	6.0	12.0	18.0	24.0	28.0
ΔC_l	0	0	0	0	0	0	0	0
	.97	-.073	-.070	-.086	-.089	-.114	-.092	-.072
	1.93	-.122	-.128	-.154	-.161	-.209	-.201	-.173
	2.90	-.154	-.178	-.208	-.222	-.292	-.327	-.299
	3.85	-.185	-.226	-.261	-.281	-.409	-.449	-.422
ΔC_n	0	0	0	0	0	0	0	0
	.97	-.030	-.030	-.030	-.024	-.037	-.033	-.028
	1.93	-.054	-.056	-.059	-.054	-.071	-.065	-.055
	2.90	-.075	-.081	-.087	-.088	-.105	-.097	-.084
	3.85	-.095	-.106	-.114	-.122	-.138	-.128	-.111
ΔC_Y	0	0	0	0	0	0	0	0
	.97	.100	.110	.100	.080	.080	.070	.090
	1.93	.180	.180	.150	.140	.150	.150	.160
	2.90	.230	.210	.180	.180	.210	.250	.270
	3.85	.290	.250	.210	.230	.260	.340	.370
ΔC_m	0	0	0	0	0	0	0	0
	.97	-.02	-.05	.08	.14	.13	.06	.01
	1.93	.16	0.00	.16	.25	.22	.14	-.08
	2.90	.20	.08	.18	.15	.26	.20	.18
	3.85	.24	.16	.20	.24	.26	.25	.17
ΔC_L	0	0	0	0	0	0	0	0
	.97	.15	-.10	-.15	-.05	-.45	-.80	-.30
	1.93	.05	-.20	-.35	-.15	-.52	-.80	-.60
	2.90	.10	-.20	-.35	-.22	-.30	-.60	-1.10
	3.85	.15	-.15	-.35	-.20	-.05	-.55	-1.50
ΔC_D	0	0	0	0	0	0	0	0
	.97	.05	.02	.02	0.00	-.20	-.14	-.10
	1.93	.13	.08	-.02	0.00	-.12	-.08	-.05
	2.90	.16	.08	.05	-.05	.08	-.10	-.17
	3.85	.20	-.05	.05	.55	.25	-.26	-.50

TABLE 4.- AERODYNAMIC COEFFICIENTS FOR THE AW/AW CONFIGURATION WITH 71° FLAPS

Coefficient	C_μ	α, deg						
		-10.0	-2.0	6.0	12.0	18.0	24.0	28.0
C_m	0	1.120	.800	.440	.220	.080	-.130	-.250
	.36	.440	.270	.110	-.020	-.230	-.530	-.680
	.77	.170	-.060	-.270	-.390	-.630	-1.000	-1.270
	1.10	-.040	-.270	-.490	-.660	-.830	-1.130	-1.280
	1.47	-.250	-.480	-.720	-.910	-1.070	-1.290	-1.470
C_L	0	-.440	.770	1.240	1.660	2.000	2.290	2.400
	.36	2.020	2.620	3.180	3.620	4.000	4.350	4.440
	.77	3.050	3.900	4.720	5.200	5.670	5.790	5.900
	1.10	3.470	4.350	5.200	5.830	6.280	6.490	6.500
	1.47	4.050	4.920	5.820	6.520	7.100	7.180	7.310
C_D	0	.260	.280	.300	.320	.370	.440	.540
	.36	.170	.250	.370	.500	.640	.810	.920
	.77	.010	.240	.510	.750	1.030	1.240	1.410
	1.10	-.190	.120	.470	.760	1.070	1.360	1.560
	1.47	-.250	.060	.460	.840	1.300	1.620	1.820
$\frac{\partial C_m}{\partial\left(\frac{q\bar{c}}{2V}\right)}$	0	-11.3	-24.0	-24.7	-18.0	0	-4.0	-9.3
	.36	-17.3	-24.7	-30.7	-25.3	-10.7	-16.7	-20.0
	.77	-22.6	-25.3	-36.0	-31.4	-22.0	-28.7	-30.7
	1.10	-24.0	-25.3	-35.4	-31.4	-24.7	-26.7	-33.3
	1.47	-25.3	-25.3	-34.7	-31.4	-27.4	-25.3	-36.0
$\frac{\partial C_m}{\partial \delta_h}$, deg^{-1}	0	-.0436	-.0629	-.0751	-.0808	-.0787	-.0787	-.0932
	.36	-.0442	-.0662	-.0788	-.0850	-.0862	-.0908	-.0981
	.77	-.0548	-.0713	-.0875	-.1000	-.1128	-.1050	-.1000
	1.10	-.0550	-.0730	-.0905	-.1035	-.1160	-.1110	-.1030
	1.47	-.0560	-.0750	-.0930	-.1068	-.1200	-.1130	-.1040
$\frac{\partial C_L}{\partial \delta_h}$, deg^{-1}	0	.0157	.0244	.0332	.0386	.0422	.0435	.0435
	.36	.0135	.0223	.0306	.0360	.0400	.0420	.0425
	.77	.0126	.0211	.0290	.0341	.0382	.0407	.0410
	1.10	.0117	.0200	.0275	.0326	.0365	.0385	.0387
	1.47	.0100	.0173	.0240	.0286	.0323	.0346	.0350
$\frac{\partial C_D}{\partial \delta_h}$, deg^{-1}	0	-.0139	-.0095	.0009	.0120	.0080	.0040	.0150
	.36	-.0139	-.0084	.0020	.0120	.0091	.0073	.0194
	.77	-.0128	-.0062	.0053	.0153	.0124	.0205	.0391
	1.10	-.0238	-.0117	-.0040	-.0042	.0060	.0141	.0207
	1.47	-.0084	-.0084	-.0040	-.0031	.0126	.0339	.0053

TABLE 4.- AERODYNAMIC COEFFICIENTS FOR THE AW/AW CONFIGURATION WITH 71° FLAPS - Continued

Coefficient	C_μ	α, deg						
		-10.0	-2.0	6.0	12.0	18.0	24.0	28.0
$\frac{\partial C_l}{\partial \delta_a}$, deg^{-1}	0	.00100	.00145	.00192	.00217	.00250	.00284	.00484
	.36	.00100	.00145	.00192	.00217	.00250	.00284	.00484
	.77	.00100	.00145	.00192	.00217	.00250	.00284	.00484
	1.10	.00100	.00145	.00192	.00217	.00250	.00284	.00484
	1.47	.00100	.00145	.00192	.00217	.00250	.00284	.00484
$\frac{\partial C_n}{\partial \delta_a}$, deg^{-1}	0	.00042	.00037	.00033	.00012	.00003	.00000	-.00033
	.36	.00042	.00037	.00033	.00012	.00003	.00000	-.00033
	.77	.00042	.00037	.00033	.00012	.00003	.00000	-.00033
	1.10	.00042	.00037	.00033	.00012	.00003	.00000	-.00033
	1.47	.00042	.00037	.00033	.00012	.00003	.00000	-.00033
$\frac{\partial C_Y}{\partial \delta_a}$, deg^{-1}	0	-.00025	-.00050	-.00092	-.00108	-.00167	-.00266	-.00400
	.36	-.00025	-.00050	-.00092	-.00108	-.00167	-.00266	-.00400
	.77	-.00025	-.00050	-.00092	-.00108	-.00167	-.00266	-.00400
	1.10	-.00025	-.00050	-.00092	-.00108	-.00167	-.00266	-.00400
	1.47	-.00025	-.00050	-.00092	-.00108	-.00167	-.00266	-.00400
$\frac{\partial C_l}{\partial \delta_r}$, deg^{-1}	0	.00170	.00140	.00120	.00150	.00180	.00130	.00030
	.36	.00130	.00110	.00100	.00110	.00120	.00100	.00060
	.77	.00090	.00080	.00080	.00070	.00060	.00060	.00090
	1.10	.00060	.00070	.00080	.00060	.00040	.00050	-.00009
	1.47	.00020	.00040	.00040	.00040	.00040	.00030	-.00100
$\frac{\partial C_n}{\partial \delta_r}$, deg^{-1}	0	-.00220	-.00220	-.00180	-.00160	-.00120	-.00060	-.00018
	.36	-.00320	-.00240	-.00210	-.00210	-.00200	-.00170	-.00120
	.77	-.00330	-.00280	-.00300	-.00280	-.00300	-.00280	-.00280
	1.10	-.00360	-.00330	-.00330	-.00320	-.00320	-.00310	-.00290
	1.47	-.00370	-.00350	-.00410	-.00330	-.00420	-.00340	-.00310
$\frac{\partial C_Y}{\partial \delta_r}$, deg^{-1}	0	.00800	.00800	.00700	.00600	.00500	.00400	.00180
	.36	.00750	.00750	.00700	.00620	.00630	.00630	.00500
	.77	.00700	.00700	.00700	.00680	.00710	.00800	.00900
	1.10	.00650	.00740	.01000	.01280	.00980	.01000	.01100
	1.47	.00610	.00750	.01200	.01350	.01200	.01200	.01300

TABLE 4.- AERODYNAMIC COEFFICIENTS FOR THE AW/AW CONFIGURATION WITH 71° FLAPS - Continued

Coefficient	C_μ	α, deg						
		-10.0	-2.0	6.0	12.0	18.0	24.0	28.0
$\frac{\partial C_l}{\partial \delta_{sp}}$, deg^{-1}	0	.00217	.00214	.00180	.00140	.00080	.00013	-.00033
	.36	.00217	.00214	.00180	.00140	.00080	.00013	-.00033
	.77	.00217	.00214	.00180	.00140	.00080	.00013	-.00033
	1.10	.00217	.00214	.00180	.00140	.00080	.00013	-.00033
	1.47	.00217	.00214	.00180	.00140	.00080	.00013	-.00033
$\frac{\partial C_n}{\partial \delta_{sp}}$, deg^{-1}	0	.00011	-.00020	-.00053	-.00070	-.00043	-.00047	-.00047
	.36	.00011	-.00020	-.00053	-.00070	-.00043	-.00047	-.00047
	.77	.00011	-.00020	-.00053	-.00070	-.00043	-.00047	-.00047
	1.10	.00011	-.00020	-.00053	-.00070	-.00043	-.00047	-.00047
	1.47	.00011	-.00020	-.00053	-.00070	-.00043	-.00047	-.00047
$\frac{\partial C_Y}{\partial \delta_{sp}}$, deg^{-1}	0	-.00116	-.00116	.00000	.00041	.00066	.00106	.00106
	.36	-.00116	-.00116	.00000	.00041	.00066	.00106	.00106
	.77	-.00116	-.00116	.00000	.00041	.00066	.00106	.00106
	1.10	-.00116	-.00116	.00000	.00041	.00066	.00106	.00106
	1.47	-.00116	-.00116	.00000	.00041	.00066	.00106	.00106
$\frac{\partial C_m}{\partial \delta_{sp}}$, deg^{-1}	0	.00300	.00533	.00500	.00467	.00566	.00700	.00733
	.36	.00300	.00533	.00500	.00467	.00566	.00700	.00733
	.77	.00300	.00533	.00500	.00467	.00566	.00700	.00733
	1.10	.00300	.00533	.00500	.00467	.00566	.00700	.00733
	1.47	.00300	.00533	.00500	.00467	.00566	.00700	.00733
$\frac{\partial C_L}{\partial \delta_{sp}}$, deg^{-1}	0	-.00200	-.00333	-.00500	-.00583	-.00633	-.00500	-.01500
	.36	-.00200	-.00333	-.00500	-.00583	-.00633	-.00500	-.01500
	.77	-.00200	-.00333	-.00500	-.00583	-.00633	-.00500	-.01500
	1.10	-.00200	-.00333	-.00500	-.00583	-.00633	-.00500	-.01500
	1.47	-.00200	-.00333	-.00500	-.00583	-.00633	-.00500	-.01500
$\frac{\partial C_D}{\partial \delta_{sp}}$, deg^{-1}	0	.00133	.00133	.00133	.00133	.00066	.00066	-.00166
	.36	.00133	.00133	.00133	.00133	.00066	.00066	-.00166
	.77	.00133	.00133	.00133	.00133	.00066	.00066	-.00166
	1.10	.00133	.00133	.00133	.00133	.00066	.00066	-.00166
	1.47	.00133	.00133	.00133	.00133	.00066	.00066	-.00166

TABLE 4. - AERODYNAMIC COEFFICIENTS FOR THE AW/AW CONFIGURATION WITH 71° FLAPS - Concluded

Coefficient	C_μ	α, deg						
		-10.0	-2.0	6.0	12.0	18.0	24.0	28.0
C_{l_β}, deg^{-1}	0	-.0045	-.0045	-.0045	-.0050	-.0055	-.0055	-.0030
	.36	-.0050	-.0050	-.0050	-.0055	-.0060	-.0060	-.0040
	.77	-.0055	-.0055	-.0055	-.0060	-.0065	-.0065	-.0050
	1.10	-.0085	-.0085	-.0085	-.0065	-.0060	-.0050	-.0030
	1.47	-.0115	-.0115	-.0115	-.0070	-.0050	-.0040	-.0020
C_{n_β}, deg^{-1}	0	.0023	.0030	.0030	.0035	.0033	.0018	.0009
	.36	.0030	.0024	.0024	.0042	.0039	.0036	.0018
	.77	.0016	.0018	.0018	.0050	.0041	.0044	.0030
	1.10	.0018	.0020	.0020	.0055	.0058	.0059	.0043
	1.47	.0019	.0022	.0022	.0060	.0063	.0065	.0060
C_{Y_β}, deg^{-1}	0	-.0140	-.0140	-.0140	-.0155	-.0180	-.0170	-.0160
	.36	-.0140	-.0147	-.0147	-.0185	-.0230	-.0230	-.0200
	.77	-.0160	-.0155	-.0155	-.0215	-.0240	-.0245	-.0210
	1.10	-.0165	-.0185	-.0185	-.0215	-.0250	-.0261	-.0220
	1.47	-.0190	-.0215	-.0215	-.0215	-.0255	-.0266	-.0230
C_{l_p}	0	-.3730	-.5330	-.3470	-.0934	-.2400	-.1000	-.1200
	.36	-.4660	-.4930	-.2670	-.1870	-.1670	.0133	.0067
	.77	-.5600	-.4530	-.1870	-.2800	-.0866	.1200	.1330
	1.10	-.5400	-.4270	-.1870	-.2930	-.1870	.0934	.1470
	1.47	-.5200	-.3930	-.1870	-.3060	-.2930	.0667	.1600
C_{n_p}	0	-.047	-.033	-.113	-.107	-.120	-.067	-.040
	.36	-.067	-.080	-.140	-.167	-.187	-.147	-.120
	.77	-.080	-.120	-.160	-.213	-.253	-.200	-.173
	1.10	-.087	-.140	-.173	-.240	-.307	-.253	-.180
	1.47	-.093	-.160	-.180	-.253	-.347	-.307	-.187
C_{l_r}	0	.213	.380	.534	.587	.633	.320	.320
	.36	.274	.440	.546	.567	.520	.340	.313
	.77	.333	.507	.560	.546	.413	.360	.313
	1.10	.287	.520	.554	.520	.480	.293	.227
	1.47	.240	.534	.546	.493	.546	.227	.147
C_{n_r}	0	-.240	-.200	-.206	-.253	-.220	-.293	-.226
	.36	-.187	-.213	-.227	-.260	-.267	-.326	-.226
	.77	-.147	-.227	-.240	-.266	-.307	-.353	-.226
	1.10	-.140	-.273	-.280	-.273	-.307	-.366	-.313
	1.47	-.133	-.320	-.320	-.280	-.313	-.380	-.400

TABLE 5.- AERODYNAMIC COEFFICIENTS FOR THE AW/EBF CONFIGURATION WITH 71° FLAPS

Coefficient	C_μ	α, deg						
		-10.0	-2.0	5.0	12.0	18.0	24.0	28.0
C_m	0	1.120	.800	.440	.220	.080	-.130	-.250
	.36	.440	.270	.110	-.020	-.230	-.530	-.680
	.77	.170	-.060	-.270	-.390	-.630	-1.000	-1.270
	1.10	-.040	-.270	-.490	-.660	-.830	-1.130	-1.280
	1.47	-.250	-.480	-.720	-.910	-1.070	-1.290	-1.470
C_L	0	-.440	.770	1.240	1.660	2.000	2.290	2.400
	.36	2.020	2.620	3.180	3.620	4.000	4.350	4.440
	.77	3.050	3.900	4.720	5.200	5.670	5.790	5.900
	1.10	3.470	4.350	5.200	5.830	6.280	6.490	6.500
	1.47	4.050	4.920	5.820	6.520	7.100	7.180	7.310
C_D	0	.260	.280	.300	.320	.370	.440	.540
	.36	.170	.250	.370	.500	.640	.810	.920
	.77	.010	.240	.510	.750	1.030	1.240	1.410
	1.10	-.190	.120	.470	.760	1.070	1.360	1.560
	1.47	-.250	.060	.460	.840	1.300	1.620	1.820
$\frac{\partial C_m}{\partial\left(\frac{q\bar{c}}{2V}\right)}$	0	-11.3	-24.0	-24.7	-18.0	0.0	-4.0	-9.3
	.36	-17.3	-24.7	-30.7	-25.3	-10.7	-16.7	-20.0
	.77	-22.6	-25.3	-36.0	-31.4	-22.0	-28.7	-30.7
	1.10	-24.0	-25.3	-35.4	-31.4	-24.7	-26.7	-33.3
	1.47	-25.3	-25.3	-34.7	-31.4	-27.4	-25.3	-36.0
$\frac{\partial C_m}{\partial \delta_h}$	0	-.1088	-.1038	-.0575	-.0240	-.0100	-.0040	.0010
	.36	-.1033	-.1145	-.0750	-.0422	-.0228	-.0092	-.0064
	.77	-.0970	-.1266	-.0948	-.0629	-.0374	-.0151	-.0149
	1.10	-.0923	-.1328	-.1096	-.0778	-.0484	-.0204	-.0216
	1.47	-.0874	-.1338	-.1242	-.0914	-.0593	-.0274	-.0289
$\frac{\partial C_L}{\partial \delta_h}$	0	.0600	.0344	.0396	.0286	.0400	-.0050	.0050
	.36	.0485	.0387	.0442	.0343	.0411	-.0076	-.0006
	.77	.0354	.0436	.0494	.0408	.0424	-.0106	-.0069
	1.10	.0298	.0475	.0527	.0448	.0432	-.0090	-.0100
	1.47	.0321	.0517	.0546	.0471	.0435	-.0005	-.0100
$\frac{\partial C_D}{\partial \delta_h}$	0	.0090	.0070	.0100	.0180	.0095	.0075	.0080
	.36	.0034	.0072	.0107	.0173	.0149	.0103	.0099
	.77	-.0029	.0074	.0116	.0164	.0210	.0135	.0120
	1.10	-.0062	.0082	.0124	.0168	.0243	.0150	.0127
	1.47	-.0068	.0101	.0136	.0191	.0253	.0150	.0120

TABLE 5. - AERODYNAMIC COEFFICIENTS FOR THE AW/EBF CONFIGURATION WITH 71° FLAPS - Continued

Coefficient	C_μ	α, deg						
		-10.0	-2.0	6.0	12.0	18.0	24.0	28.0
$\frac{\partial C_l}{\partial \delta_a}$, deg^{-1}	0	.00100	.00145	.00192	.00217	.00250	.00284	.00484
	.36	.00100	.00145	.00192	.00217	.00250	.00284	.00484
	.77	.00100	.00145	.00192	.00217	.00250	.00284	.00484
	1.10	.00100	.00145	.00192	.00217	.00250	.00284	.00484
	1.47	.00100	.00145	.00192	.00217	.00250	.00284	.00484
$\frac{\partial C_n}{\partial \delta_a}$, deg^{-1}	0	.00042	.00037	.00033	.00012	.00003	.00000	-.00033
	.36	.00042	.00037	.00033	.00012	.00003	.00000	-.00033
	.77	.00042	.00037	.00033	.00012	.00003	.00000	-.00033
	1.10	.00042	.00037	.00033	.00012	.00003	.00000	-.00033
	1.47	.00042	.00037	.00033	.00012	.00003	.00000	-.00033
$\frac{\partial C_Y}{\partial \delta_a}$, deg^{-1}	0	-.00025	-.00050	-.00092	-.00108	-.00167	-.00266	-.00400
	.36	-.00025	-.00050	-.00092	-.00108	-.00167	-.00266	-.00400
	.77	-.00025	-.00050	-.00092	-.00108	-.00167	-.00266	-.00400
	1.10	-.00025	-.00050	-.00092	-.00108	-.00167	-.00266	-.00400
	1.47	-.00025	-.00050	-.00092	-.00108	-.00167	-.00266	-.00400
$\frac{\partial C_l}{\partial \delta_r}$, deg^{-1}	0	.00263	.00219	.00188	.00231	.00270	.00195	.00045
	.36	.00240	.00195	.00174	.00208	.00238	.00176	.00061
	.77	.00213	.00178	.00158	.00181	.00203	.00153	.00079
	1.10	.00192	.00165	.00145	.00159	.00173	.00135	.00093
	1.47	.00167	.00149	.00130	.00135	.00141	.00115	.00110
$\frac{\partial C_n}{\partial \delta_r}$, deg^{-1}	0	-.00375	-.00338	-.00277	-.00240	-.00190	-.00087	.00026
	.36	-.00384	-.00352	-.00303	-.00272	-.00229	-.00147	-.00053
	.77	-.00395	-.00367	-.00333	-.00307	-.00273	-.00216	-.00143
	1.10	-.00403	-.00380	-.00356	-.00337	-.00309	-.00272	-.00216
	1.47	-.00413	-.00394	-.00383	-.00369	-.00350	-.00335	-.00298
$\frac{\partial C_Y}{\partial \delta_r}$, deg^{-1}	0	.01250	.01250	.01025	.00900	.00825	.00500	.00275
	.36	.01213	.01213	.01034	.00928	.00871	.00630	.00433
	.77	.01171	.01171	.01045	.00960	.00924	.00778	.00612
	1.10	.01136	.01136	.01053	.00985	.00967	.00897	.00758
	1.47	.01098	.01098	.01063	.01014	.01015	.01032	.00921

TABLE 5.- AERODYNAMIC COEFFICIENTS FOR THE AW/EBF CONFIGURATION WITH 71° FLAPS - Continued

Coefficient	C_μ	α, deg						
		-10.0	-2.0	6.0	12.0	18.0	24.0	28.0
$\frac{\partial C_l}{\partial \delta_{sp}}$, deg^{-1}	0	.00217	.00214	.00180	.00140	.00080	.00013	-.00033
	.36	.00217	.00214	.00180	.00140	.00080	.00013	-.00033
	.77	.00217	.00214	.00180	.00140	.00080	.00013	-.00033
	1.10	.00217	.00214	.00180	.00140	.00080	.00013	-.00033
	1.47	.00217	.00214	.00180	.00140	.00080	.00013	-.00033
$\frac{\partial C_n}{\partial \delta_{sp}}$, deg^{-1}	0	.00011	-.00020	-.00053	-.00070	-.00043	-.00047	-.00047
	.36	.00011	-.00020	-.00053	-.00070	-.00043	-.00047	-.00047
	.77	.00011	-.00020	-.00053	-.00070	-.00043	-.00047	-.00047
	1.10	.00011	-.00020	-.00053	-.00070	-.00043	-.00047	-.00047
	1.47	.00011	-.00020	-.00053	-.00070	-.00043	-.00047	-.00047
$\frac{\partial C_Y}{\partial \delta_{sp}}$, deg^{-1}	0	-.00116	-.00116	.00000	.00041	.00066	.00106	.00106
	.36	-.00116	-.00116	.00000	.00041	.00066	.00106	.00106
	.77	-.00116	-.00116	.00000	.00041	.00066	.00106	.00106
	1.10	-.00116	-.00116	.00000	.00041	.00066	.00106	.00106
	1.47	-.00116	-.00116	.00000	.00041	.00066	.00106	.00106
$\frac{\partial C_m}{\partial \delta_{sp}}$, deg^{-1}	0	.00300	.00533	.00500	.00467	.00566	.00700	.00733
	.36	.00300	.00533	.00500	.00467	.00566	.00700	.00733
	.77	.00300	.00533	.00500	.00467	.00566	.00700	.00733
	1.10	.00300	.00533	.00500	.00467	.00566	.00700	.00733
	1.47	.00300	.00533	.00500	.00467	.00566	.00700	.00733
$\frac{\partial C_L}{\partial \delta_{sp}}$, deg^{-1}	0	-.00200	-.00333	-.00500	-.00583	-.00633	-.00500	-.01500
	.36	-.00200	-.00333	-.00500	-.00583	-.00633	-.00500	-.01500
	.77	-.00200	-.00333	-.00500	-.00583	-.00633	-.00500	-.01500
	1.10	-.00200	-.00333	-.00500	-.00583	-.00633	-.00500	-.01500
	1.47	-.00200	-.00333	-.00500	-.00583	-.00633	-.00500	-.01500
$\frac{\partial C_D}{\partial \delta_{sp}}$, deg^{-1}	0	.00133	.00133	.00133	.00133	.00066	.00066	-.00166
	.36	.00133	.00133	.00133	.00133	.00066	.00066	-.00166
	.77	.00133	.00133	.00133	.00133	.00066	.00066	-.00166
	1.10	.00133	.00133	.00133	.00133	.00066	.00066	-.00166
	1.47	.00133	.00133	.00133	.00133	.00066	.00066	-.00166

TABLE 5.- AERODYNAMIC COEFFICIENTS FOR THE AW/EBF CONFIGURATION WITH 71° FLAPS - Concluded

Coefficient	C_μ	α, deg						
		-10.0	-2.0	6.0	12.0	18.0	24.0	28.0
$\frac{\partial C_l}{\partial \beta}$, deg^{-1}	0	.0018	-.0023	-.0040	-.0035	-.0021	-.0016	-.0018
	.36	-.0001	-.0023	-.0038	-.0037	-.0034	-.0043	-.0059
	.77	-.0020	-.0023	-.0037	-.0041	-.0047	-.0069	-.0100
	1.10	-.0017	-.0027	-.0035	-.0048	-.0052	-.0073	-.0108
	1.47	-.0013	-.0031	-.0033	-.0056	-.0056	-.0076	-.0113
$\frac{\partial C_n}{\partial \beta}$, deg^{-1}	0	.0023	.0029	.0028	.0027	.0029	.0016	.0002
	.36	.0030	.0037	.0039	.0039	.0053	.0032	.0018
	.77	.0037	.0046	.0052	.0052	.0049	.0048	.0035
	1.10	.0037	.0047	.0054	.0052	.0053	.0053	.0044
	1.47	.0037	.0049	.0056	.0051	.0058	.0058	.0053
$\frac{\partial C_Y}{\partial \beta}$, deg^{-1}	0	-.0170	-.0170	-.0170	-.0160	-.0190	-.0180	-.0150
	.36	-.0220	-.0230	-.0250	-.0250	-.0250	-.0250	-.0200
	.77	-.0270	-.0300	-.0330	-.0340	-.0320	-.0320	-.0250
	1.10	-.0280	-.0330	-.0350	-.0340	-.0330	-.0360	-.0330
	1.47	-.0300	-.0360	-.0370	-.0350	-.0340	-.0390	-.0410
$\frac{\partial C_l}{\partial\left(\frac{pb}{2V}\right)}$	0	-.3730	-.5330	-.3470	-.0934	-.2400	-.1000	-.1200
	.36	-.4660	-.4930	-.2670	-.1870	-.1670	.0133	.0067
	.77	-.5600	-.4530	-.1870	-.2800	-.0866	.1200	.1330
	1.10	-.5400	-.4270	-.1870	-.2930	-.1870	.0934	.1470
	1.47	-.5200	-.3930	-.1870	-.3060	-.2930	.0667	.1600
$\frac{\partial C_n}{\partial\left(\frac{pb}{2V}\right)}$	0	-.047	-.033	-.113	-.107	-.120	-.067	-.040
	.36	-.067	-.080	-.140	-.167	-.187	-.147	-.120
	.77	-.080	-.120	-.160	-.213	-.253	-.200	-.173
	1.10	-.087	-.140	-.173	-.240	-.307	-.253	-.180
	1.47	-.093	-.160	-.180	-.253	-.347	-.307	-.187
$\frac{\partial C_l}{\partial\left(\frac{rb}{2V}\right)}$	0	.213	.380	.534	.587	.633	.320	.320
	.36	.274	.440	.546	.567	.520	.340	.313
	.77	.333	.507	.560	.546	.413	.360	.313
	1.10	.287	.520	.554	.520	.480	.293	.227
	1.47	.240	.534	.546	.493	.546	.227	.147
$\frac{\partial C_n}{\partial\left(\frac{rb}{2V}\right)}$	0	-.240	-.200	-.206	-.253	-.220	-.293	-.226
	.36	-.187	-.213	-.227	-.260	-.267	-.326	-.226
	.77	-.147	-.227	-.240	-.266	-.307	-.353	-.226
	1.10	-.140	-.273	-.280	-.273	-.307	-.366	-.313
	1.47	-.133	-.320	-.320	-.280	-.313	-.380	-.400

TABLE 6.- COCKPIT CONTROL CHARACTERISTICS

	Control		
	Column	Wheel	Pedal
Force gradient, N/cm (lb/in.)	11.4 (6.5)	4.55 (2.6)	35 (20)
Breakout force, N (lb)	8.9 (2.0)	8.9 (2.0)	44.5 (10)
Travel, cm (in.)	Forward: 14.6 (5.75) Aft: 25.7 (10.1)	[a]±20.3 (±8.0)	±12.7 (±5)

[a]±60°.

TABLE 7.- PILOT RATING SCALE
[From ref. 17]

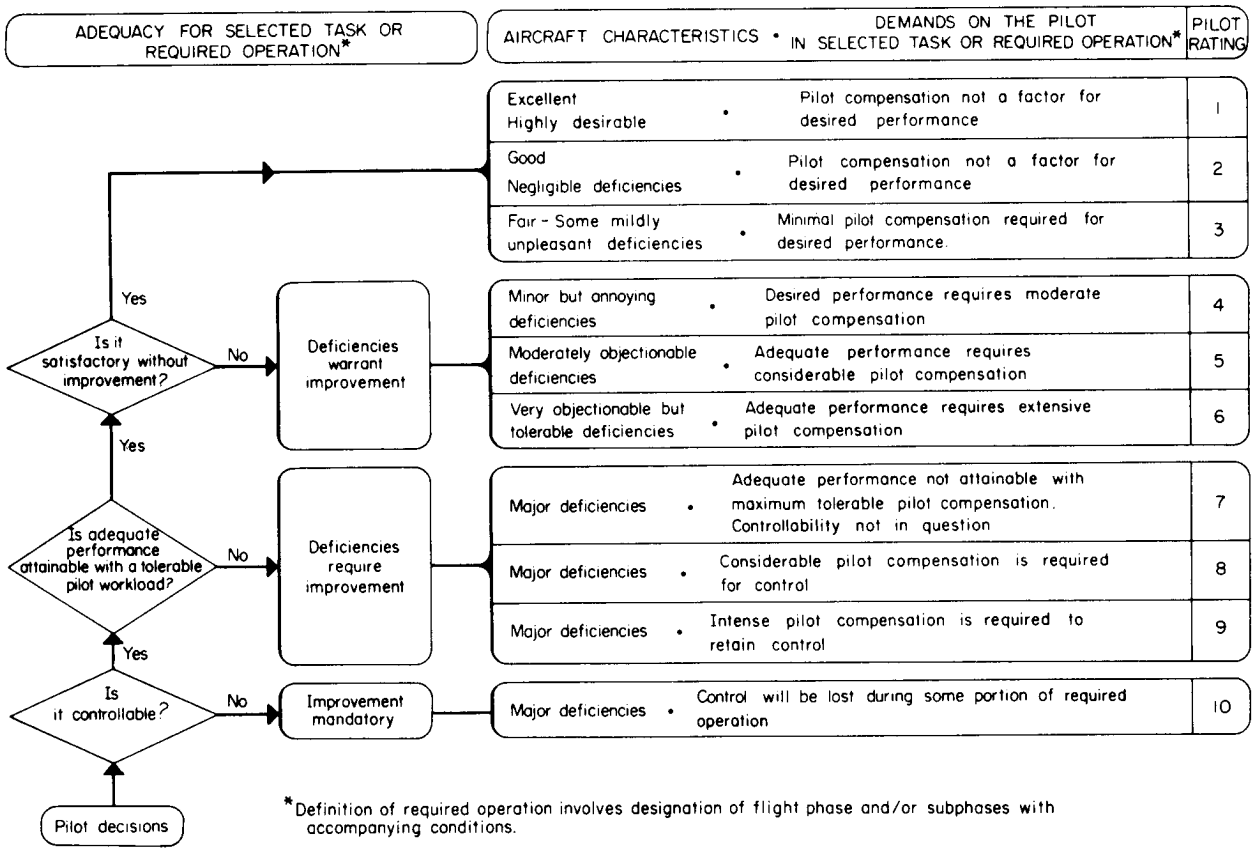

*Definition of required operation involves designation of flight phase and/or subphases with accompanying conditions.

TABLE 8.- PILOT RATINGS OF LATERAL-DIRECTIONAL CONTROL SYSTEMS

[EBF approach configuration; 70 knots]

	Pilot rating	
	Four-engine approach	Engine-out transient
Basic airplane	8	10
Roll and yaw damper (δ_r/r = -1.0 deg/deg/sec, δ_a/p = -1.0 deg/deg/sec)	6	--
Turn coordinator (δ_r/p = -0.93 deg/deg/sec)	6	--
Roll and yaw damper, turn coordinator	4	--
Roll and sideslip rate damper, turn coordinator (δ_r/r = 1.0 deg/deg/sec, δ_r/φ = 0.28 deg/deg)	3	--
Roll and sideslip rate damper, turn coordinator, aileron-to-rudder interconnect (δ_r/δ_a = 0.2 deg/deg)	2.5	6
Roll and sideslip rate damper, turn coordinator, aileron-to-rudder interconnect, bank angle command ($\delta_a = \left(1+\frac{1}{s}\right)(\delta_w - \varphi - p)$)	2.5	3.5

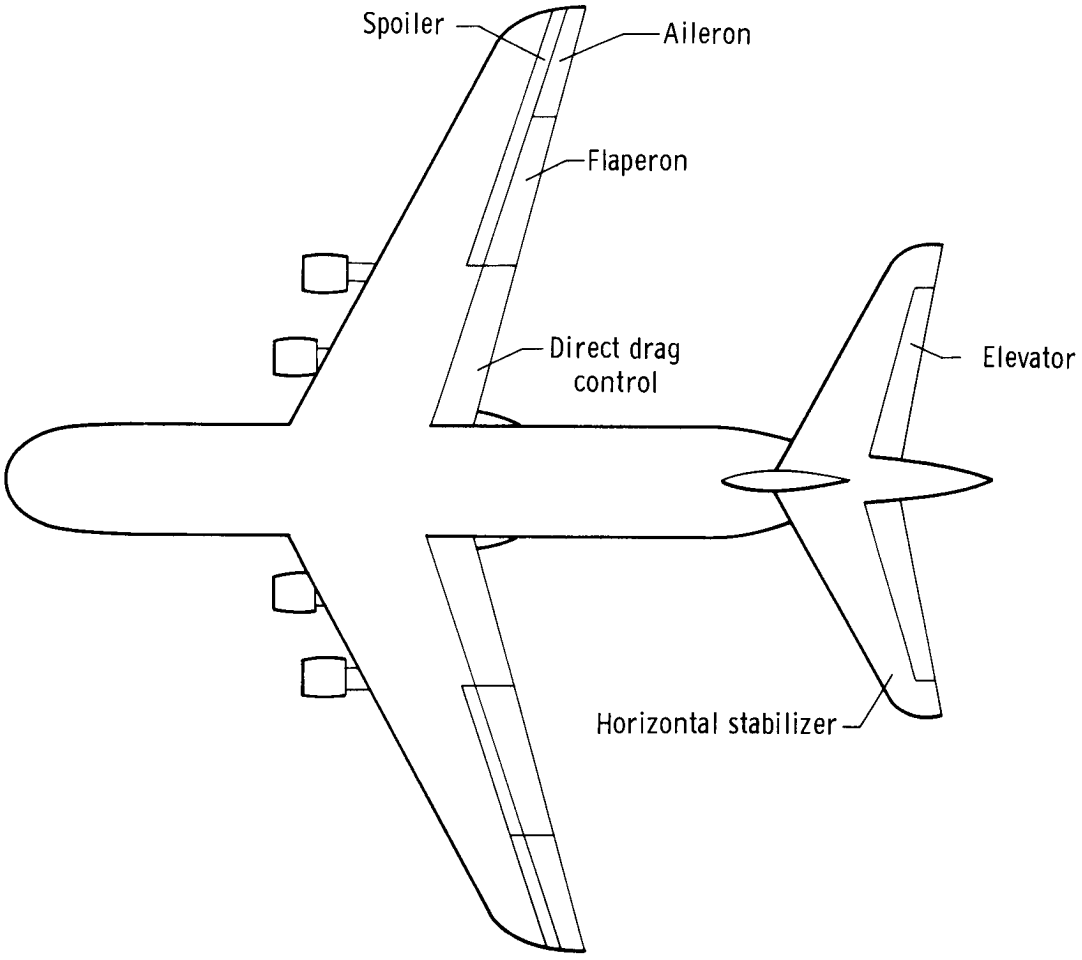

(a) EBF configuration.

Figure 1. Airplane configurations.

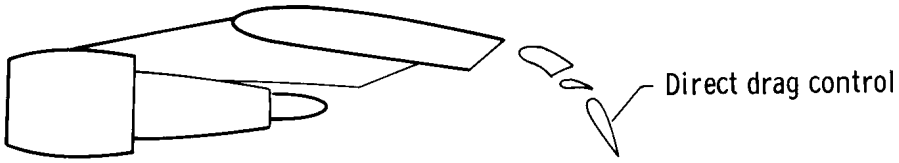

(b) EBF flap detail.

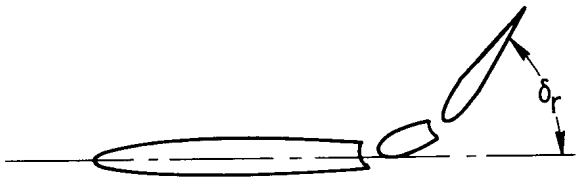

(c) EBF double-hinged rudder.

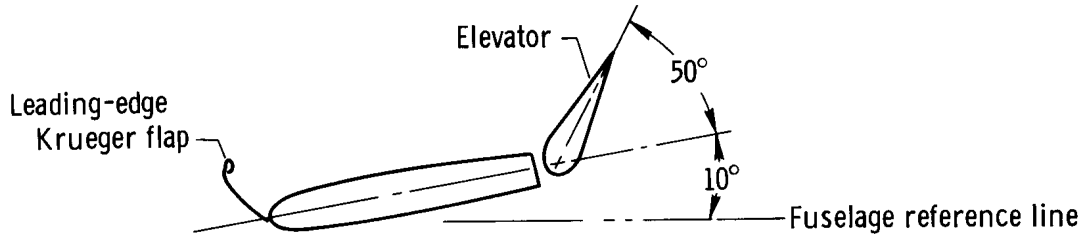

(d) EBF horizontal tail detail with full trailing-edge-up deflection.

Figure 1. Continued.

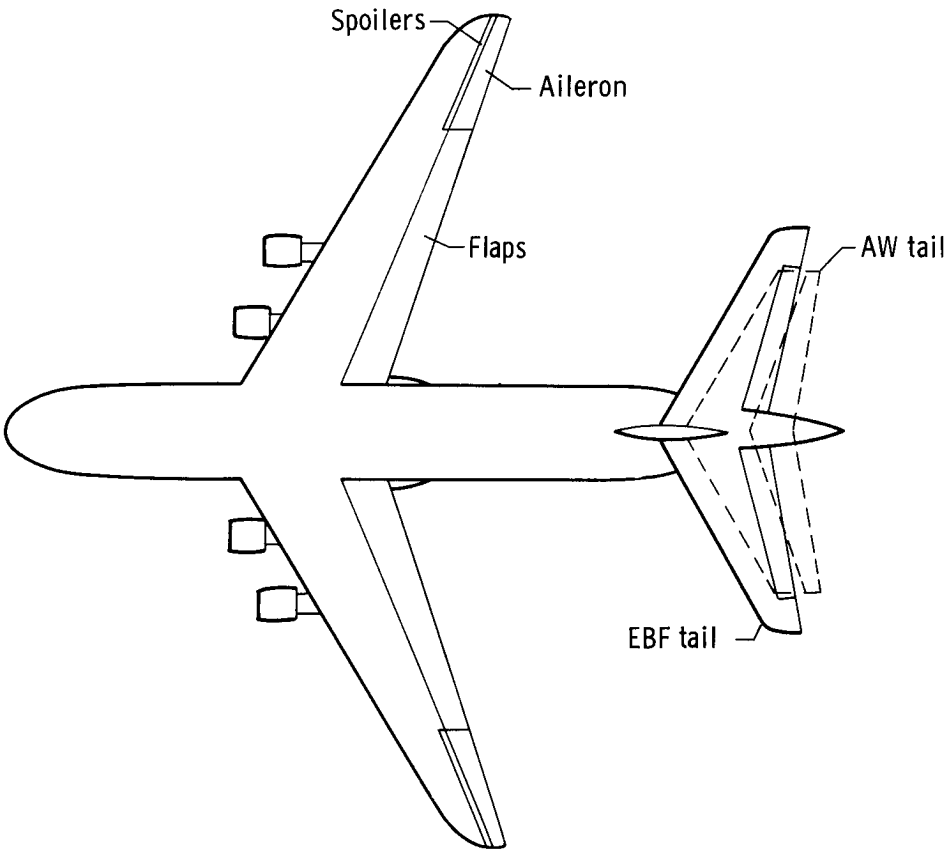

(e) AW/AW and AW/EBF configurations.

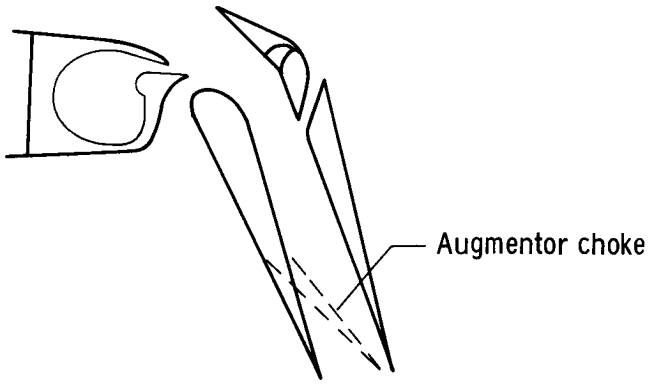

(f) AW flap detail.

Figure 1. Concluded.

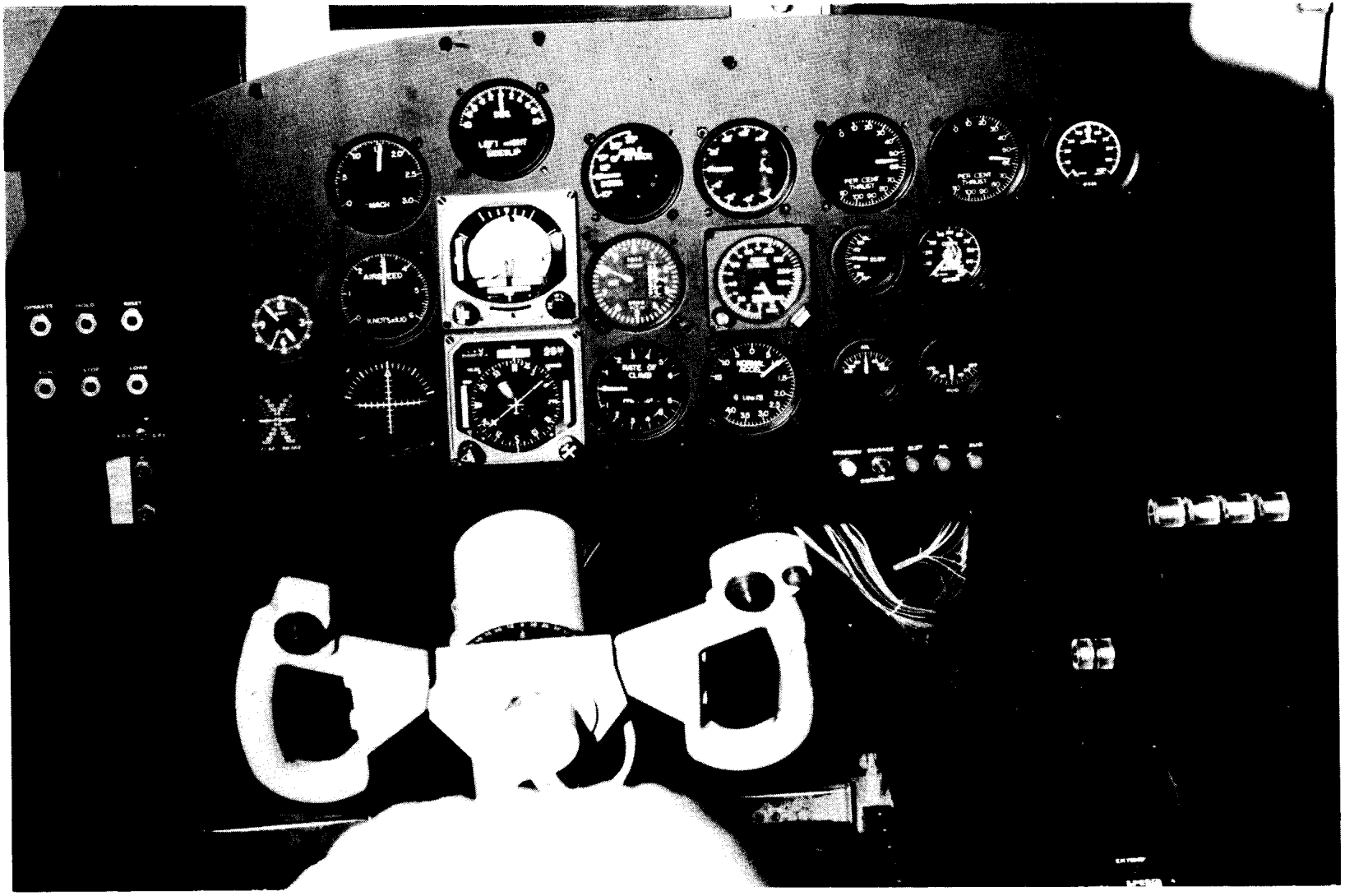

Figure 2. Simulator cockpit.

E-23280

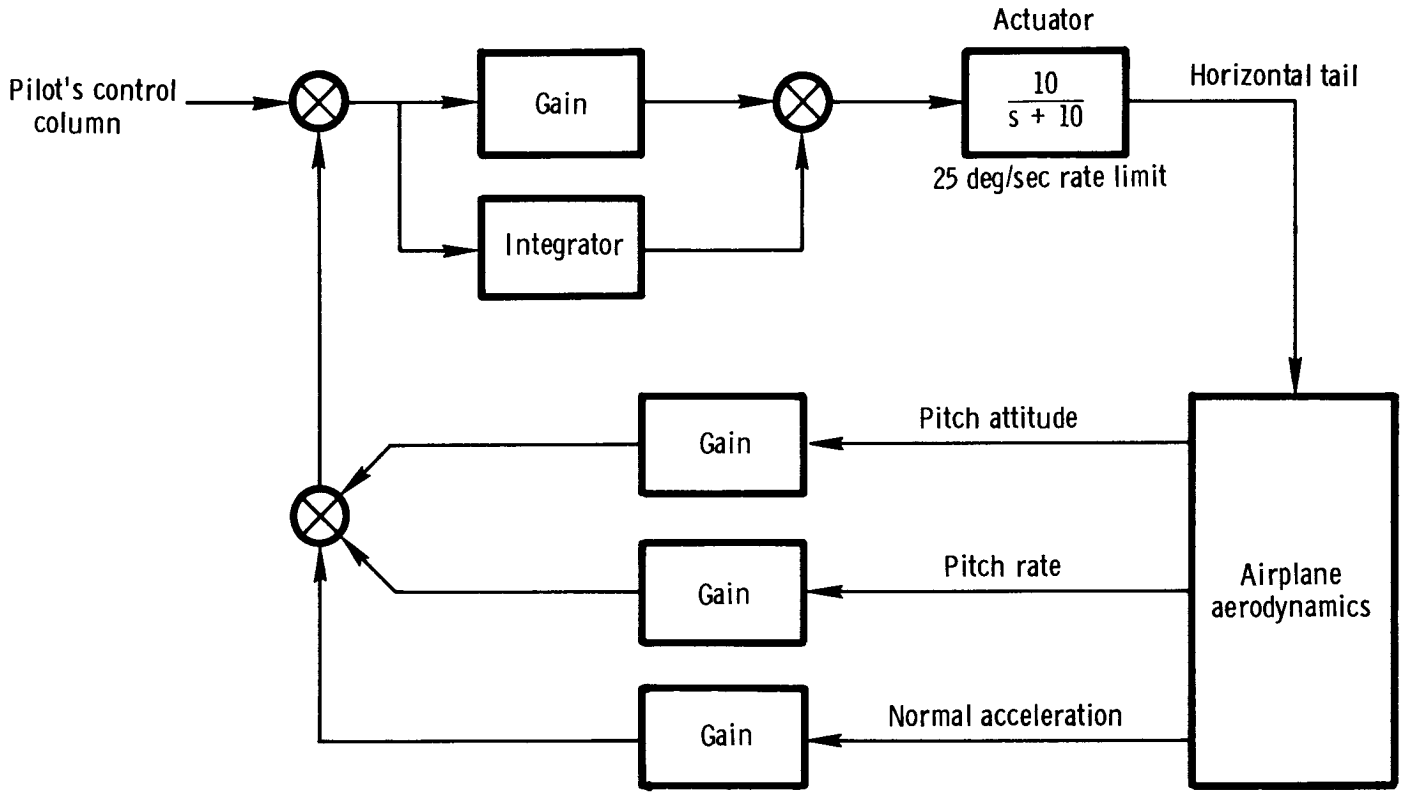

(a) Pitch axis.

Figure 3. Control system block diagrams.

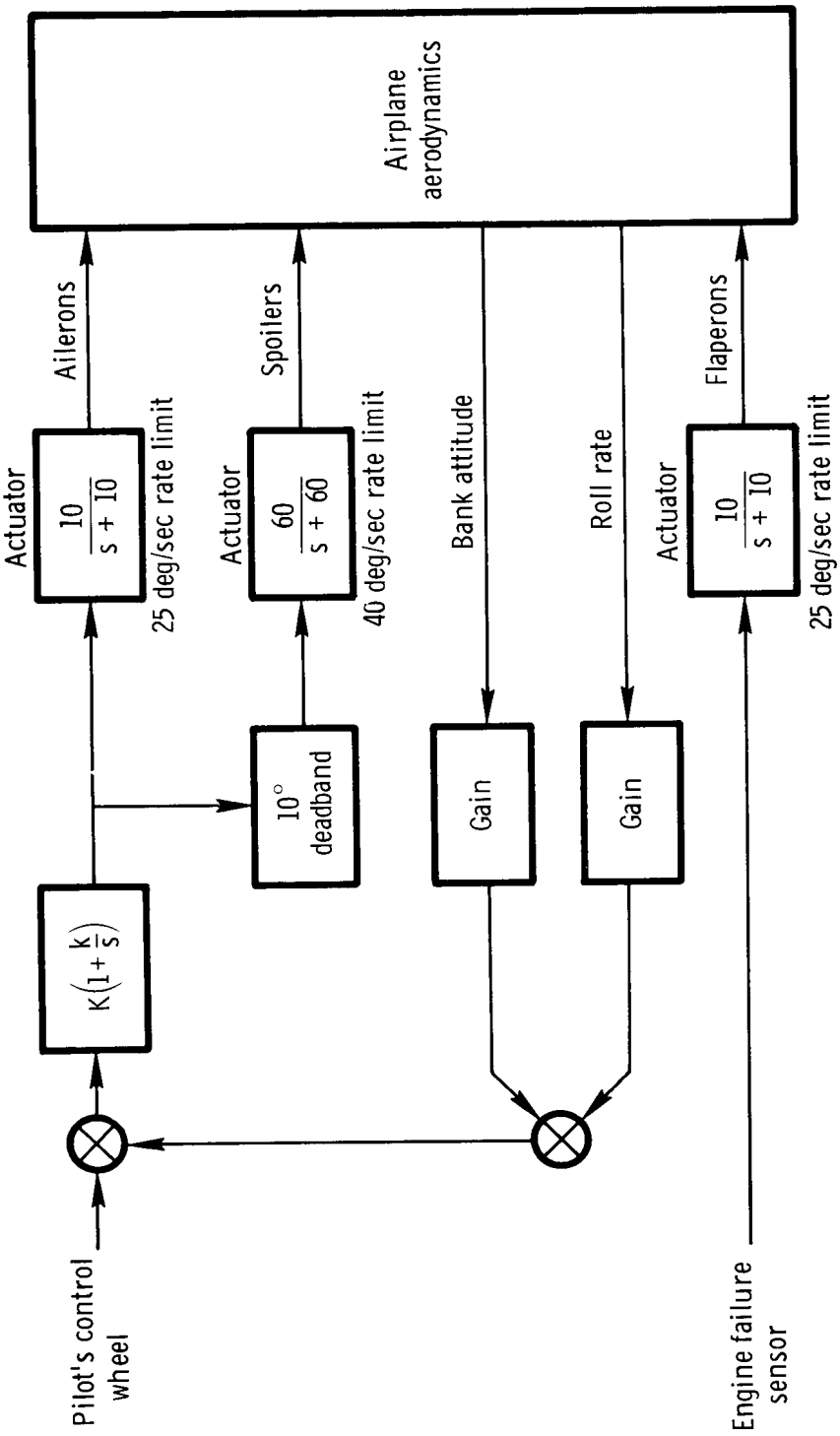

(b) Roll axis.

Figure 3. Continued.

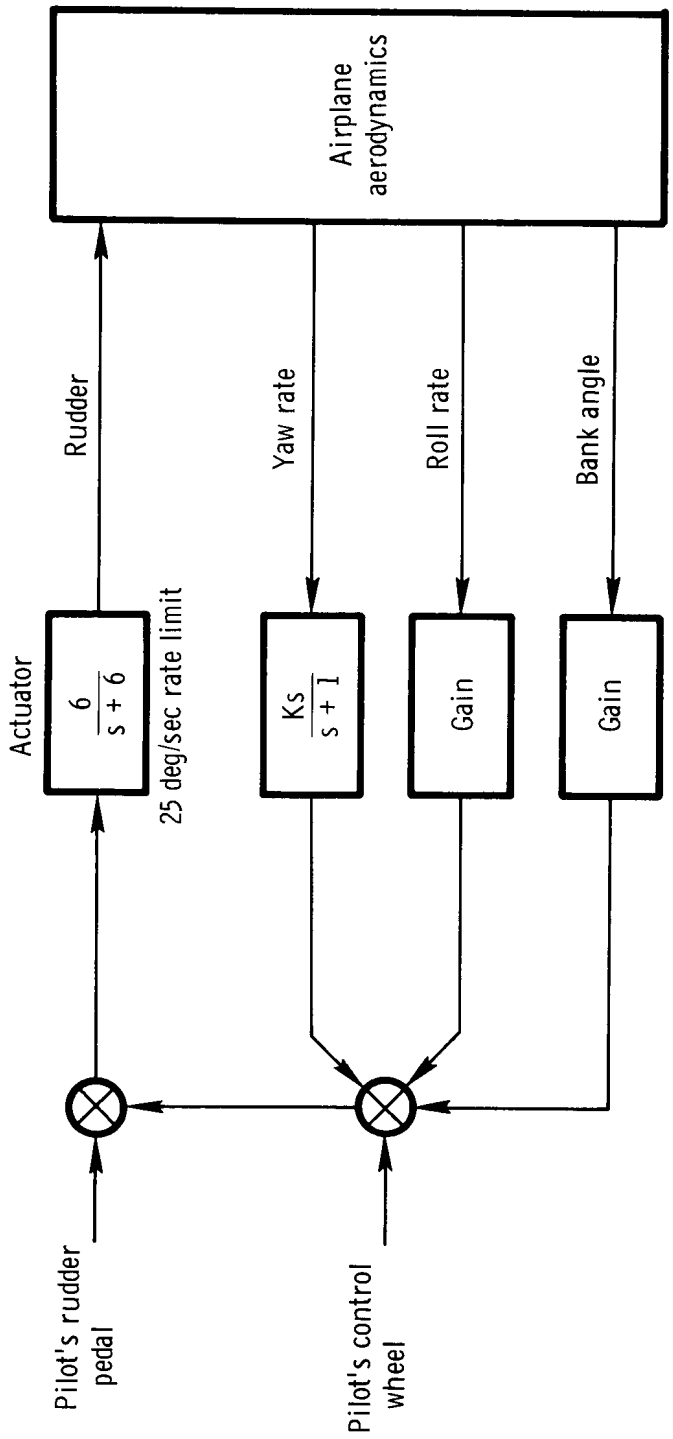

(c) Directional axis.

Figure 3. Concluded.

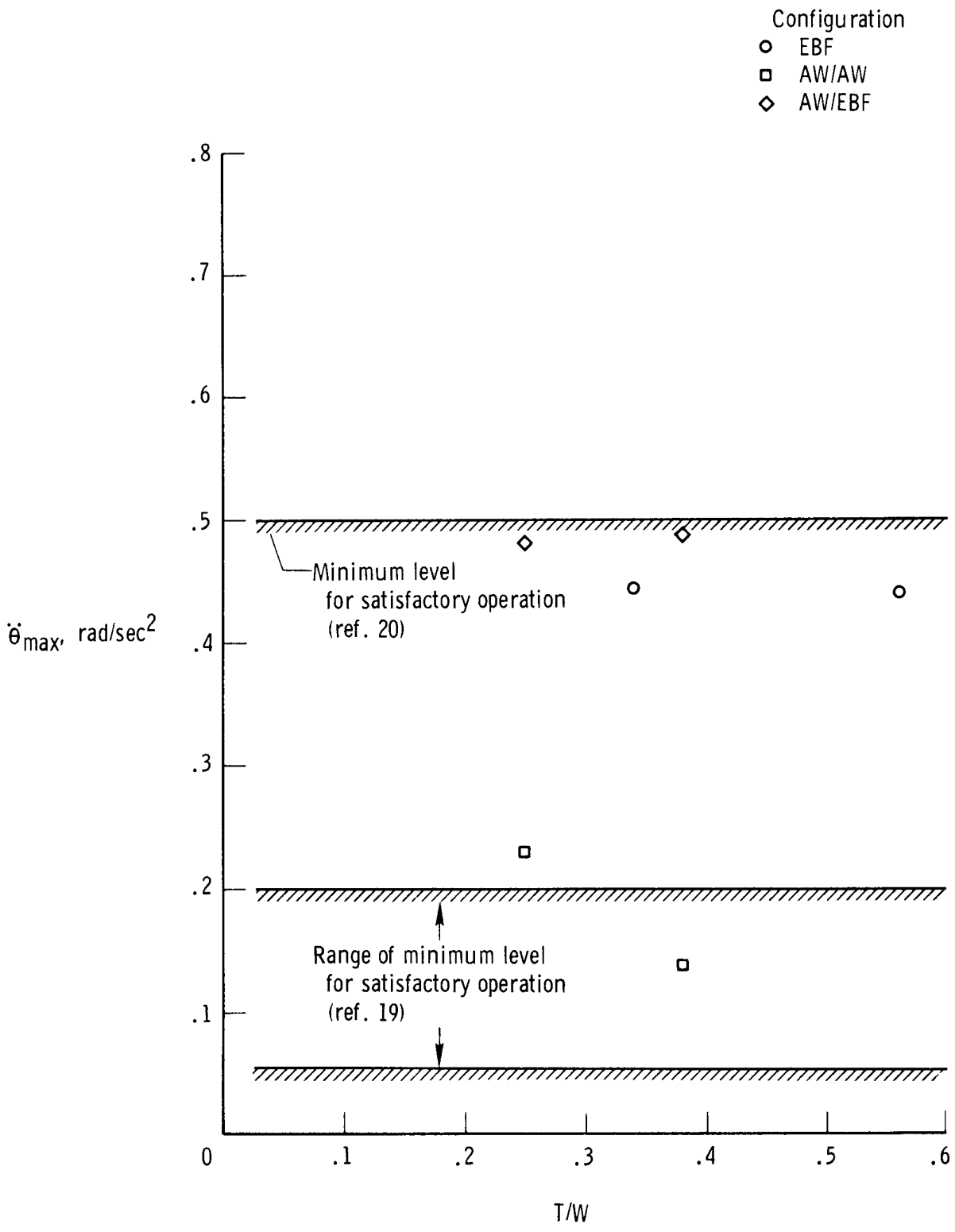

Figure 4. Comparison of maximum pitch control power available from trim with criteria from references 19 and 20. Approach configuration; 70 knots.

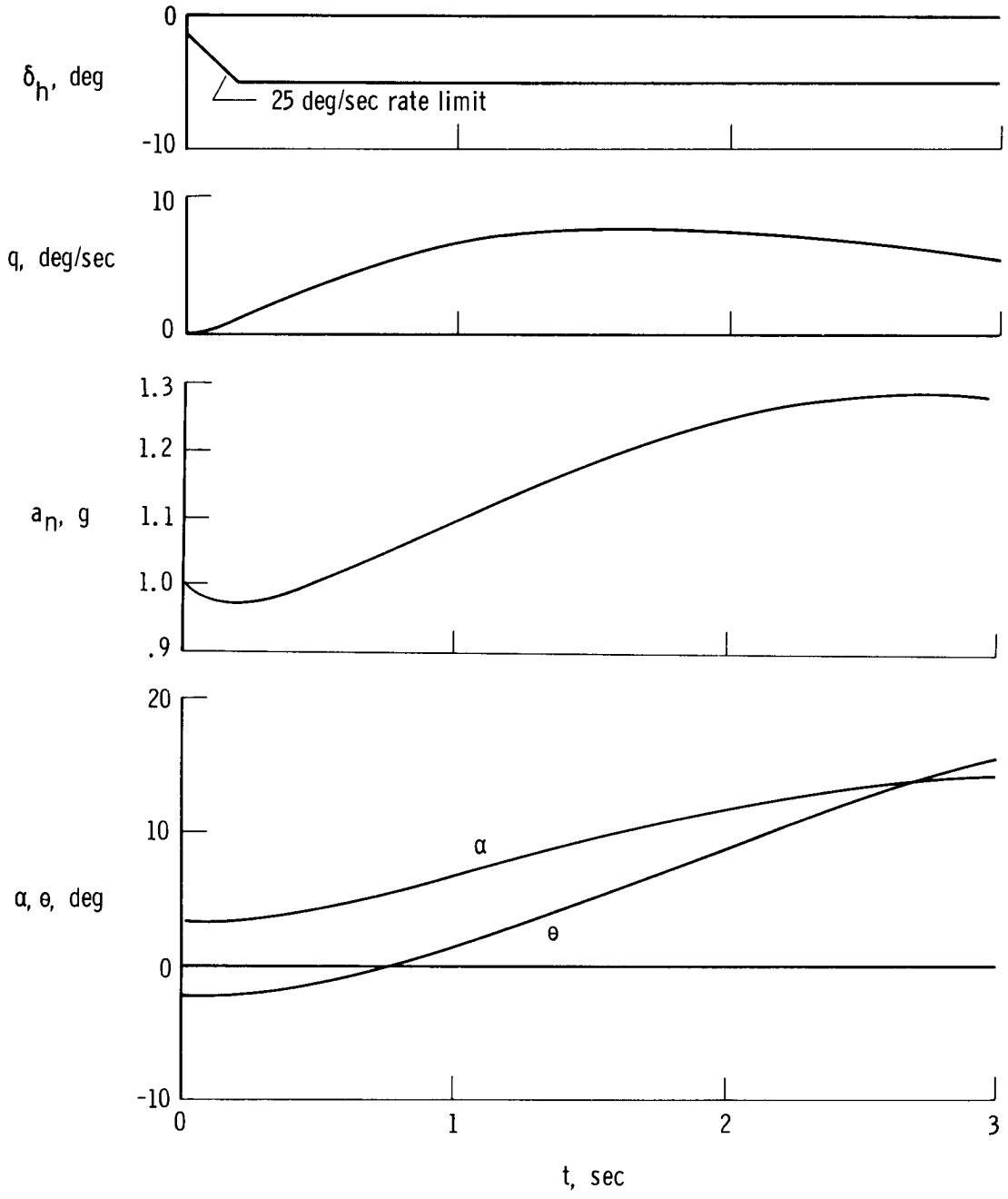

Figure 5. Time history of airplane response to a longitudinal control column step input from trim. EBF approach configuration; 70 knots.

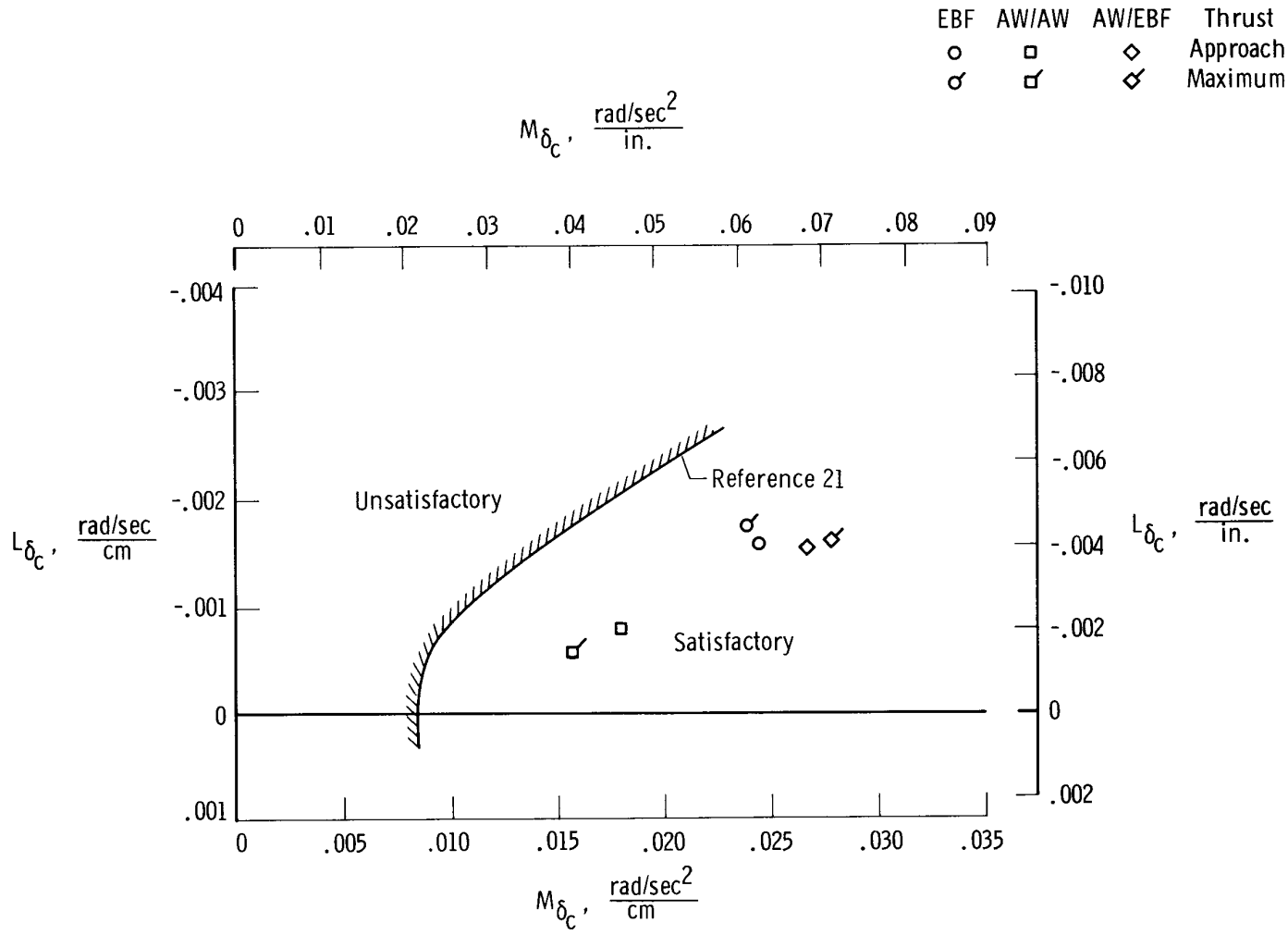

Figure 6. Comparison of characteristics of lift loss and pitching moment due to column displacement with criterion from reference 21. Approach configuration; 70 knots.

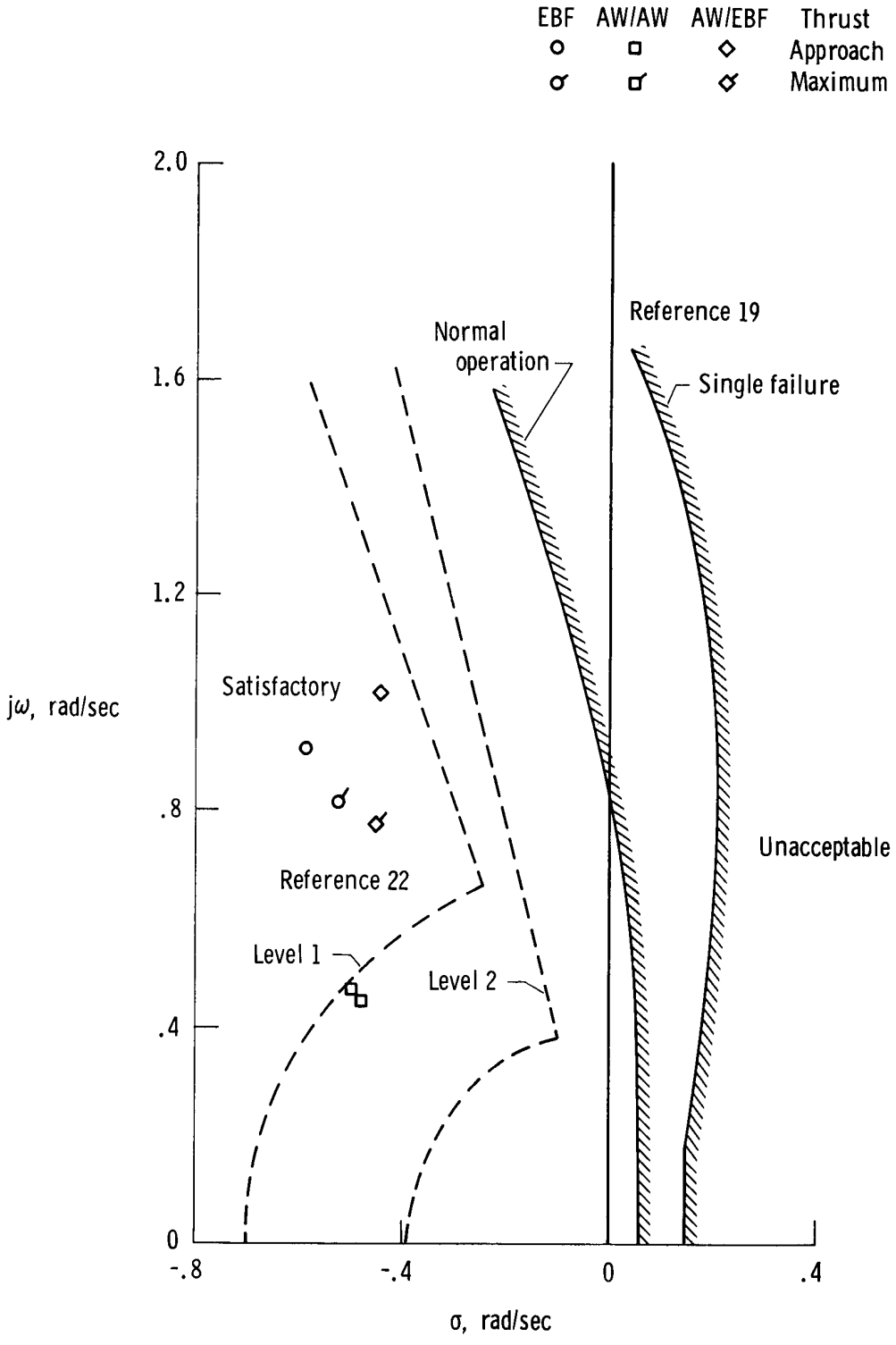

Figure 7. Comparison of longitudinal frequency and damping characteristics with criteria from references 19 and 22. Approach configuration; 70 knots.

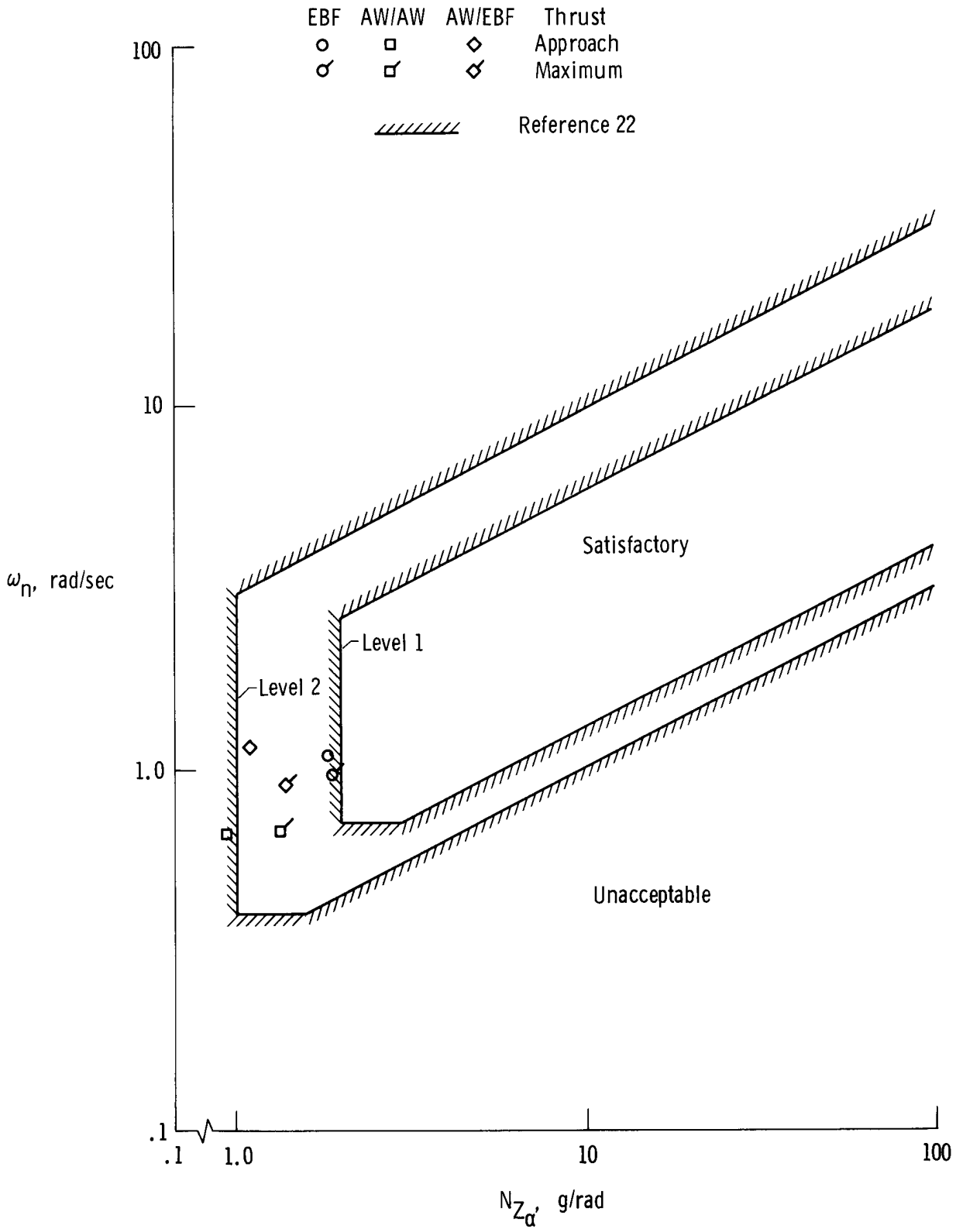

Figure 8. Comparison of longitudinal short-period characteristics with criterion from reference 22. Approach configuration; 70 knots.

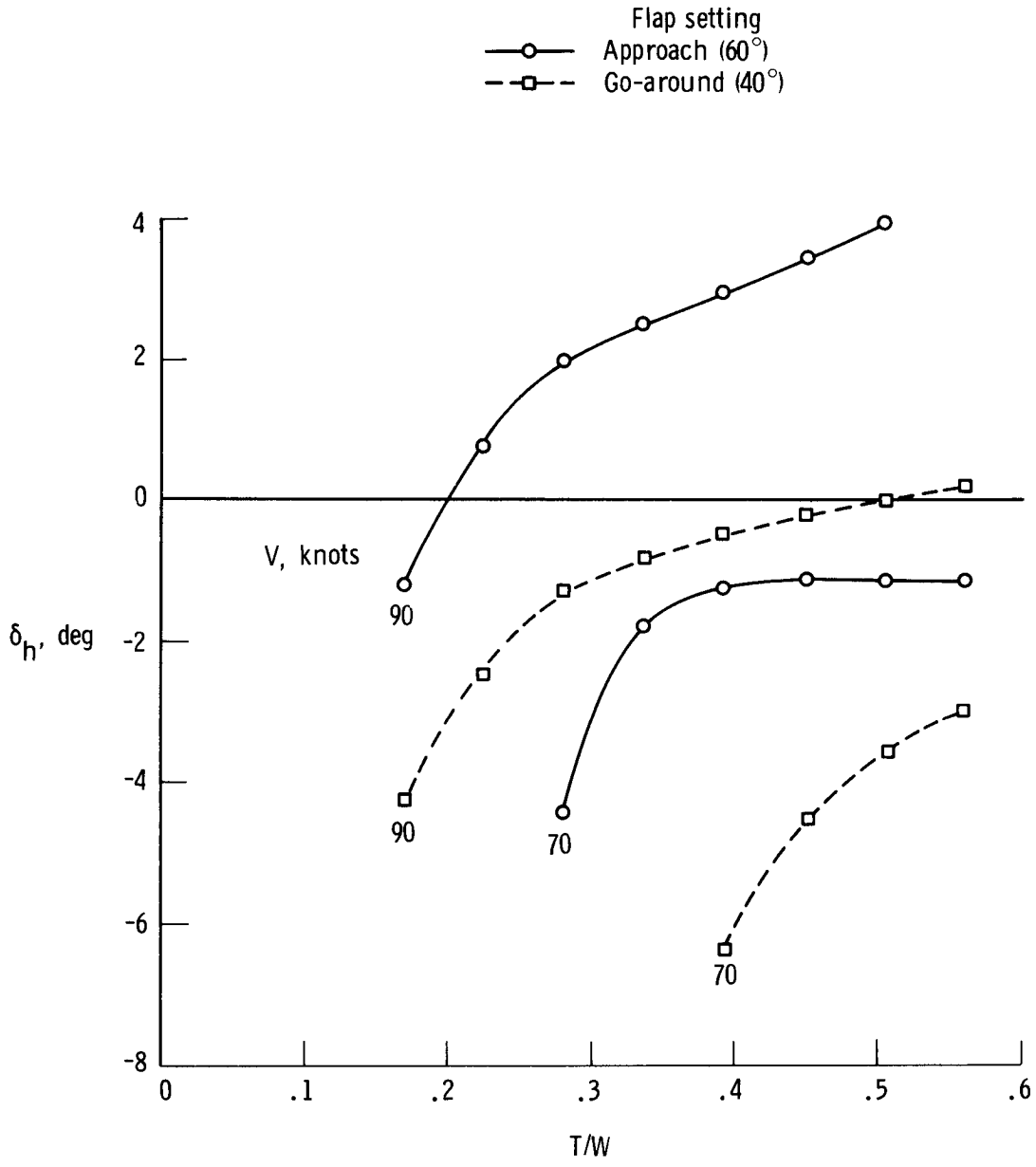

(a) EBF configuration.

Figure 9. Longitudinal control required for steady-state trim.

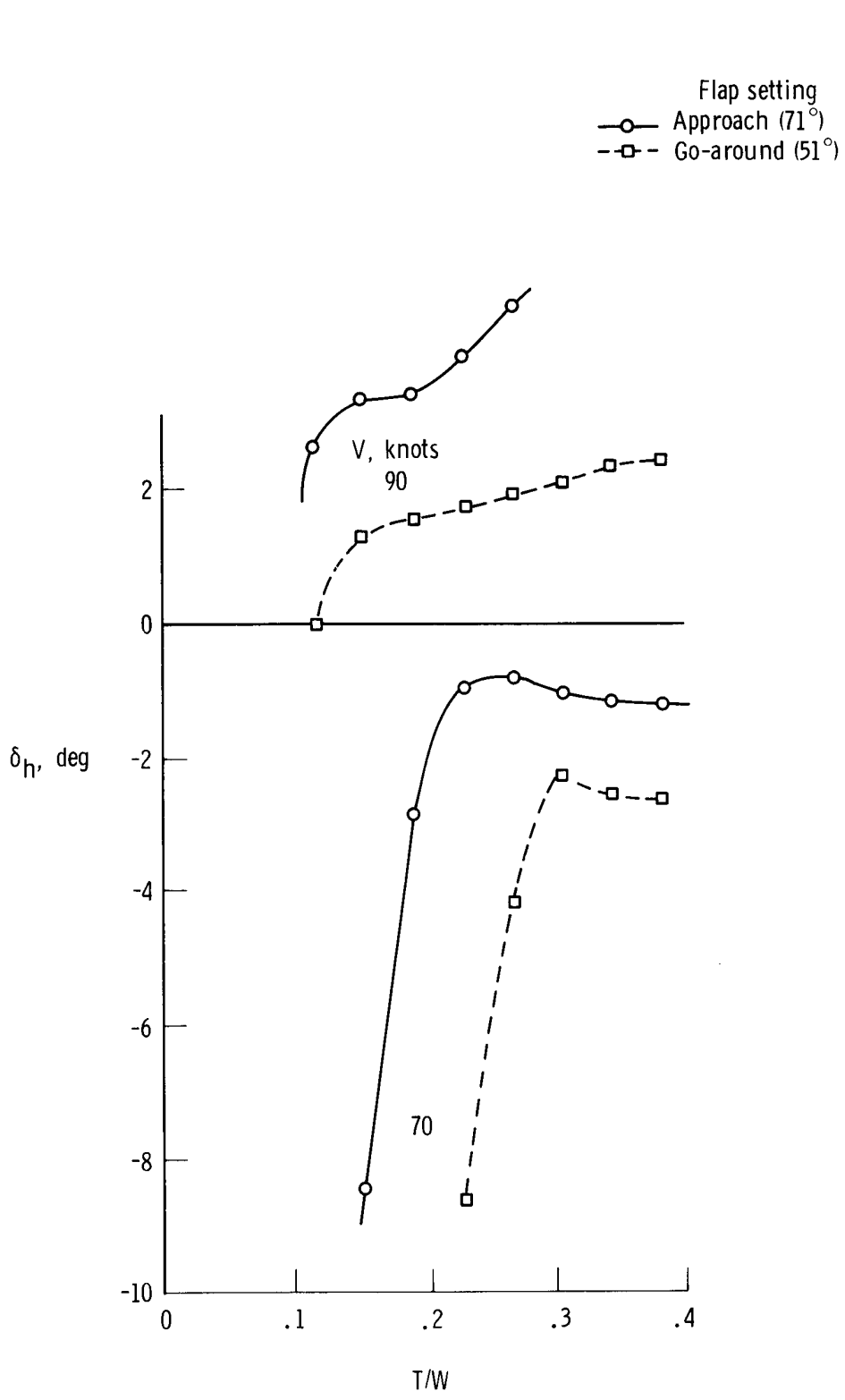

(b) AW/EBF configuration.

Figure 9. Continued.

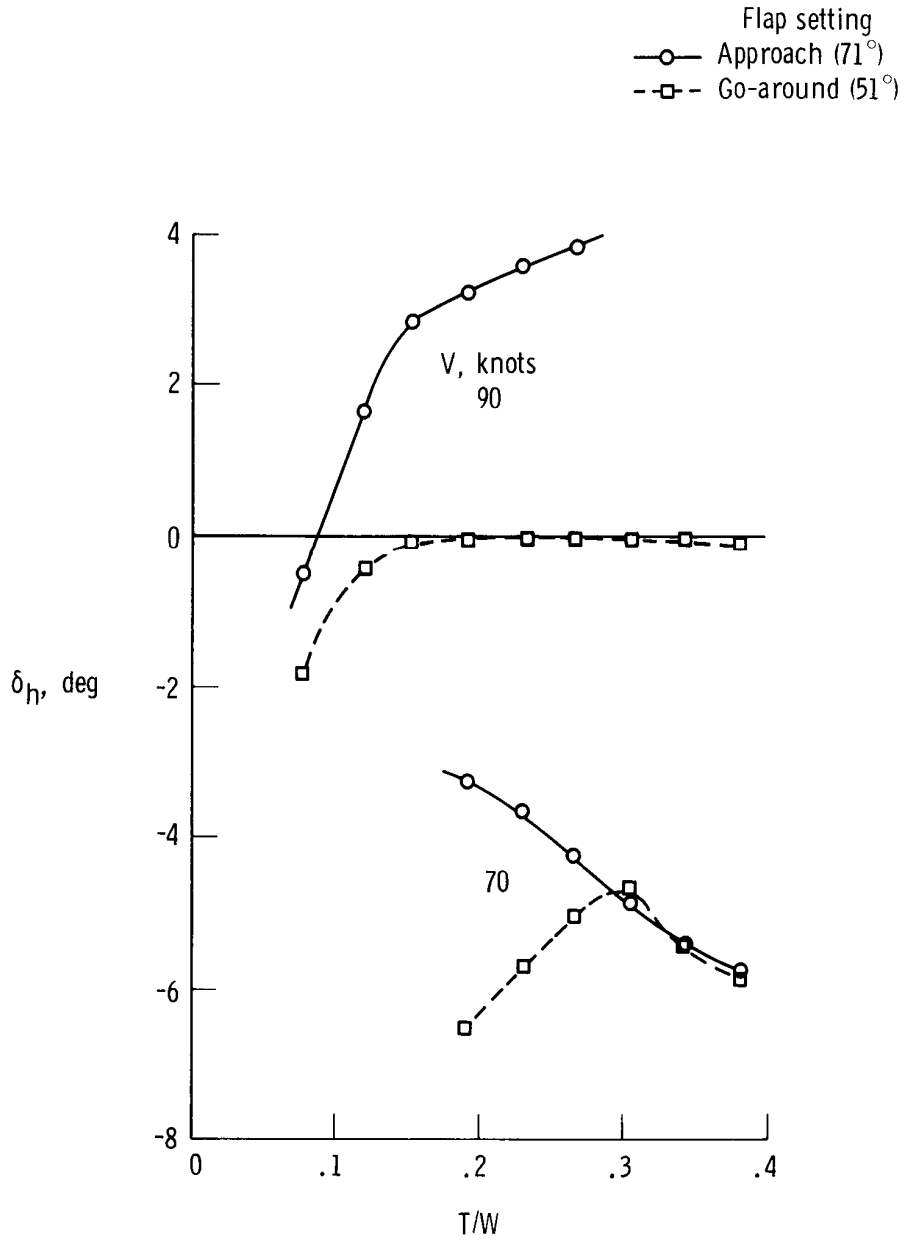

(c) AW/AW configuration.

Figure 9. Concluded.

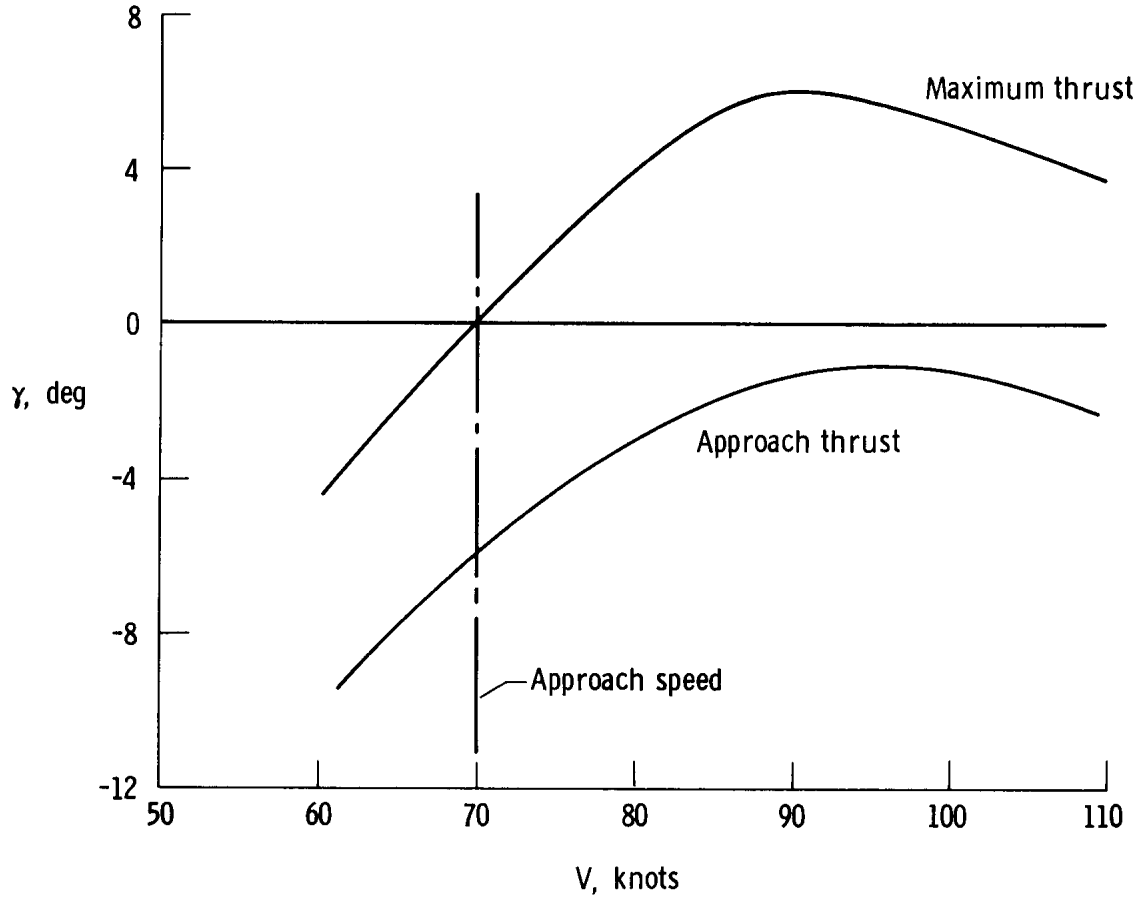

(a) Determination of flight path stability for EBF configuration.

Figure 10. Flight path stability characteristics.

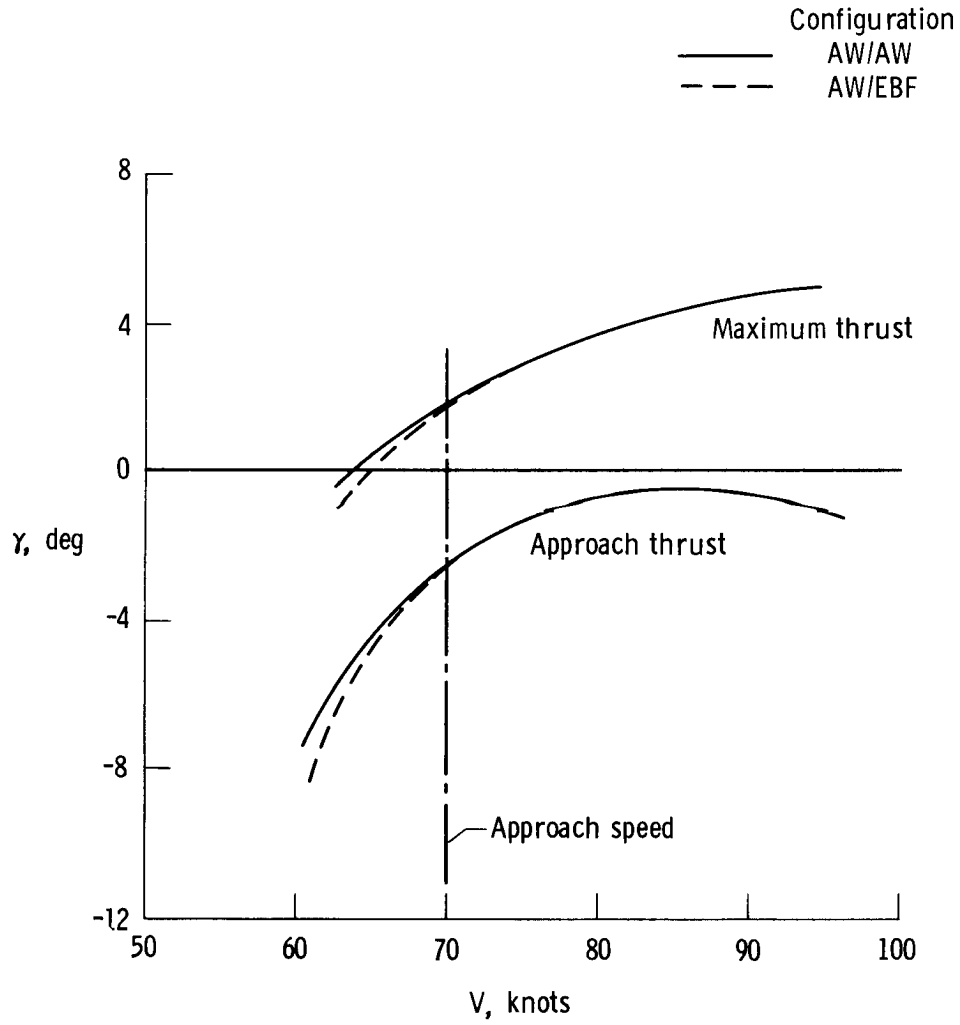

(b) Determination of flight path stability for AW configurations.

Figure 10. Continued.

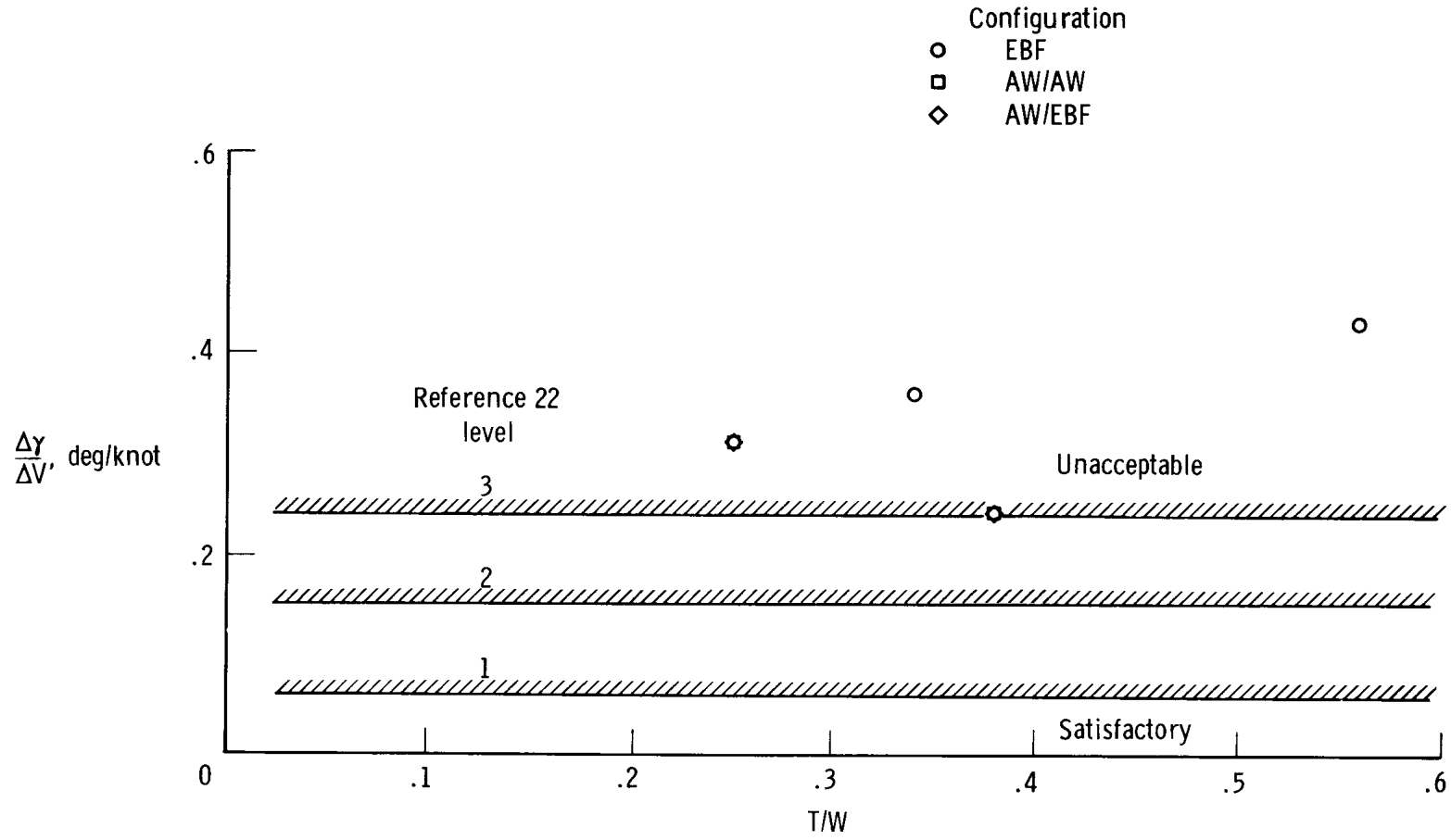

(c) Comparison of flight path stability with criterion of reference 22. Approach configuration; 70 knots.

Figure 10. Concluded.

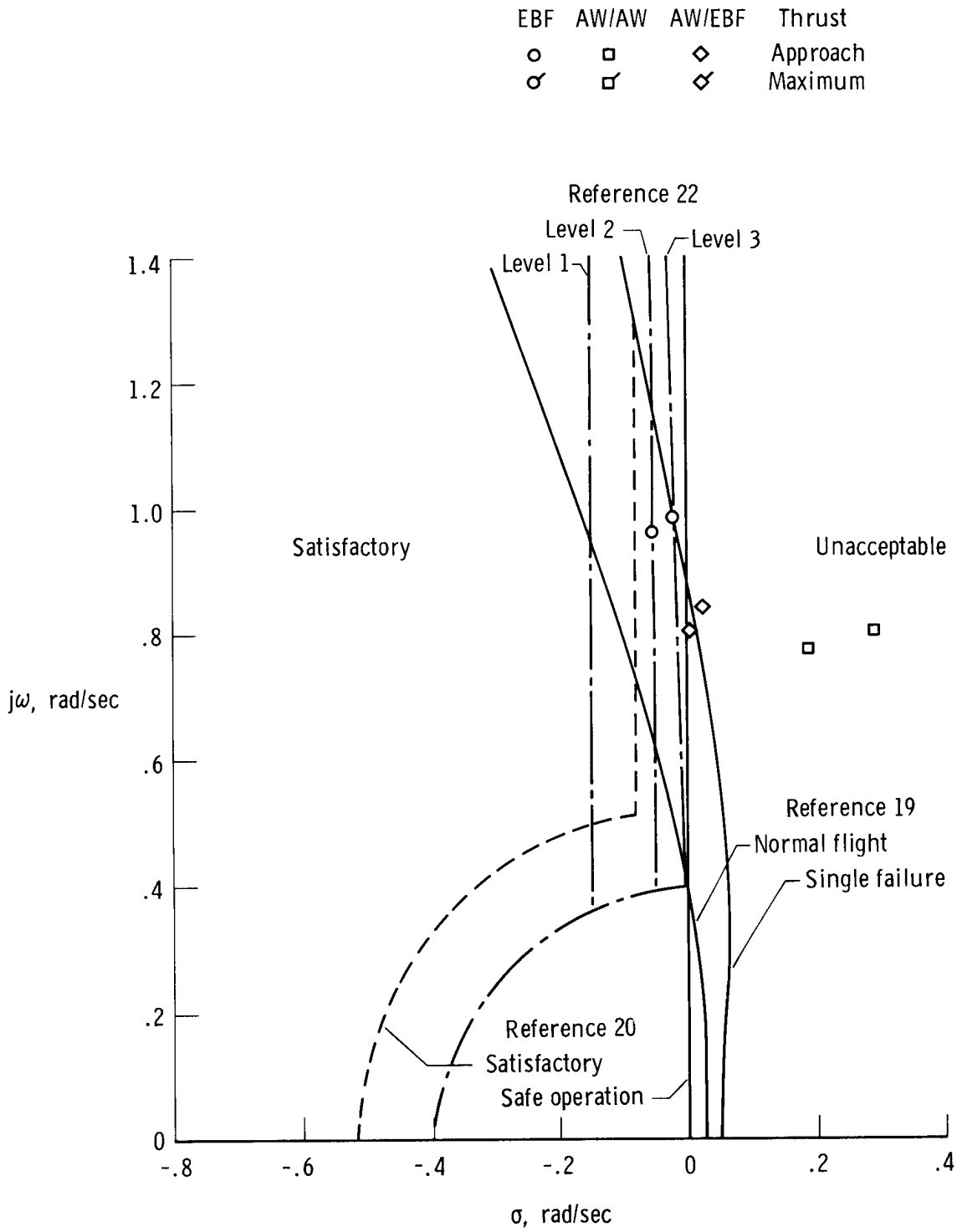

Figure 11. Comparison of lateral-directional frequency and damping characteristics with criteria from references 19, 20, and 22. Approach configuration; 70 knots.

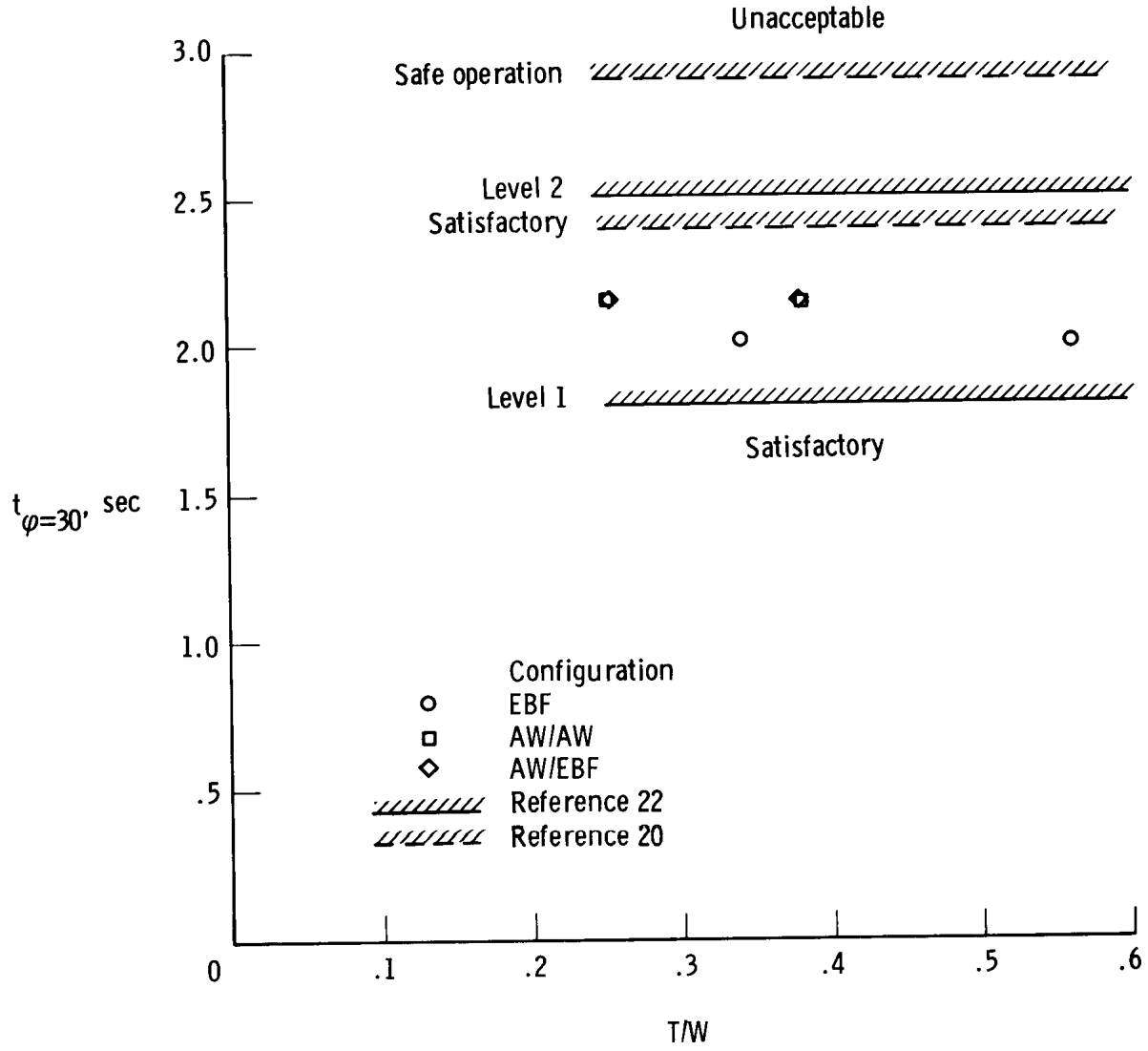

Figure 12. Time to bank to 30° for control wheel step input. Four-engine approach configuration; 70 knots.

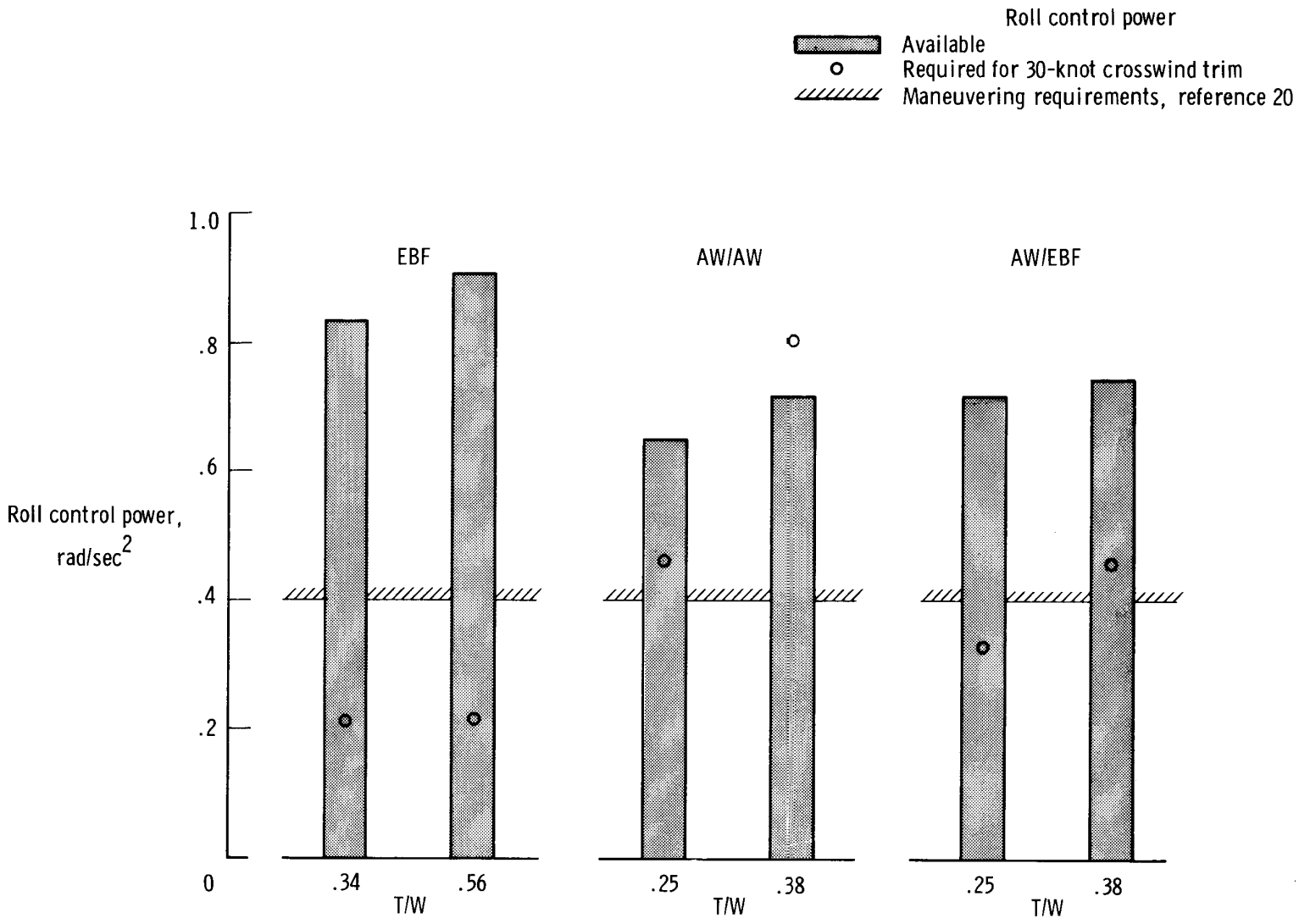

Figure 13. Available and required roll control power. Approach configuration; 70 knots.

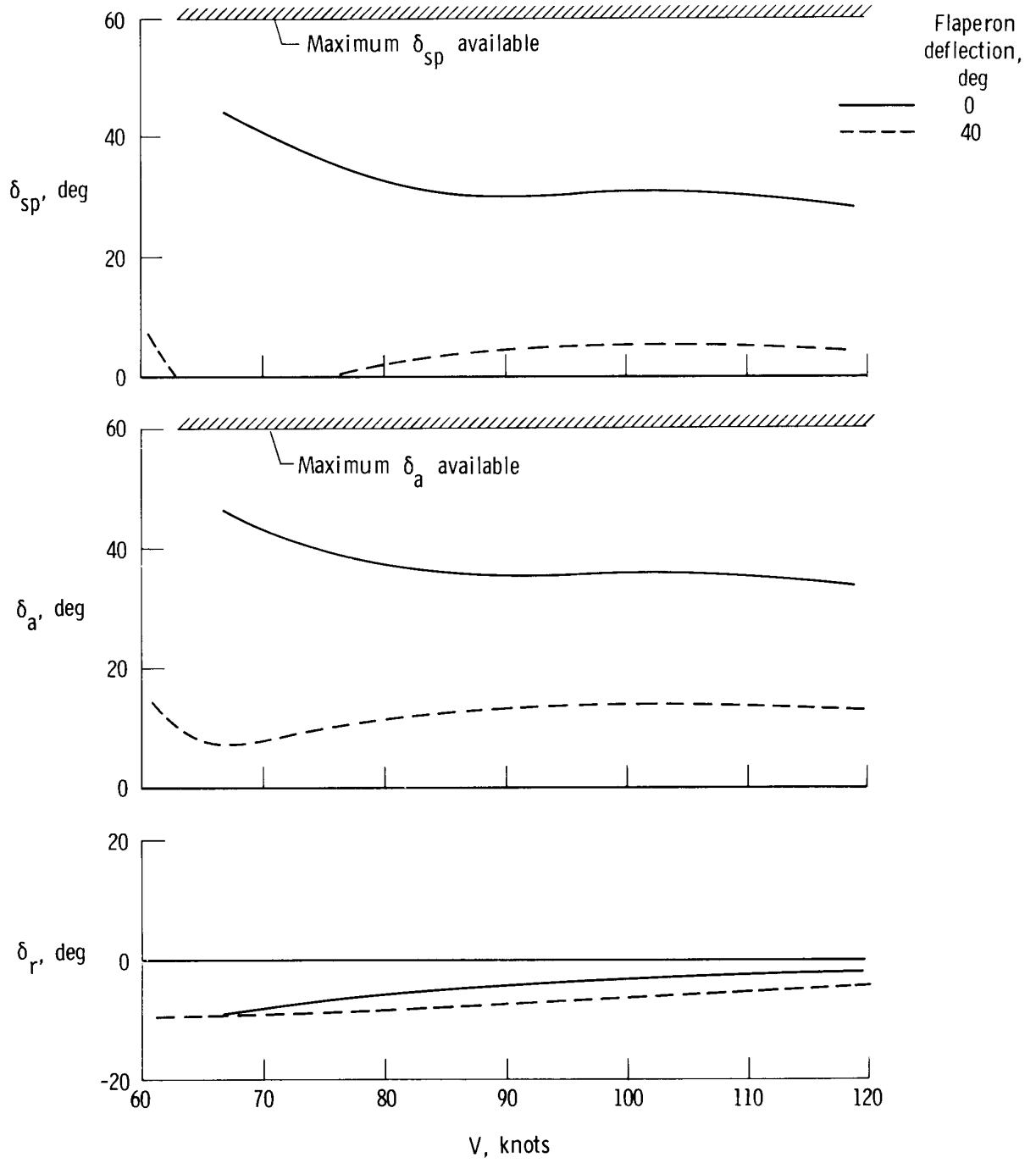

Figure 14. Lateral-directional trim required for engine-out condition. EBF approach configuration; maximum thrust; constant heading; $\beta = 0°$.

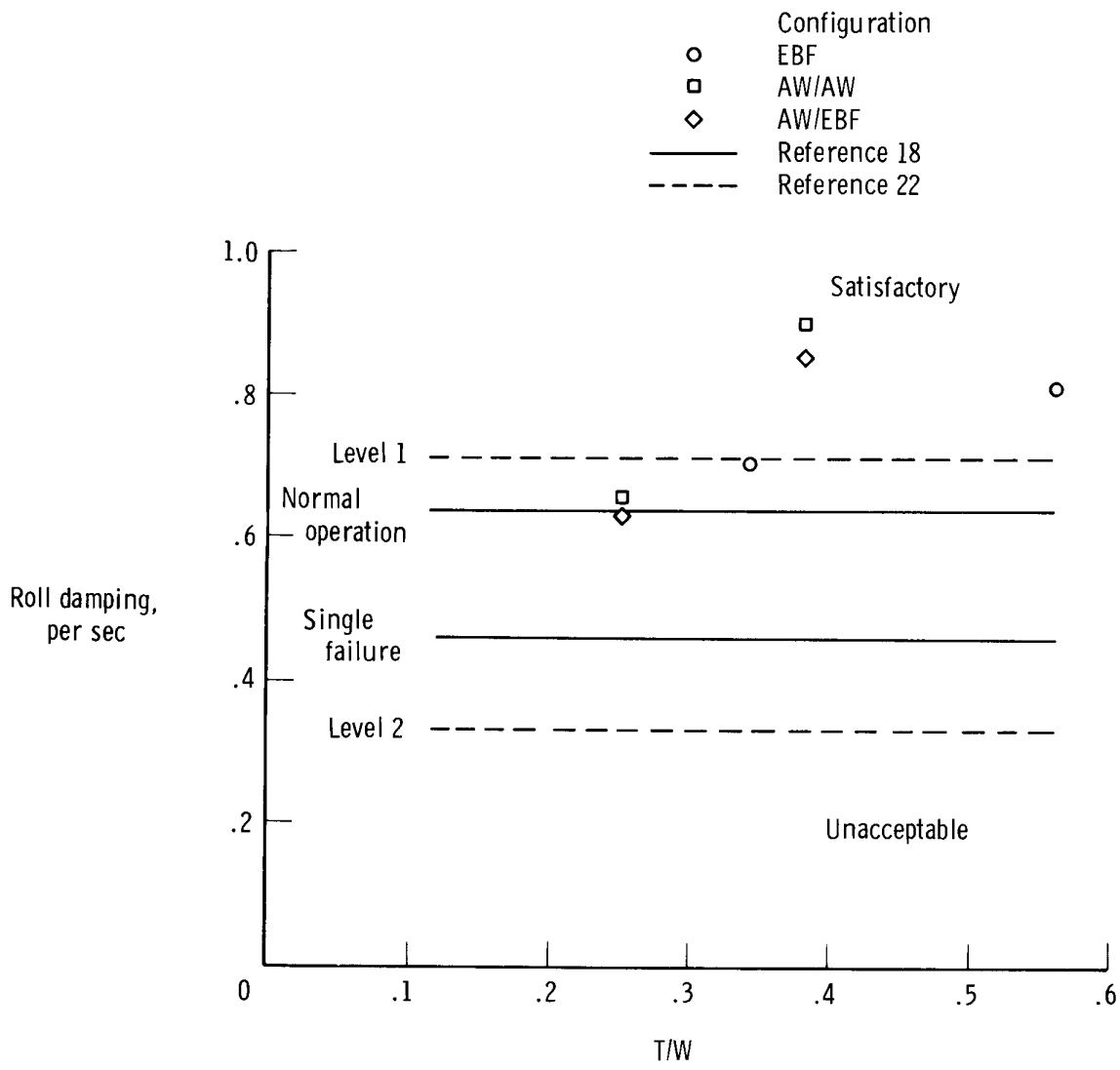

Figure 15. Comparison of roll damping characteristics with criteria from references 18 and 22. Approach configuration; 70 knots.

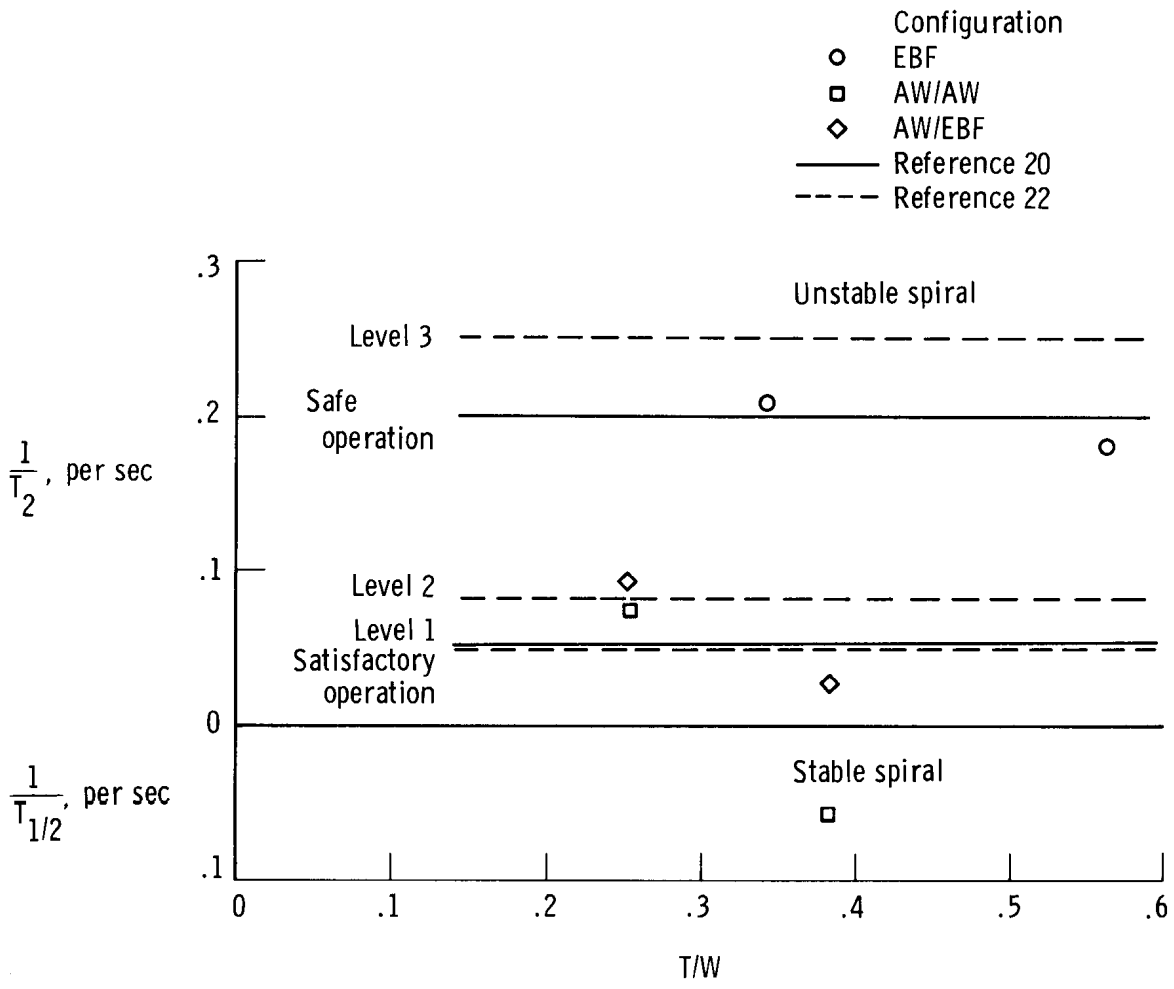

Figure 16. Comparison of spiral characteristics with criteria from references 20 and 22. Approach configuration; 70 knots.

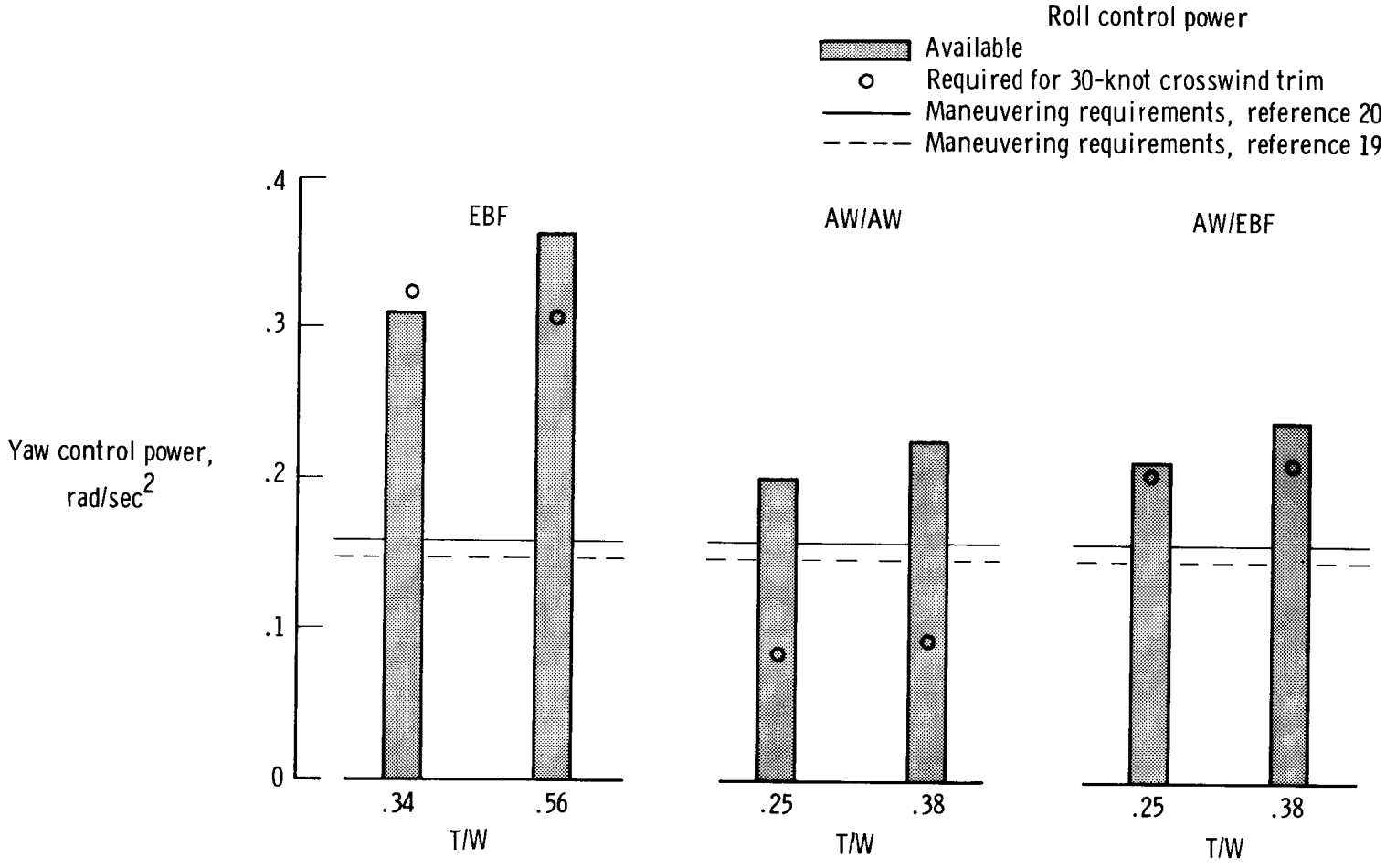

Figure 17. Available and required yaw control power. Approach configuration; 70 knots.

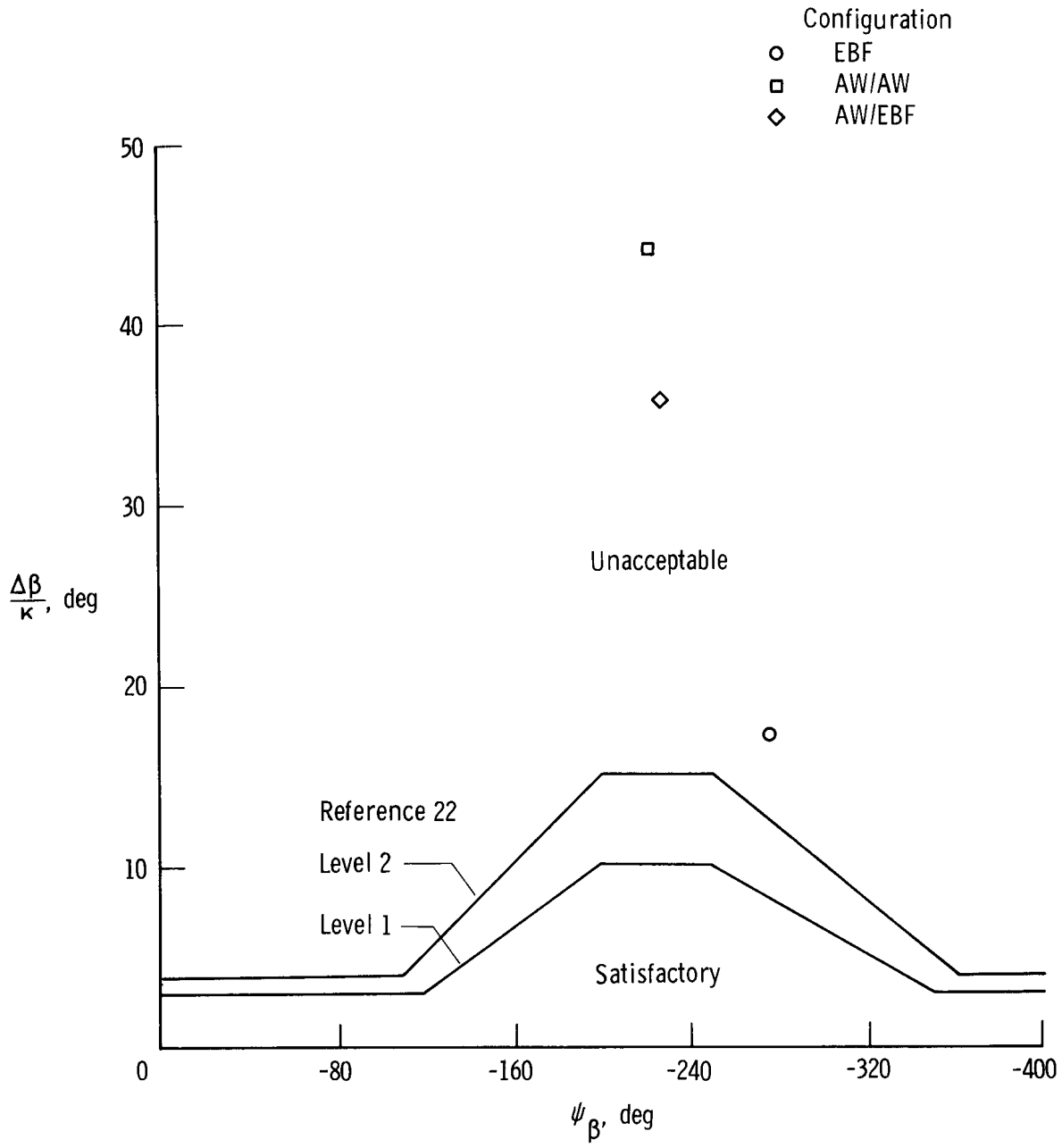

(a) Comparison with reference 22.

Figure 18. Roll-yaw coupling characteristics. Landing configuration; 70 knots.

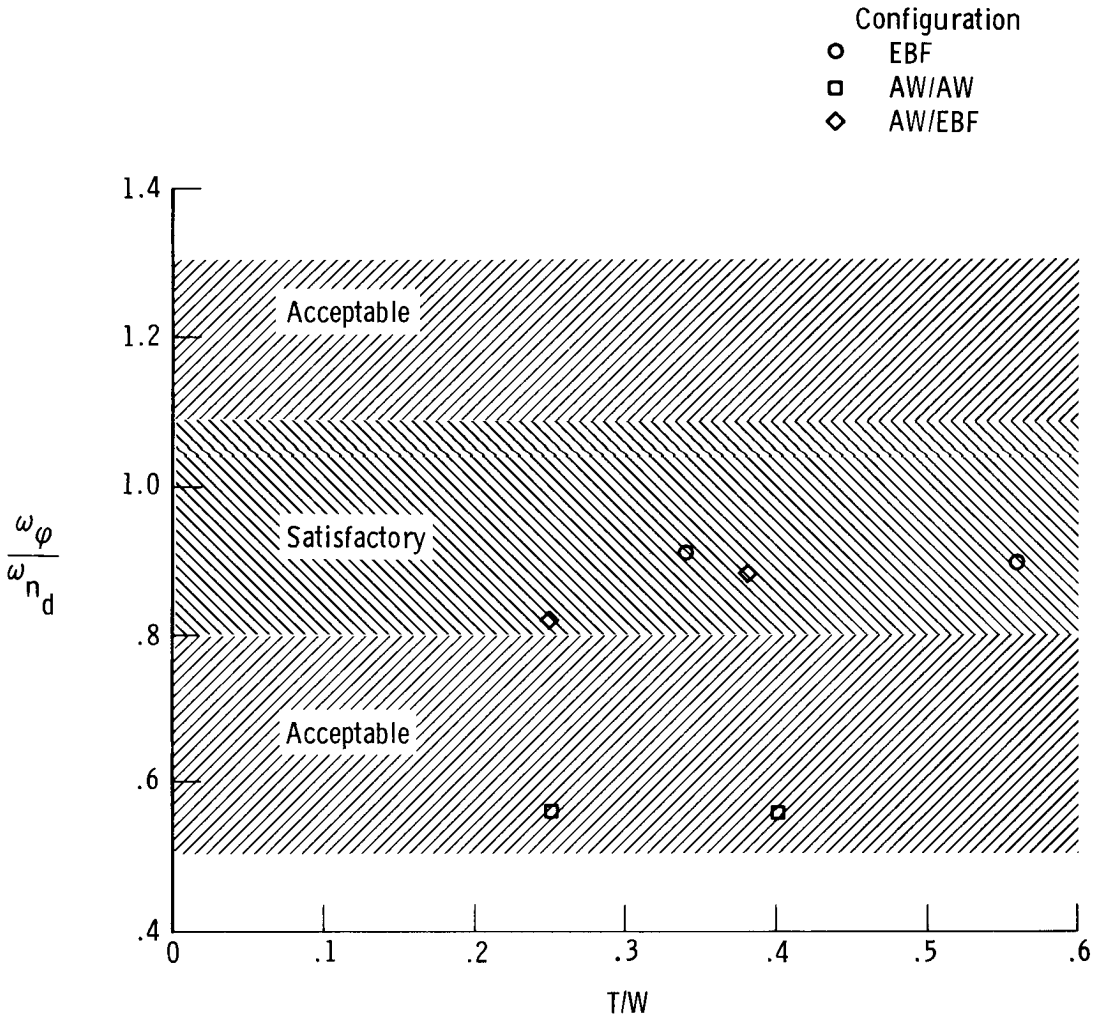

(b) Comparison with reference 24.

Figure 18. Concluded.

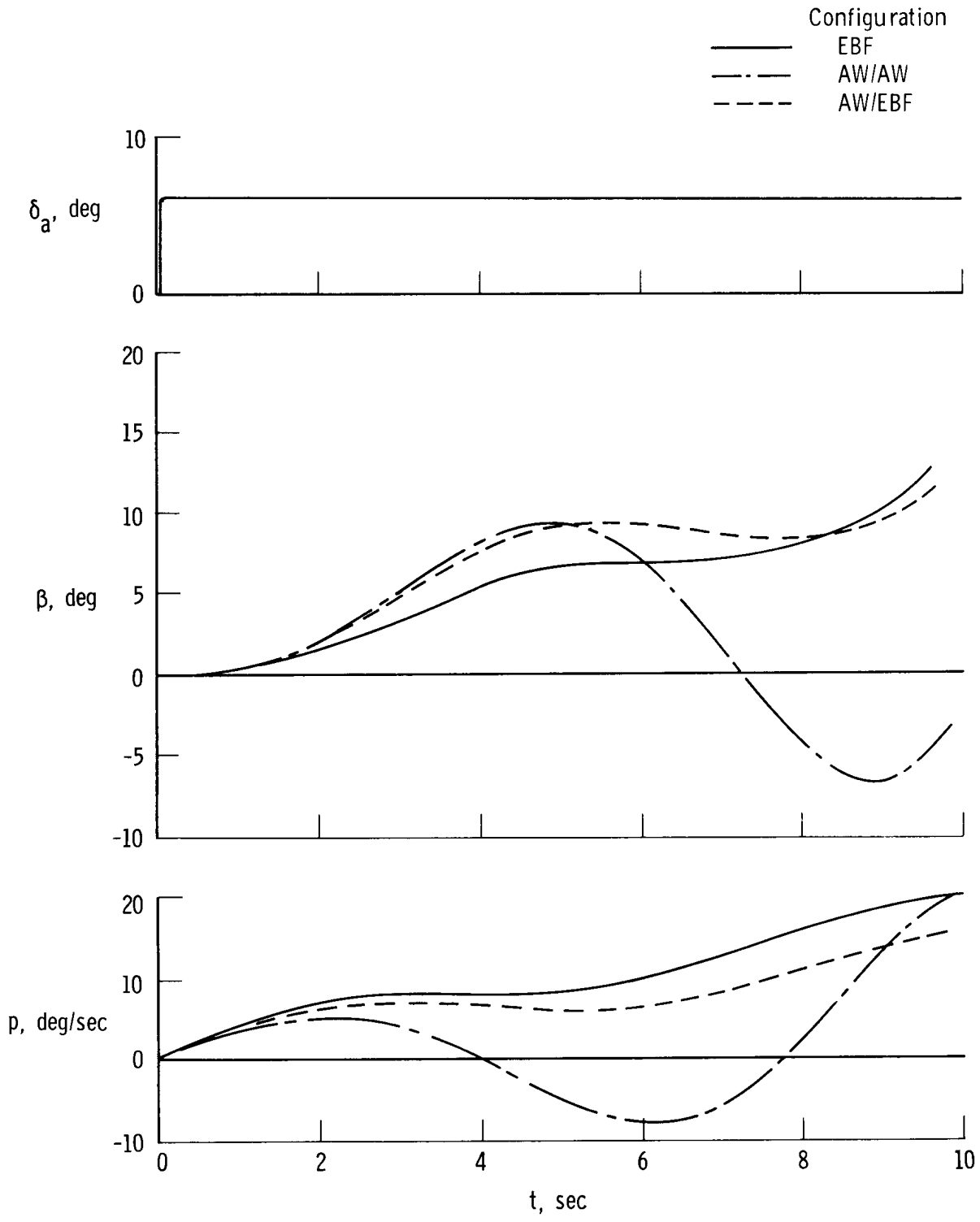

Figure 19. Time history of lateral-directional response to an aileron step input. Approach configuration; 70 knots.

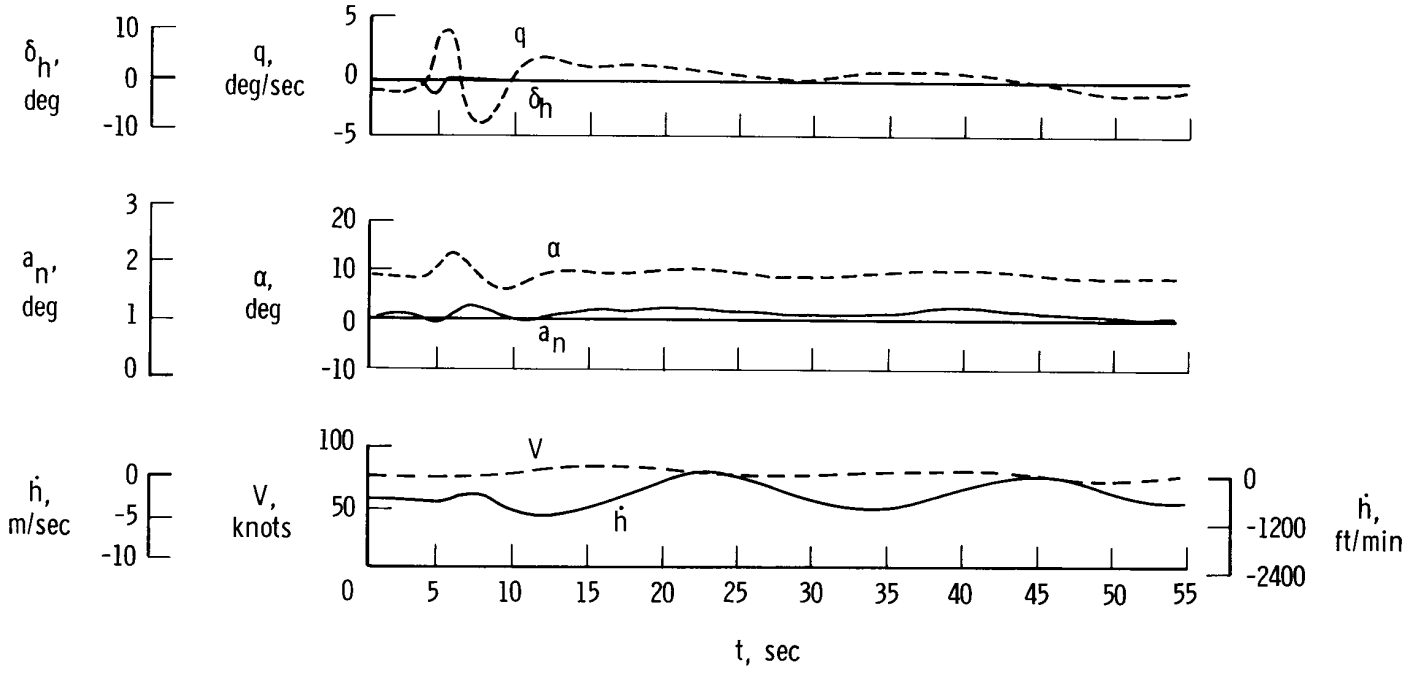

Figure 20. Time history of a longitudinal pulse illustrating the phugoid response. EBF landing configuration; 70 knots.

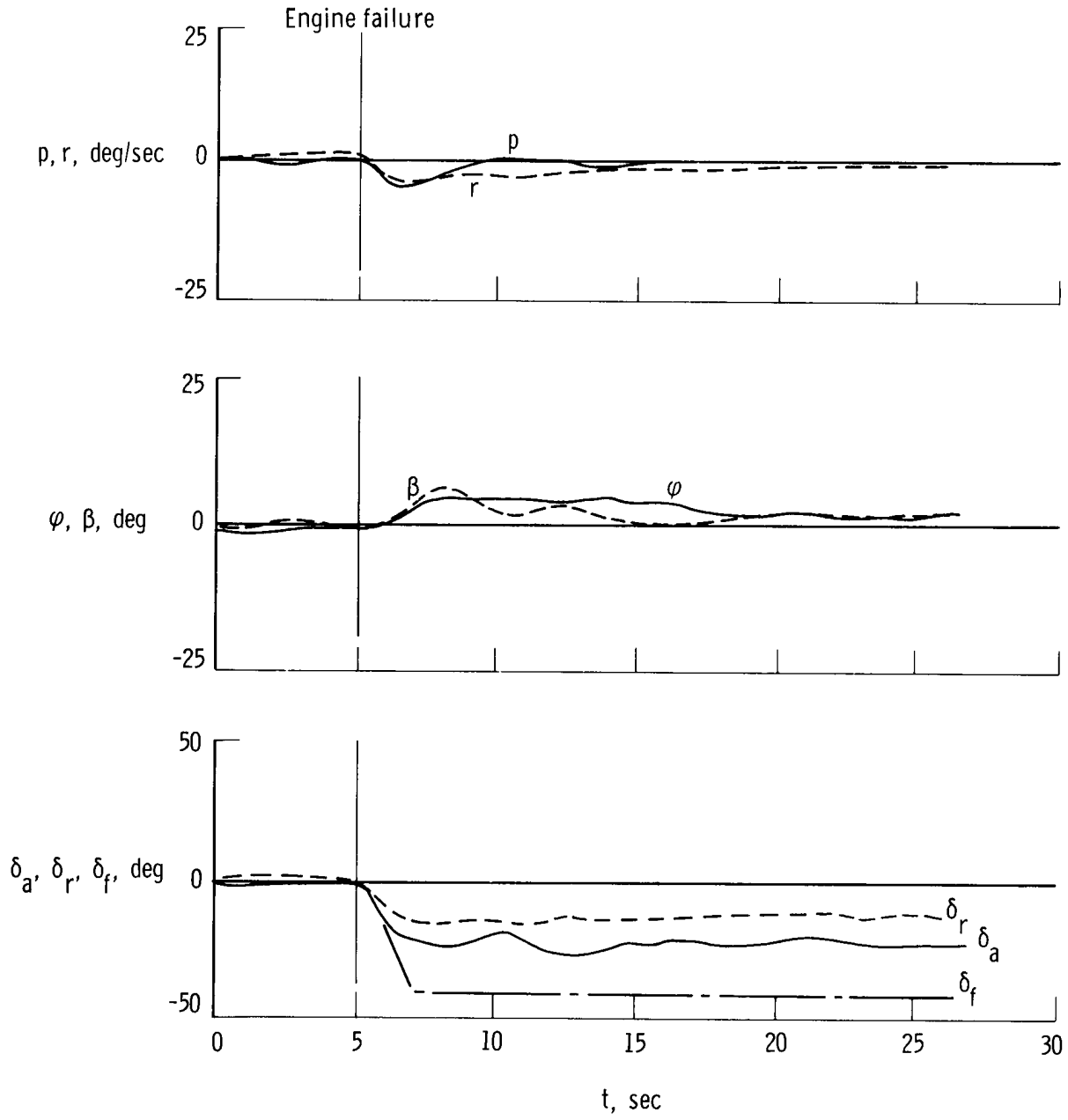

Figure 21. Time history of an engine failure. EBF landing configuration; stability augmentation on; 100 percent power.

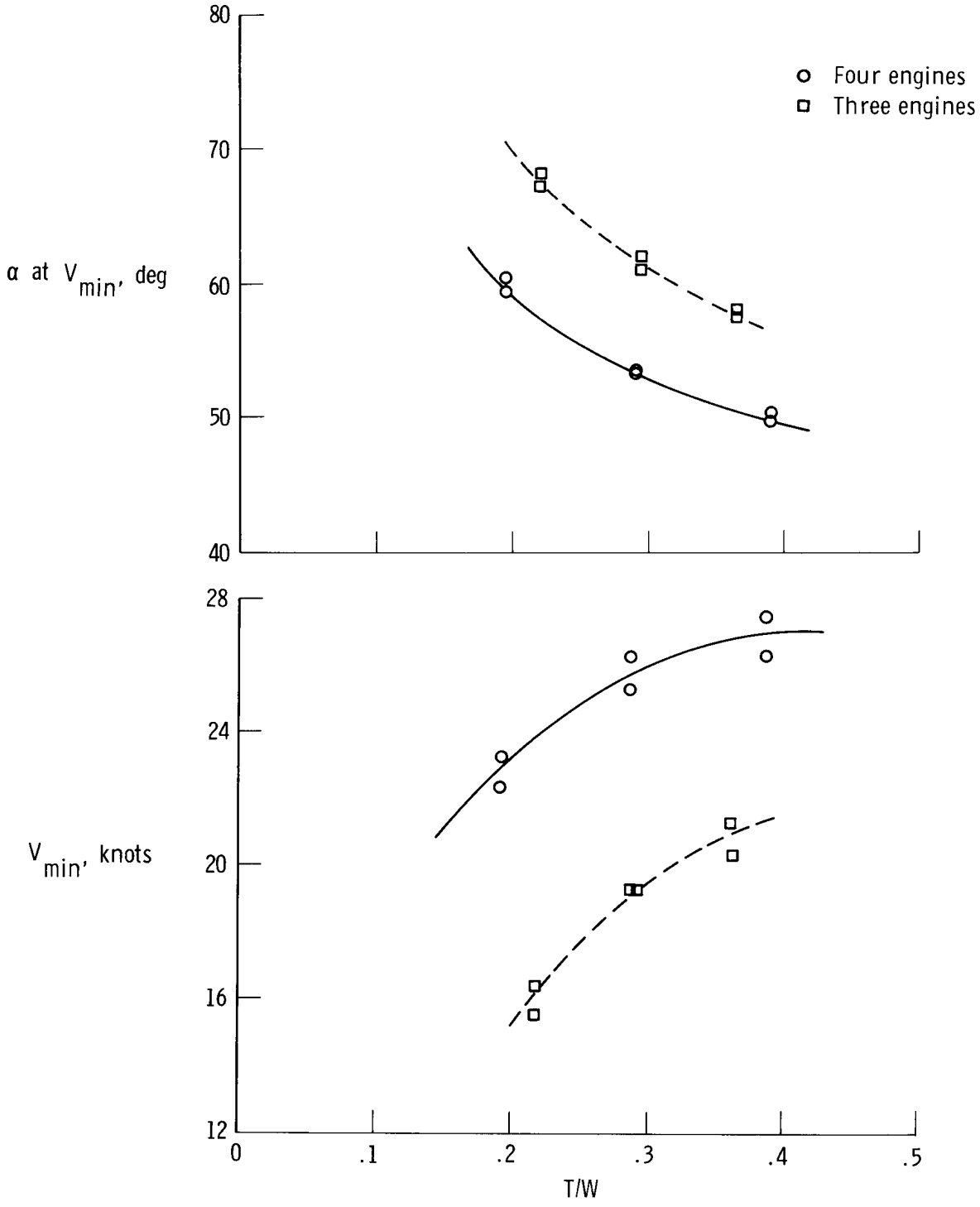

(a) EBF configuration.

Figure 22. Minimum speeds for three- and four-engine operation. Approach configuration; W/S = 3590 N/m^2 (75 lb/ft^2).

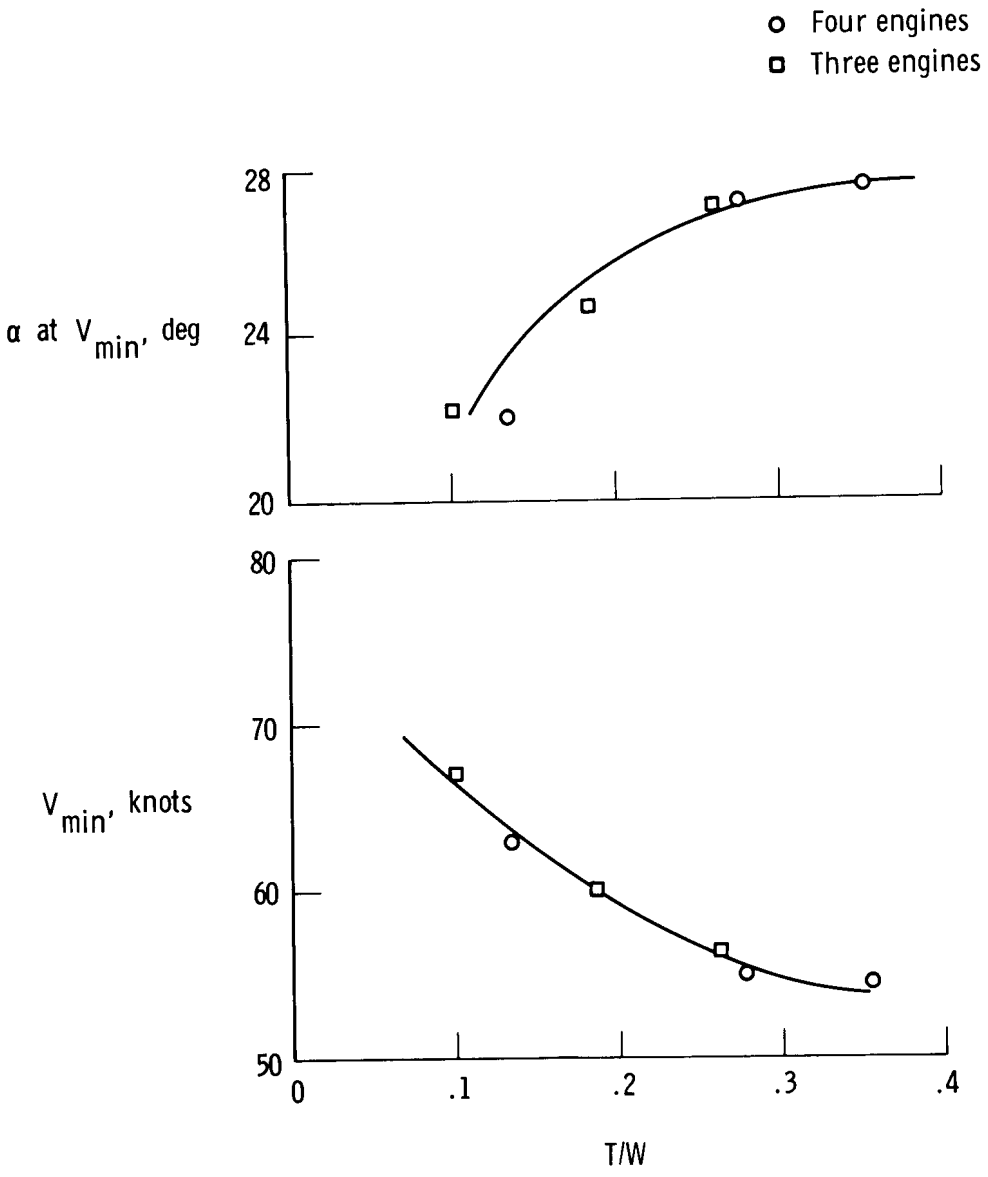

(b) AW/AW configuration.

Figure 22. Continued.

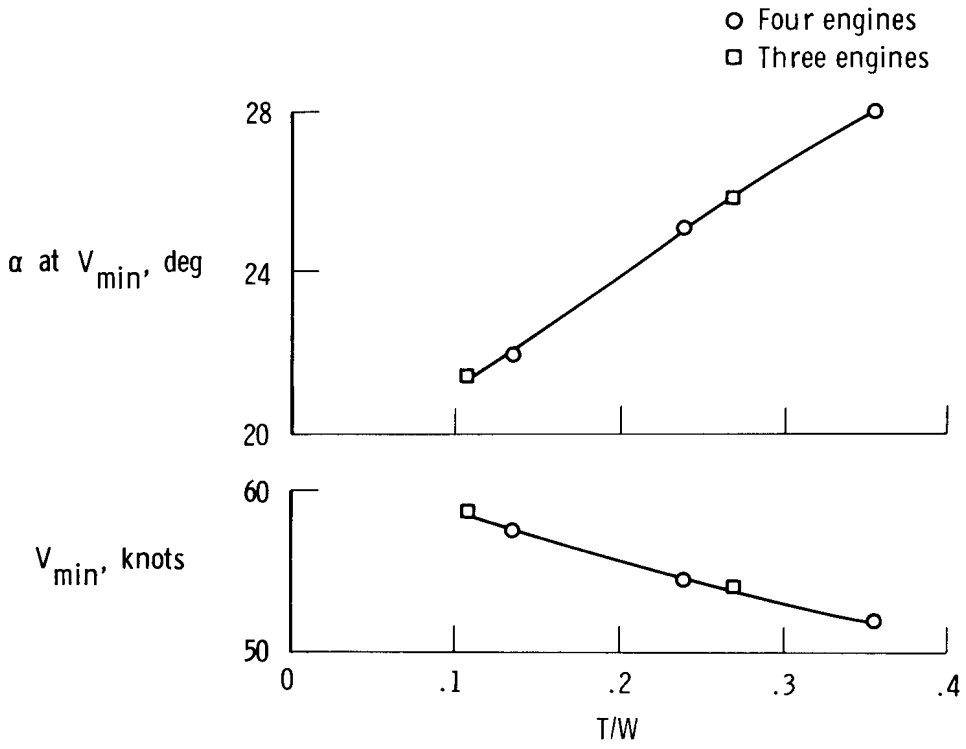

(c) AW/EBF configuration.

Figure 22. Concluded.

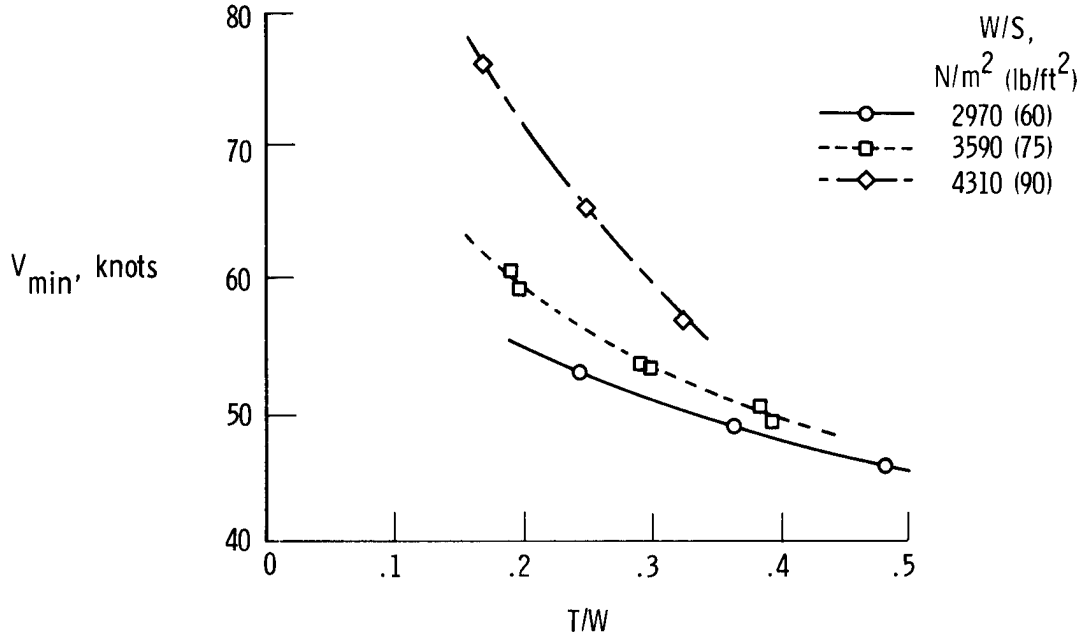

(a) Four engines.

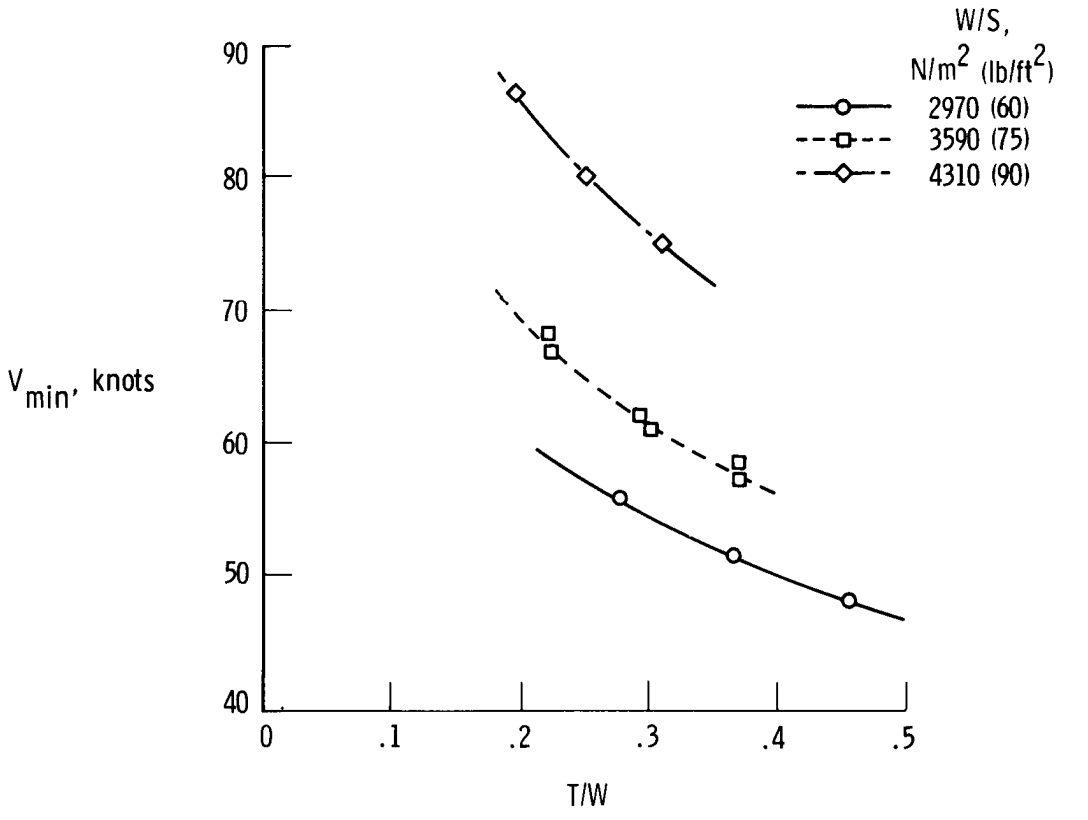

(b) Three engines.

Figure 23. Effect of wing loading on minimum speed. EBF approach configuration.

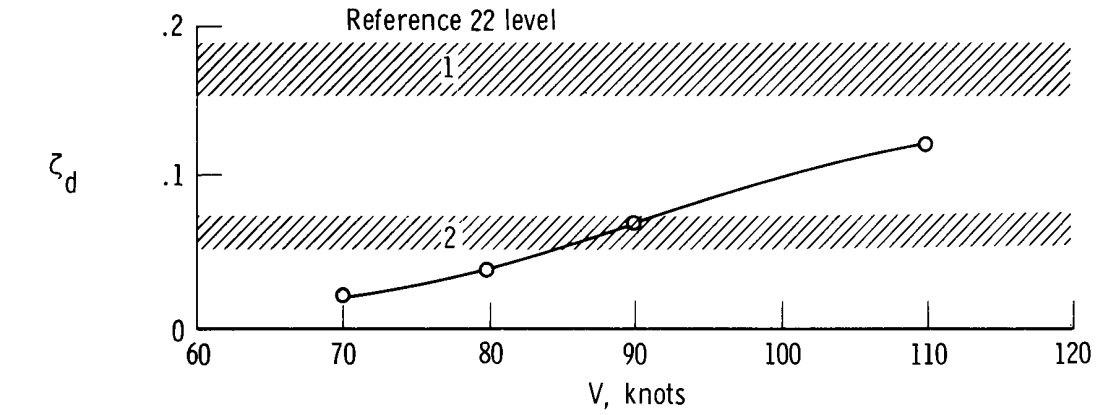

(a) Dutch-roll damping ratio.

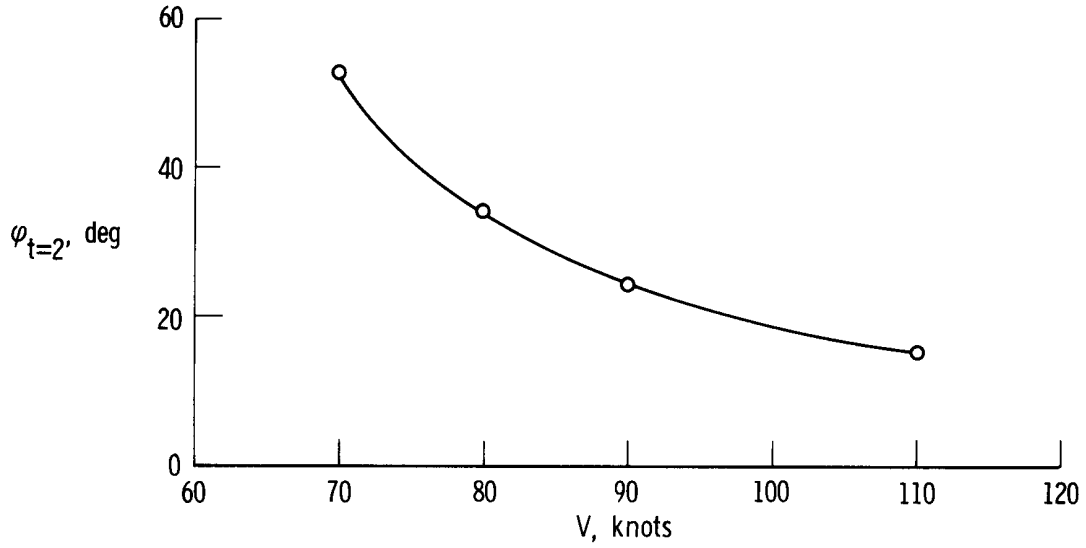

(b) Bank angle response due to engine failure.

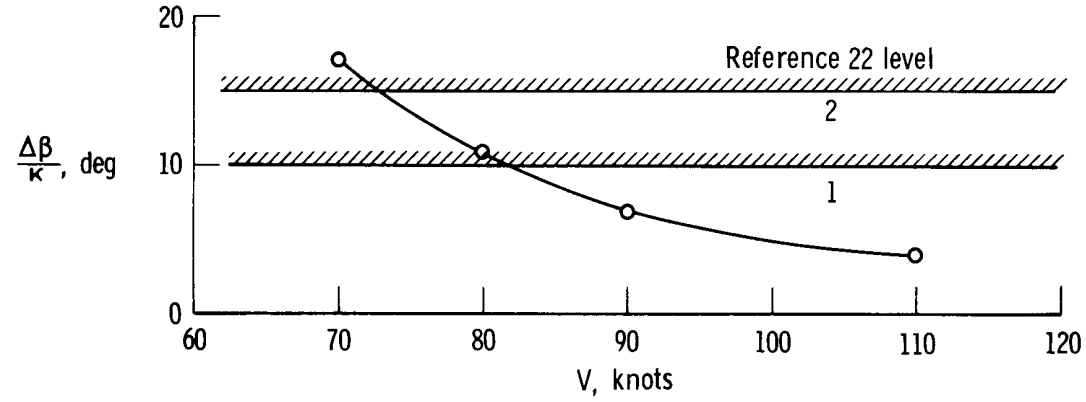

(c) Roll-yaw coupling parameter.

Figure 24. Effect of speed on EBF landing configuration characteristics.

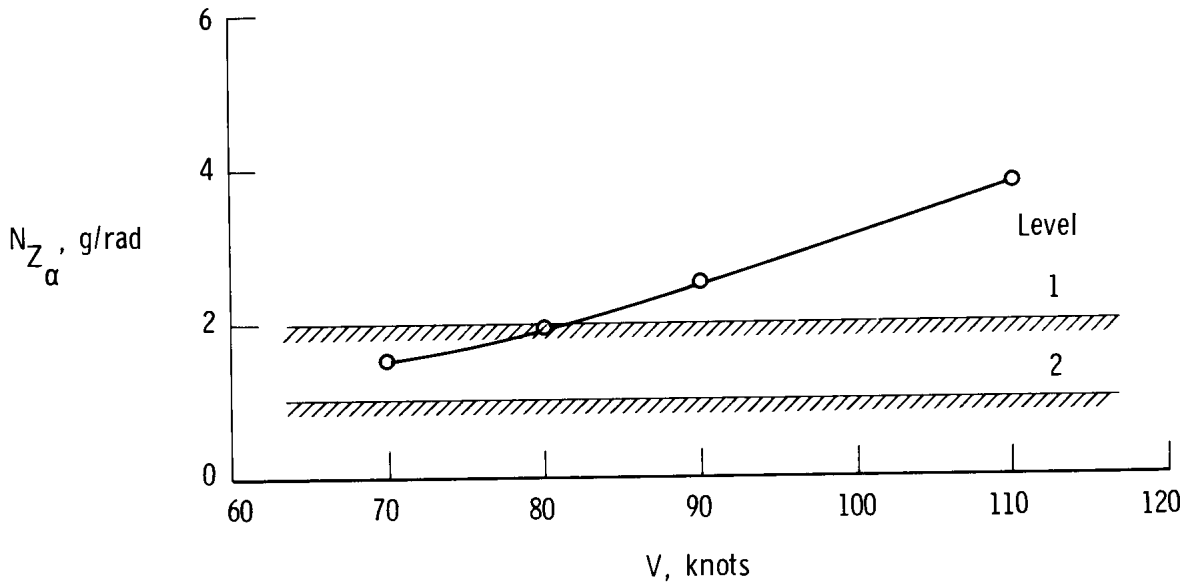

(d) Acceleration sensitivity.

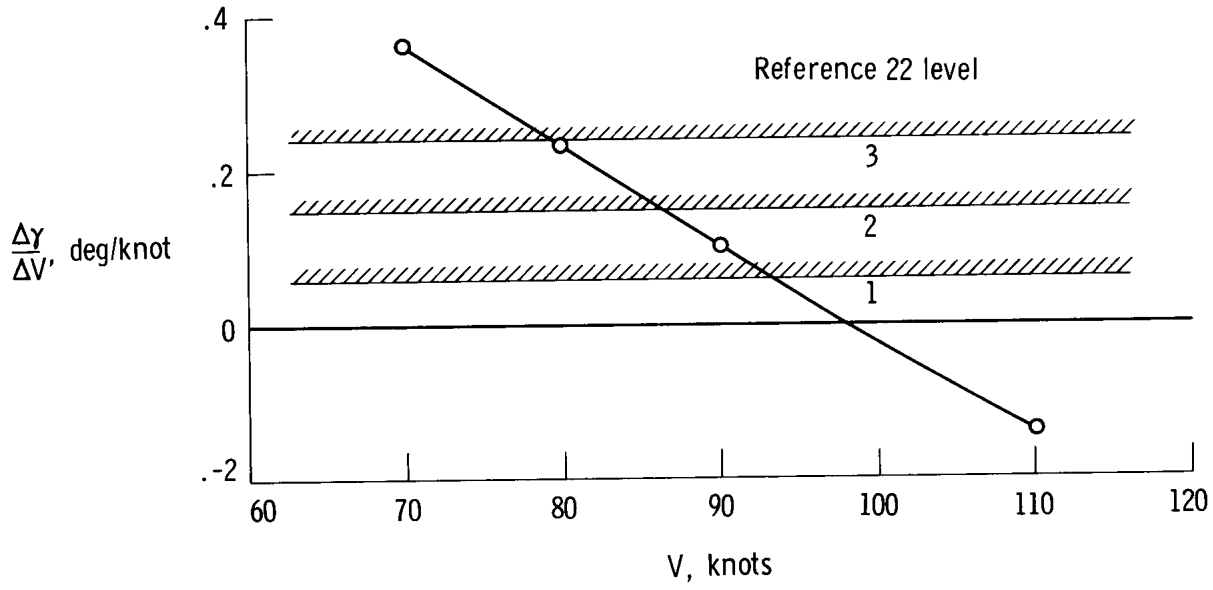

(e) Flight path stability parameter.

Figure 24. Concluded.

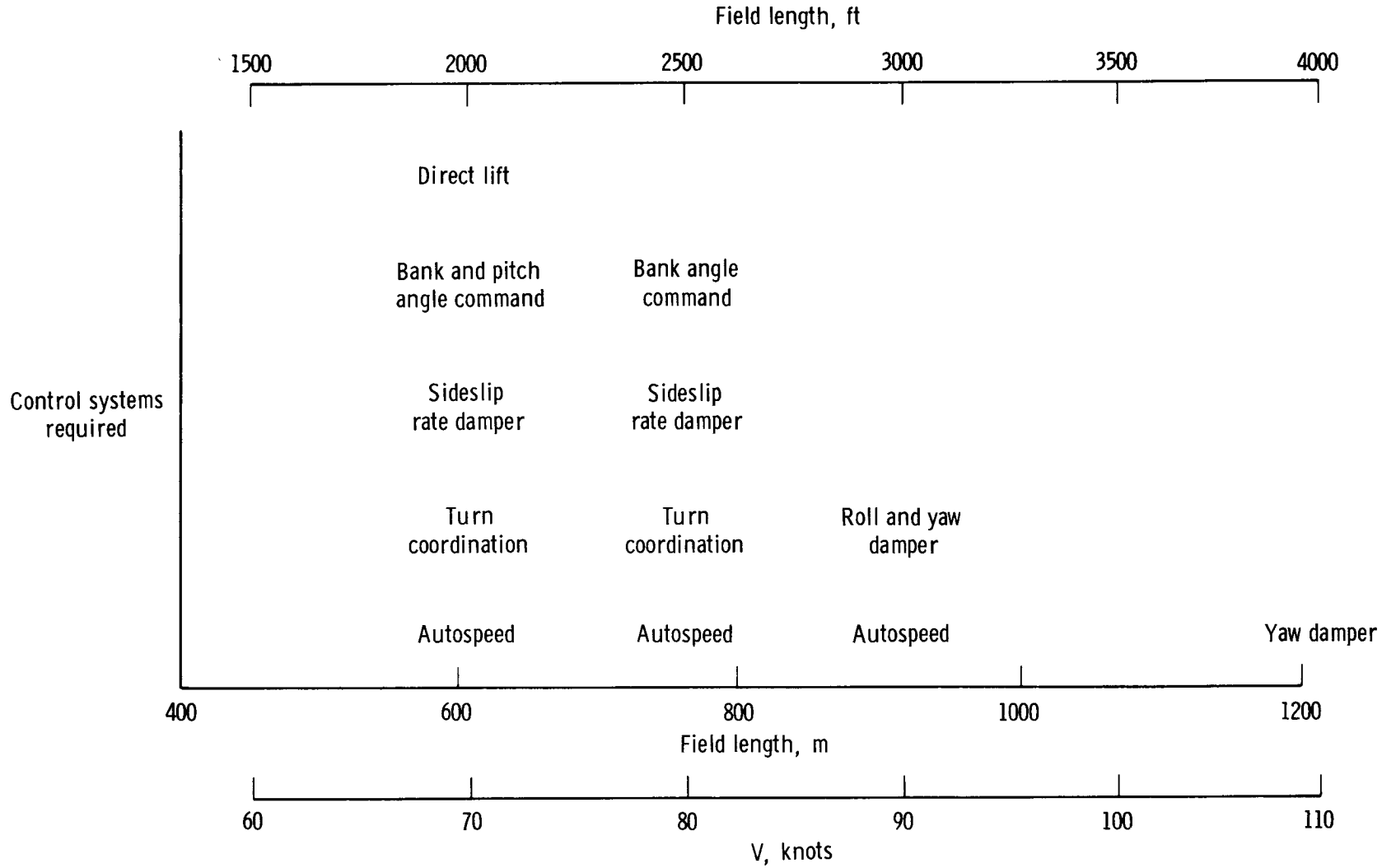

Figure 25. Summary of control system requirements as a function of speed and field length for EBF landing configuration.